The role of mTOR for the development and function of mouse thymic epithelium

Inauguraldissertation
zur
Erlangung der Würde eines Doktors der Philosophie
vorgelegt der
Philosophisch-Naturwissenschaftlichen Fakultät
der Universität Basel

von

Caroline Berkemeier

von Fribourg (FR) und Ligerz (BE)

Basel, 2013

Genehmigt von der Philosophisch-Naturwissenschaftlichen Fakultät

auf Antrag von

Fakultätsverantwortlicher & Dissertationsleiter:	Prof. Dr. Georg A. Holländer
Korreferent:	Prof. Dr. Antonius Rolink

Basel, den 18.06.2013

Dekan: Prof. Dr. Jörg Schibler

Acknowledgement

The presented work was carried out in the laboratory of Pediatric Immunology at the University of Basel under the supervision and guidance of Prof. Dr. med. Georg A. Holländer. He supported me from the moment I shyly asked for the possibility to join his lab, until last corrections of this thesis, and was never short of time to provide fruitful ideas, suggestions and comments.

Also, I would like to thank Prof. Dr. Antonius Rolink and Prof. Dr. Michael Hall for taking the time to read and evaluate my thesis.

Dr. Thomas Barthlott, Annick Peter, Katrin Hafen, Dr. Saulius Zuklys I thank for sharing their expert knowledge with me on many occasions, in theoretical aspects as well as in practical work. In addition, I am very grateful for the support and collegiality of all other members of the Pediatric Immunology laboratory and would like to thank them for creating a very pleasant working environment and for providing me with some distraction from the work whenever necessary.

Finally, I would like to thank my family and Alex for being there when I needed them.

Contents

Chapter 1

Introduction

1.1 Immune system

Over the past million years, a powerful and highly sophisticated system has evolved to protect our bodies from microbes, toxins and other pathogens, that surround us constantly. This system of defense — composed of a complex network of soluble factors and cells — is called "the immune system". A central feature of the immune system is its ability to distinguish between harmless "self" and pathogenic "non-self" structures, in order to only mount immune responses against potentially dangerous, foreign antigens.

An immune response can generally be divided into two phases; an initial phase of recognition, responsible for the selectivity of the reaction, followed by an effector phase. To reach selectivity and thus to prevent a reaction against autologous cells, pathogen recognition is based upon the presence of characteristic "foreign" markers and the concomitant absence of particular markers, expressed by "self"-tissue (Medzhitov and Janeway, 2002). During the effector phase, diverse highly efficient mechanisms are activated, aiming for the destruction and elimination of the intruding pathogens. These potentially lethal mechanisms have developed from the continuous threat by pathogens and are extremely potent and dangerous. Therefore, a tight regulation of the immune response is of great significance to restrict its effects to harmful substances. Numerous examples of humans with a defective immunity illustrate how important a perfectly balanced immune system is; a lack of immunity tends to result in an increased susceptibility to infectious diseases; such as in case of severe combined immunodeficiency (SCID). Conversely, an excessive and overshooting immune response directed against self-antigens can lead to severe autoimmune diseases, like Lupus erythemytosus. Finally, an inappropriate reaction against otherwise harmless substances can be the origin of allergies.

Knowledge about the fundamental principles of the immune system has also enabled us to benefit from its strength. The well-directed application

of specifically chosen, small doses of antigen, i.e. a "vaccine", can generate immunological memory that thus helps us to be protected from experiencing serious illnesses.

Globally, the immune system can be subdivided into two evolutionary different branches: the "innate" and the "adaptive" immune system. These two systems can be discriminated by the main players involved, their immune receptors and therefore the speed and specificity of the reaction. Although both systems are very closely linked and in certain areas even seamlessly merged, this division helps to illustrate the different general strategies and mechanisms through which we are able to protect and defend ourselves against pathogens or infectious diseases.

1.1.1 Innate immune system

The variety of immunological processes that are to our disposal without any previous exposition to microbes are summarized under the term "innate immunity". Through a number of fixed germ-line encoded receptors, patterns of microbial or viral structures are recognized in order to activate defense mechanisms. Prior to the activation of any of these mechanisms, pathogens need to overcome the first line of defense, represented by tight epithelial cell layers in the skin and mucosal membranes. In addition to these physical barriers, the synthesis of antimicrobial proteins and maintenance of an acidic environment are effective chemical means for the earliest elimination of microbes. Once pathogens succeed in intruding into the epithelium, different strategies take action that are known as second line of defense. The recruitment of immune cells, such as macrophages, neutrophils, eosinophils, natural killer cells (NK cells) and dendritic cells (DC) plays a major role here. Through pattern recognition receptors (PRR), these cells are able to detect vital components of foreign pathogens referred to as pathogen-associated molecular patterns (PAMPs), which are shared by groups of related microbes but are inexistent in healthy host cells. PAMPs are usually very essential molecules for the survival and function of the pathogen, including mannans, present in the yeast cell wall, double-stranded RNA (dsRNA) from viruses, bacterial and viral unmethylated CpG DNA and various bacterial cell-wall components such as lipopolysaccharides (LPS), lipopeptides, peptidoglycans and teichoic acids (Tsan and Gao, 2004).

The first PRRs that have been characterized are the so-called Toll-like receptors (TLR) (Medzhitov et al., 1997; Takeda et al., 2003), of which ten (named TLR1-10) are currently known to be expressed in humans. Together with the other PRRs, they can be classified according to their ability to promote either of two principal immune reactions: the initiation of phagocytosis or the activation of pro-inflammatory pathways via the release of cytokines and interferones. In neutrophils, monocytes, macrophages, mast cells and DCs, activation of PRRs leads directly to phagocytosis of the recognized

pathogen. Beside the removal of the perturbing agent, phagocytosis renders these cells also able to recruit cells of the adaptive immune system by presenting parts of the engulfed structures to them.

Another non-cellular component of innate immunity is the *complement system* (Ricklin et al., 2010). This system comprises a compilation of plasma proteins, which initiate a cascade of proteolytic reactions after mannose- or antibody-binding. The binding is achieved by covering the microbial surfaces with fragments that can be bound by phagocytic receptors on macrophages. Since the plasmatic molecules that facilitate phagocytosis are called opsonins, this special way of cellular removal is termed *opsonisation*. Some opsonins represent also targets for cellular destruction through activation of NK cells, whereas other components of the complement system contribute to the attraction of neutrophils and macrophages via their activity as chemotactic agents.

Together, these processes dominate the reaction against pathogens for the first four to five days and provide thus the early defense against infections. However, already during this initial phase of defense, several innate immune mechanisms aim for the activation and priming of the adaptive immune response, such as the release of inflammatory cytokines or the presentation of pathogenic antigens that have been processed after phagocytosis. Thereby, the innate immune system achieves to overcome its limitations of having only a restricted repertoire of pathogen recognition and lacking the ability to form a long-lasting memory against newly encountered pathogens, through the rapid involvement of the adaptive immune response.

1.1.2 Adaptive immune system

In contrast to the innate immunity, the adaptive immune system is an evolutionary young defense strategy, which is only present in vertebrates and cartilaginous fish. It is characterized by the specific immune response that is mounted after activation of unique antigen recognition receptors. These receptors are present on thymus-derived lymphocytes (T-cells) or bursa-derived lymphocytes (B-cells). They have undergone somatic gene recombination in order to provide each immune cell with the ability to recognize an exclusive antigen. Moreover, due to a process called allelic exclusion, only one of the two inherited alleles for the immune receptor is expressed in the process of successful rearrangement. As a result, mature B-cells or T-cells only express a single antigen receptor specificity. This specificity for a single receptor requires an exceptionally high diversity of immune receptors for the recognition of theoretically any potential pathogen or toxin. There are approximately 2 x 10^7 different T-cell receptors (TCR) at any given time point in a human.

T-cells and B-cells are the major cellular components of the adaptive immune system. They arise from a common haematopoietic stem cell that

is generated in the bone marrow. Resident stem cells in the bone marrow are able to directly differentiate into the B-cell lineage. Stem cells that are released into the blood, can, however, enter the thymus, where they encounter a unique microenvironment promoting the initiation and support of T-cells. In addition to these two primary sites of lymphocyte generation, other organs are also of great significance for the immune system. These organs include lymph nodes and the lymphoid follicles in tonsils, spleen, adenoids, skin and Peyer's patches that are belonging to the mucosa-associated-lymphoid-tissue (MALT). Populated by lymphocytes, plasma cells and macrophages, these tissues are ready to encounter antigens that pass through their epithelia and can subsequently mount an immune response.

To generate an adaptive immune response, microbes need to be phagocytised by cells of the innate immune system. By transporting components of the ingested material back to the surface, these phagocytes are able to engage T-cells through piecewise presentation of antigens. Subsequent to receptor-stimulation, activated lymphocytes expand clonally in order to increase the number of receptor-specific leucocytes. These leucocytes are able to recognize the currently threatening pathogen, and differentiate into effector cells. In the case of B-cells, encountering an antigen leads to the differentiation into antibody-secreting plasma cells. The released antibodies represent soluble lymphocyte-receptors, that constitute the humoral (from latin hūmōrālis; for moisture, bodily fluid) part of the adaptive immunity in allusion to their site of action. The outcome of T-cell activation leads to the establishment of cell-mediated immunity and engages the differentiation of T-lymphocytes into specialized effector cells. In addition to the general division of T-cells into the functionally different $CD4^{pos}$ and $CD8^{pos}$ T-cells, antigen-stimulation leads to a further subdivision of the $CD4^{pos}$ T-cells. According to their cytokine profile, they can be classified either as T_H1-cells or T_H2-cells. The production of interferon (IFN)-γ, tumour necrosis factor (TNF)-β, interleukin (IL)-2 and other pro-inflammatory cytokines supports the cell-mediated immunity and inflammation in T_H1-weighted T-cells. In contrast, T_H2-cells produce — amongst others — IL-4, IL-5, IL10, and IL-13 and thus provide help to B-cells and partially inhibit the functions of phagocytic cells. The interaction of T_H2-weighted T-cells with B-cells, and the partial converse effects of T_H1- or T_H2-cytokines illustrate once more the close dependency and interrelationship between the different immune branches and the complexity of the immune system.

Altogether, the humoral and the cellular arm of the acquired immune system represent a highly specific and flexible defence against different types of infections. While antibodies function to eliminate extracellular pathogens, activated T-cells combat intracellular microbes, together providing a global protection at different sites of action.

Another unique feature of acquired immunity is the generation of a long-term memory after first antigen-encounter. After a primary immune

response against a newly recognized antigen has been mounted, a second exposure to the same antigen will lead to a larger and more rapid immune response. In contrast to primary immune responses, which are mediated by immunological unexperienced T-cells ("naïve" T-cells , $T_{\text{naïve}}$) that have not recognized their antigen yet, secondary immune responses are mounted by cells that were induced during the first antigen encounter, ("memory" T-cells, T_{mem}). In mice, surface expression of CD62L is indicative of $T_{\text{naïve}}$, whereas T_{mem} typically lack CD62L but express CD44.

The list of the main effectors in the adaptive immune system is completed by regulatory T-cells (T_{reg}). These $CD4^{pos}$ T-cells are characterized by their potential to modulate and abrogate immune responses after successful elimination of invading organisms. As they also suppress the activation of other T-cells, they are able to prevent pathological self-reactivity. Therefore, T_{reg} are often linked to the maintenance of tolerance against "self" and the prevention of autoimmunity. Still, many open questions about T_{reg} and their mode of action remain unanswered. So far, the cell's immuno-suppressive potential is ascribed to the release of the anti-inflammatory cytokines IL-10 and tumour growth factor (TGF)β which in turn inhibit the activation of T_H1-and T_H2-cells and the production of antibodies.

Characteristically, T_{reg} express the transcription factor forkhead box P3 (FoxP3) and the α-chain of the IL-2 receptor, namely CD25. IL-2 is necessary for the growth, proliferation and differentiation of T-cells into the effector T-cells mentioned above. Expressing the IL-2 receptor α-chain, T_{reg} are able to bind and internalize IL-2, which leads to the deprivation of IL-2 for the effector T-cells. After elimination of the infection, the immune response contracts and returns to a resting state, until another infection needs to be combated.

In comparison to the immediacy of the innate immune system, the acquired immune system only becomes fully active within several days. This delay can be ascribed to the different immunological strategies applied by both systems. In order to recognize any conceivable antigen, immune receptors of the adaptive immune system are highly divers. As a result, there are only very few cells, recognizing a specific epitope. Therefore, antigen encounter first leads to an extensive proliferation of the specific T- and B-cells that have been activated. Typically, this cellular expansion takes several days. During this time, the protection against infectious agents relies on the innate immune system. In summary, the seamless collaboration of both, the innate and the adaptive arm of the immune defence provide us with a highly complex defensive system and supplies both instant protection against invading pathogens and long-termed immunity through the generation of memory.

1.2 Thymus

The thymus is a bilobed organ located in the central compartment of the thoracic cavity, positioned behind the sternum and in front of the heart. As a primary lymphoid organ, the thymus is the site for the formation and maturation of functional T-cells (Miller, 1964). Because of their potent functions in the defence against pathogens and transformed cells, mature T-cells harbour also the potential to be harmful against the host. Indeed, their antigen receptor rearranges randomly to facilitate the recognition of any potential antigen. Hence, a reliable and careful selection of T-cells during their development is essential. The thymic stromal micro-environment is responsible for this selection. It guarantees that T-cells survive only if they have successfully rearranged a receptor with the potential to react to foreign antigens but have been rendered tolerant to self-peptides. The thymic stroma is mainly composed of two types of thymic epithelial cells (TEC), which are in close contact to developing thymocytes and which exert distinct functions relevant for T-cell maturation: cortical thymic epithelial cells (cTEC) and medullary TEC (mTEC). These functions include the attraction of T-cell precursors from the blood, the subsequent maturation, selection, and eventually the export of functional T-cells. Importantly, the interactions of the thymic epithelium with thymocytes are bidirectional. Data obtained from mice with a block in T-cell maturation have shown, that an unperturbed T-cell development is also a prerequisite for the establishment of a functional thymic epithelium (Holländer et al., 1995; Shakib et al., 2009).

The following subsections will provide a brief overview of the development, anatomy and function of the thymus and characterize the complex interplay between TEC and thymocytes in more detail.

1.2.1 Development

Initial phases of thymus development

The vertebrate thymus constitutes cells that originate from all three embryonic germ layers; endoderm-derived epithelium, neuroectoderm-derived neural crest cells, and mesoderm-derived haematopoietic cells and endothelial cells (Smith, 1965; Moore and Owen, 1967; Owen and Ritter, 1969; Le Douarin and Jotereau, 1975; Le Douarin et al., 1976). A unique aspect of thymus development is the organization of the thymic epithelial cells. In contrast to other epithelial organs, TEC do not form a sheet of cells positioned on a basement membrane (BM), but build a 3-dimesional network, devoid of the BM scaffold. The initial formation of the thymic premordium occurs at early stages of embryogenesis (E9.5 to E11.5) and involves interactions between epithelial cells of the 3^{rd} pharyngeal pouch (3pp) endoderm and mesenchymal cells, derived from the neural crest (Cordier and Haumont, 1980; Manley, 2000). The process of thymic organogenesis can be divided

into a sequence of several consecutive steps, starting with the initial positioning of the 3pp at embryonic day 9.5 (E9.5). Analysis of spontaneous and gene targeted mutations have shown that this positioning depends on several transcription factors, including T-box1 (Tbx1), homeobox A3 (Hoxa3) (Manley and Capecchi, 1995; Chisaka and Capecchi, 1991), paired box gene 1 (Pax1) (Wallin et al., 1996), Pax9 (Peters et al., 1998; Hetzer-Egger et al., 2002), eyes absent 1 homologue (Eya1) (Xu et al., 2002), and sine oculis-related homeobox 1 homologue (Six1)6 (Xu et al., 2002). With the onset of the expression of the glial cells missing homologue 2 (Gcm2) around E10 (Gordon et al., 2001), the patterning and outgrowth of the primordial is initiated (Nehls et al., 1994), leading to the generation of regional differences within the cells of the growing rudiment. As a result two individual organs evolve from the 3pp primordium. While cells of the dorsal part of the 3pp develop into the parathyroid under the control of Gcm2, the ventral aspect of the 3pp gives rise to the thymus anlage, a formation that is critically dependent on the expression of the transcription factor Foxn1 (Nehls et al., 1994). Foxn1 message can be detected in the 3pp derivates of embryos at gestational day 10.5 using reverse transcription polymerase chain reaction RT PCR, however high-level Foxn1 expression is only found after E11.25 (Gordon et al., 2001). Studies in nude mice, in which the Foxn1 gene is mutated (Flanagan, 1966; Pantelouris, 1968), have shown that Foxn1 is not required for the initial formation of the thymus rudiment. However, in the absence of Foxn1, any further differentiation of the thymus anlage is blocked, including its colonization with lymphocyte progenitors.

Entry of thymocyte progenitor cells and thymus patterning

The initial attraction of haematopoietic precursor cells to enter the thymus primordium is initiated at E11.5 (Owen and Ritter, 1969). At this time point, the thymus is not yet vascularized, and precursor attraction is executed only by release of chemokines. In this context, chemokine (C-C motif) ligand 25 (Ccl25), which is embryonally controlled by Foxn1, and chemokine (C-C motif) ligand 21 (Ccl21) have been implicated in this process (Bleul and Boehm, 2001). Analysis of mice which have a naturally occurring deficiency for Ccl21 (plt/plt mice) or mice that lack Ccr9, the ligand for Ccl25 revealed a significantly lower number of thymocytes (Wurbel et al., 2001; Liu et al., 2005) at the age of E14.5 or E17.5, respectively, indicating the importance of these two chemokines in early thymic precursor seeding. The experimental use of antibodies against Ccl21, Ccl25, and (C-X-C motif) ligand 12 Cxcl12 to block their function confirmed the relevance of Ccl21 and Ccl25 for early haematopoietic colonisation, whereas neutralization of Cxcl12 did not result in an impaired thymocyte seeding (Ara et al., 2003). Initial lymphoid colonisation occurs before significant changes in TEC differentiation can be observed. This fact gave rise to the

question whether thymocyte precursor may play any role in inducing developmental differentiation of the thymus stroma during this very early phase of thymus organogenesis. To address this question, TEC differentiation was analysed in recombination-activating gene 2/ common cytokine receptor γ-chain-deficient (RAG 2/ γc) and Ikaros-null mice (Klug et al., 2002) — two mutant mouse models that show a block in early lymphocyte differentiation. Until E13.5, thymic development and TEC differentiation was unperturbed, which led to the conclusion that despite of their early occurrence in the thymus, initial patterning of the thymic epithelial compartment does not depend on inductive signals from haematopoietic cells.

Late phases of thymus development; Thymocyte-TEC crosstalk

The later differentiation of TEC and the formation of the medullary compartment is highly dependent on "crosstalk" between thymic epithelium and lymphoid cells (Ritter and Boyd, 1993; Nitta et al., 2011). Although the precise mechanisms that regulate the initial and late-stage differentiation of cortical and medullary TEC are still not fully understood, data from mutant mouse studies imply the role of several factors for the establishment and maintenance of the epithelial compartment. Transgenic mice that carry a mutant human CD3 ϵ chain, display a maturational block of thymocytes at the CD44^{pos} CD25^{pos} stage (Holländer et al., 1995). In these mice, cortical epithelial cells fail to expand and organize normally. This patterning defect can be reverted to normal thymopoiesis, once the mice are reconstituted by normal bone marrow precursor cells. However, the rescue fails and results only partially in a normal stromal compartment when the reconstitution is attempted at adult stages. This finding led to the conclusion that unperturbed epithelial differentiation and organization relies not only on signals provided from developing thymocytes but also on a temporal window of developmental opportunity. Though the cortical stroma requires active crosstalk with thymocytes committed to the T-cell lineage for its development (Naspetti et al., 1997; Wang et al., 1997), maturation of the medulla depends on the presence of mature single positive (SP) α/β or γ/δTCR^{high} thymocytes. In mice deficient for ZAP-70 or TCR α, where T-cell development is blocked prior to positive or negative selection, the formation of the medulla is strongly impaired, resulting in a reduction of medullary cells in the thymus (Surh et al., 1992; Naspetti et al., 1997). Even though the mTEC compartment is hypocellular, the expression of markers typically associated with mTEC differentiation is not altered (e.g. Autoimmune Regulator (AIRE) and tissue-restricted antigens genes). Thus, even in the absence of signals from positively selected thymocytes, the expression of functional molecules on mTEC is not affected (Hikosaka et al., 2008). The medullary compartment is also contracted in a mouse model in which positively selected thymocytes are not able to migrate to the medulla following

positive selection due to a lack of Ccr7 expression (Ueno et al., 2004). However, reduction in the number of mTEC is less severe in these mutant mice when compared to that of the aforementioned ZAP-70 or TCR α knockout mice. This finding strongly suggests that the defect in medulla formation is rather linked to the lack of interactions with positively selected thymocytes than a consequence of a general absence of thymocytes in the medulla. In addition, numerous studies have revealed that signals mediated by members of the TNFR superfamily, including lymphotoxin β (LTβ), receptor activator for NF-κB (RANK), and CD40, play an essential role in organizing the medullary thymic epithelial cell compartment (White et al., 2010). In this context, RANKL and its respective receptor on TEC has been identified as potent mediator of thymic crosstalk, as its enforced expression was shown to restore mTEC cellularity in mouse models with impaired positive selection (Hikosaka et al., 2008). More recently, another cell type has been implicated to play a role in mTEC development and differentiation, namely lymphoid tissue inducer (LTi) cells. The appearance of these $CD4^{pos}CD3^{neg}$ cells *in situ* was found to be temporally linked to the development of mTEC during embryogenesis (Rossi et al., 2007). Indeed, RORγ-deficient mice, which lack LTi cells, display a reduced number of specialized mTEC, marked by the expression of AIRE. This effect was causally linked to the lack of TEC-directed RANKL signalling mediated by LTi cells.

Epithelial-mesenchymal interactions

Mesenchymal cells, initially derived from both the pharyngeal mesoderm and the neural crest contribute to the outer thymic capsule (Le Lièvre and Le Douarin, 1975), the interlobular septae (Jiang et al., 2000), and the intrathymic network of fibroblasts (Yamazaki et al., 2005), from as early on as E11.5. A functional importance of neural crest-derived cells during thymus development was suggested by experiments in which removal or reduction of mesenchymal cells in the pharyngeal region resulted in either a complete absence or a significant reduction of thymus cellularity (Bockman and Kirby, 1984).

It is still not fully understood how mesenchymal cells support thymus morphogenesis, but a possible molecular link between neural crest mesenchyme and epithelial cells is provided via fibroblast growth factors (FGF) and their receptors (FGFR), respectively. Fgfr2-IIIb is expressed on TEC as early as E13 (Revest et al., 2001), (Jenkinson et al., 2003), where it is thought to interact to Fgf7 and Fgf10, which are produced by the surrounding mesenchyme (Revest et al., 2001). The evidence for the importance of Fgfr2-IIIb results from studies of Fgfr2-IIIb -/- mice. After initially normal thymus development, thymus growth is severely stunned in these mice from E12.5 onwards (Revest et al., 2001). Other factors potentially involved in the proliferation and differentiation of immature thymic epithelia include

epidermal growth factor (EGF), insulin-like growth factors-1 (IGF 1) and -2, retinoic acid (Shinohara and Honjo, 1996; Jenkinson et al., 2003; Bhasin et al., 2004). Once epithelial cells have acquired the competence to fully support T-cell development, and the establishment of thymic vasculature is complete, the presence of neural crest-derived mesenchymal cells decreases (Yamazaki et al., 2005; Jiang et al., 2000), and further TEC differentiation becomes largely independent of ongoing mesenchymal support (Jenkinson et al., 2007). The question whether these cells persist in the thymic microenvironment to time points beyond the newborn age remained open for quite some time. Using genetic markers expressed under the promotor of Wnt1 (Danielian et al., 1998) and Sox10 (Matsuoka et al., 2005) — which are expressed in the neural plate from which neural crest-derived cells (NCCs) originate (Echelard et al., 1994; Matsuoka et al., 2005) — it was then convincingly demonstrated that NCCs constitute a major cellular component in the adult thymus. These studies furthermore demonstrated that NCCs differentiate into smooth muscle cells and perivascular cells (pericytes), which are both involved in forming a supportive network for thymic blood vessels. More recently, pericytes were identified as a source for sphingosine-1-phosphate (S1P), which promotes the egress of mature thymocytes (Matloubian et al., 2004).

1.2.2 Thymus anatomy and cellular characterization

The composition of the thymic stromal compartment is heterogenous and comprises the aforementioned thymic epithelial cells (TEC), as well as endothelium, fibroblasts, macrophages, dendritic cells (DCs) and other rare cell types. TEC represent the most abundant cell population within the thymic stroma. According to their location, function, and characteristics, they can be further subdivided into cortical and medullary TEC. The anatomic region that is located at the border between cortical and medullary TEC is defined as the cortico-medullary junction (CMJ). This region is highly enriched for vessels that are surrounded by a perivascular space, which is thought to be involved in T-cell progenitor immigration as well as in the export of newly generated T-cells to the circulation (Mori et al., 2007). The thymic cortex, which surrounds the medullary compartment, is composed of a three-dimensional meshwork of reticular cTEC. These epithelia are phenotypically best characterized by distinctive patterns of extracellular antigens (such as Ly51) and intercellular proteins (such as Keratin 8 (K8)) (Godfrey et al., 1988; Klug et al., 1998; Surh et al., 1992). mTEC which similarly form a three-dimensional stromal network in the inner core of the thymus are characterized by a reactivity with Ulex europaeus agglutinin I (UEA1) and the expression of Keratin 5 (K5). A typical feature that both epithelial cells subtypes share, and which is related to their function of antigen-presentation to developing thymocytes, is the expression of major

histocompatibility II (MHCII) molecules. Based on the amount of MHCII expression, cTEC and mTEC are further subdivided into cells with a high ($MHCII^{high}$) or low ($MHCII^{low}$) expression. The quantity of MHCII expression per TEC follows a typical kinetic over time: MHCII expression on TEC is typically low during embryonic stages and changes to a consistently higher expression after birth. By two weeks of age, a significant population of $MHCII^{low}$ TEC emerges in parallel to $MHCII^{high}$ cells. This phenotype correlates with other molecular markers of epithelial immaturity and is thus used in mice three weeks and older to identify immature TEC in both cortex and medulla. TEC with a low MHCII cell surface expression expand over time and eventually become the predominant TEC subpopulation in older mice (Gray et al., 2006). Among the $MHCII^{high}$ mTEC, expression of the Autoimmune Regulator (AIRE), which plays a crucial role in the induction of T cell tolerance towards tissue-restricted antigens (Derbinski et al., 2001; Anderson et al., 2002), can be used to further distinguish these cells into distinct, terminally differentiated subpopulations (Hamazaki et al., 2007).

mTEC and cTEC are derived from a common progenitor (Bleul et al., 2006; Rossi et al., 2006; Hamazaki et al., 2007; Shakib et al., 2009). However, the individual steps of differentiation that finally result in the generation of phenotypically and functionally cTEC or mTEC compartments remain still not fully defined, not least because TEC differentiation is regulated by cell-intrinsic factors and extrinsic factors, provided by the local environment (reviewed in Rodewald (2008); Anderson et al. (2009)).

1.2.3 Thymic function

Random rearrangements of the genetic elements that encode the different parts of the TCR are responsible for the great variability in TCR specificities generated during intrathymic T-cell development. The downside of this mechanism is the danger of generating receptors that are either non-functional in or harmful to the individual. In order to avoid propagation of useless or self-reactive T-cells, developing thymocytes undergo several selection processes, during which only those cells survive which have successfully rearranged and expressed a T-cell receptor that has specificity for self-MHC molecules presenting foreign (i. e. non-self) antigens. These essential selection processes are effected by the thymic stromal compartment.

Thymocyte development

The generation of thymocytes is dependent on a continuing input of blood-born hematopoietic precursor cells (Kadish and Basch, 1976; Lepault and Weissman, 1981; Leuchars et al., 1973) as there are no residual thymocyte progenitors present in the thymus. After seeding into the thymus at the cortico-medullary junction, immature progenitor cells undergo further dif-

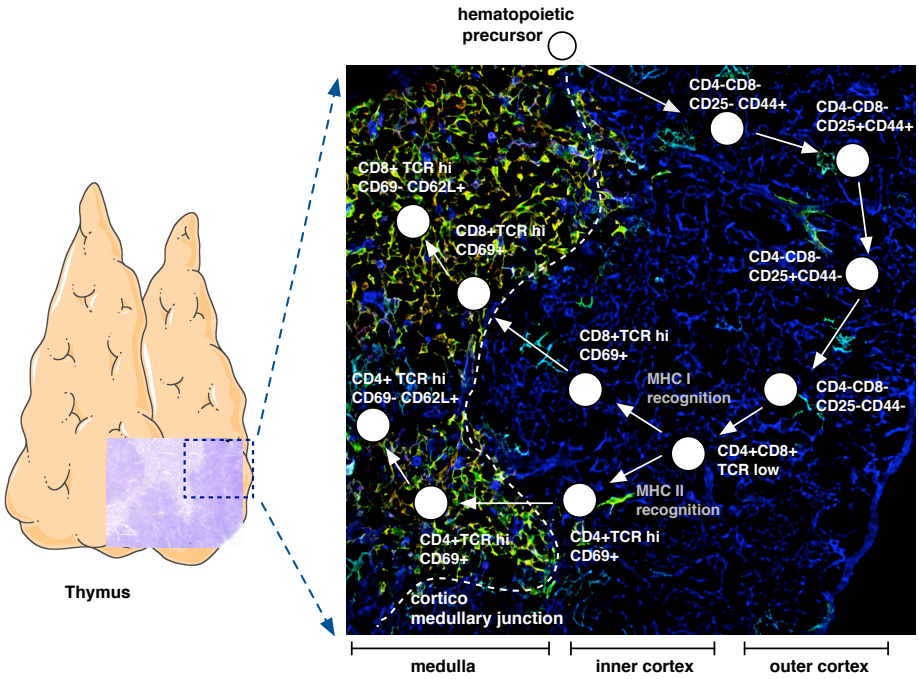

Figure 1.1: Anatomical microenvironment in the adult thymus; The thymus is a bilobed organ divided by mesenchymal septae. The two lobes are organized into discrete cortical and medullary areas, each of which is characterized by the presence of particular stromal cell types, as well as thymocyte precursors at defined maturational stages. Thymocyte differentiation can be followed phenotypically by the expression of cell-surface markers, including CD4, CD8, CD44, CD25, CD69 and CD62L, as well as the status of the T-cell receptor (TCR). Interactions between thymocytes and thymic stromal cells are known to be important in driving a complex program of T-cell maturation in the thymus, which ultimately results in the generation of self-tolerant $CD4^{pos}$ helper and $CD8^{pos}$ cytotoxic T-cells, which emigrate from the thymus to establish the peripheral T-cell pool. (TCR^{low}, expressing the TCR at low levels; TCR^{hi}, expressing the TCR at high levels.) *Adopted from Graham Anderson and Eric J. Jenkinson; Lymphostromal interactions in thymic development and function; Nature Reviews 2001*

ferentiation, which is marked by the loss of alternative lineage choices and the commitment to the T-cell lineage. During the first steps of development, the most immature thymocytes lack any expression of CD4, CD8 or CD3, and are therefore referred to as double negatives (DN) thymocytes. They undergo four distinct maturational stages, whereby each of them is characterized by the differential expression of CD44 and CD25. The earliest DN subpopulation is defined as DN1 (which includes also early thymic presursors; ETPs, which are marked by the expression Sca1), and is identified by the absence of CD25 and several lineage-associated markers (such as CD3, CD4, CD8, CD11b, CD11c, CD19, B220, F4/80, Ter119, Gr1, Nk1.1, Dx5, TCRα/β, TCRγ/δ) and expresses CD44 and high amounts of c-kit. These early thymocytes still bear the potential to develop into T-cells, dentritic cells (DC), macrophages and natural killer cells (NK), but lost their potential to differentiate to erythroid cells and megacaryoctes. In other words, they have not yet fully committed to the T-cell lineage. During their maturation, DN1 cells migrate from their site of entry, through the cortex in direction of the subcapsular region. During this journey, they transiently attain the DN2 phenotype (c-kit^{high}CD44^{pos}CD25^{pos}) and subsequently reach the DN3 stage (c-kit^{low}CD44^{neg}CD25^{pos}). At this stage, the recombinases activating genes RAG1 and 2 are expressed and catalyze the successful rearrangement of the β, γ and δ loci. In contrast to α/β T-cells, γ/δ T cells represent only a small subset of T-cells in the mature thymus. Further development and survival of thymocytes depends on signals mediated by the TCR. The TCR of DN3 thymocytes is composed of the rearranged β-chain, an invariant pre-TCR α-chain (pTα) and the CD3 complex (composed of four distinct chains; γ, δ, ϵ and ζ). Only successfully rearranged β-chains can be incorporated into the complete and functionally competent pre-TCR complex. The necessary signals required for survival and further developmental maturation and proliferation then emanate from this receptor. This event is referred to as β-selection and constitutes the first checkpoint in thymocyte development. Following β-selection, the cells become committed to the α/β lineage, start to rearrange the TCR α-chain, arrest the rearrangement of their β-chain, and attain the simultaneous expression of the co-receptors CD4 and CD8. Cells in this developmental stage are known as double positive (DP) cells and are now unresponsive to interleukin-7 (IL-7), which plays a critical role during the previous T-cell developmental stages (Fry and Mackall, 2005). These DP thymocytes represent the most abundant subset within the thymus (80% to 90%). At this and the following stages, thymocytes are subjected to distinct selection processes, leading to the death of more than 90% of the DP population. (Fig. 1.1).

Positive selection

In contrast to the TCR β chain, rearrangement of the TCR α locus is not arrested after productive rearrangement of one TCR α-chain. To terminate the TCR α locus rearrangement, a successful interaction of the TCR α/β with major histocompatibility (MHC) molecules is required, which leads to the selection of MHC-restricted TCRs (Borgulya et al., 1992; Brändle et al., 1992). The structure of the α locus facilitates multiple V/J recombination events on the same allele, resulting each time in the excision of the prior recombined DNA. This set-up allows for the testing of multiple TCR α gene rearrangements per cell, enhancing the production of useful thymocytes by increasing the frequency of positively selectable TCR α/β heterodimers (Petrie et al., 1993; Davodeau et al., 2001). However, the time for rearranging and testing functional TCR α/β complexes is short, as DP cells need to interact with MHC molecules within 3 to 4 days to receive the necessary survival signals. Consequently, cells that are not able to assemble a functionally competent MHC-restricted TCR will die by neglect.

There are two types of MHC molecules, termed MHC class I (MHCI) or MHC class II (MHCII). Developing T-cells will need to bind to either MHC class I or class II molecules to receive and transmit the aforementioned survival signal. In this process of TCR-mediated interaction of developing thymocytes with thymic stromal cells, the transmembrane proteins CD4 and CD8 play a decisive role. Their extracellular domains CD4 and CD8 are able to bind specifically to invariant determinants on MHC class II and MHC class I molecules, respectively, while their intracellular domains associate with the non-receptor protein tyrosine kinase Lck, which initiates TCR signal transduction when enzymatically activated (Doyle and Strominger, 1987; Norment et al., 1988; Shaw et al., 1989). As the co-receptors and the TCR are thought to bind to the same peptide-MHC complex, intracellular Lck is brought into close proximity with the cytosolic domains of the invariant CD3 chains associated with the engaged TCR. This consequently results in the initiation of signalling (Veillette et al., 1989b,a).

Positive selection is initiated in the cortex. This event is characterized by a sustained low-affinity engagement of the TCR with the self-peptide-MHC complex on the surface of cTEC. This interaction is only rarely successful, so that the survival of DP cells occur in 5% of these cells (Wilkinson et al., 1995; Starr et al., 2003). With positive selection, the decision to ultimately develop into either CD4 or CD8 single positive (SP) T-cells is determined. By means of TCR-transgenic mice, it was shown that CD4 or CD8 lineage commitment is defined by the MHC-restriction specificity of the respective TCR. DP thymocytes, which acquired a signal by MHCII-restricted TCRs differentiate into $CD4^{pos}$ T-cells, whereas DP thymocytes that interacted via MHC-I-restricted TCRs differentiate into $CD8^{pos}$ T-cells. However, down-regulation of CD4 or CD8 occurs asynchronously (Barthlott et al., 1997; Singer et al.,

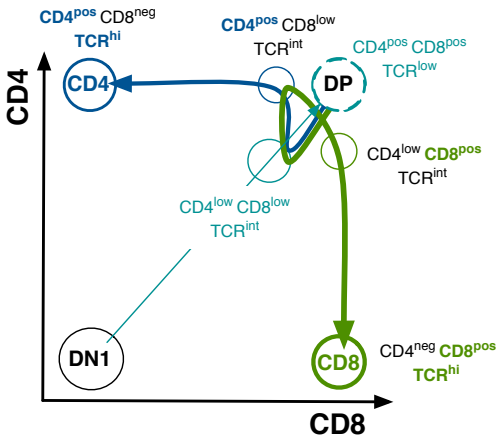

Figure 1.2: Maturation steps of late thymocytes; Developing thymocytes differ in their surface expression of the CD4 and CD8 co-receptor. Double negative (DN) cells differentiate into double positive ($CD4^{pos}CD8^{pos}$) DP thymocytes, which are the first cells to express a functional T-cell receptor (TCR). DP that are able to interact via their TCR with major histocompatibility (MHC) molecules undergo positive selection and become $CD4^{pos}CD8^{low}$ TCR^{int}. Thymocytes that have encountered MHCI molecules will further differentiate into CD8*pos*, cells that interacted with MHCII molecules differentiate into $CD4^{pos}$ mature thymocytes.

2008), resulting in a characteristic phenotype of developing SP according to their expression of CD4 or CD8 as depicted in Fig. 1.2. Distinct subsequent stages in the development of thymocytes can be identified using several cell surface markers, such as CD24, which is highly expressed in DP thymocytes, the early activation marker CD69, which gets rapidly induced after TCR interaction, and the surface expression of the TCR itself. The successful TCR-MHC-interaction also leads to the down regulation of RAG expression — precluding any further alternate TCR α/β configurations. Finally, the migration into the medulla occurs where the last steps in T-cell maturation are accomplished.

Negative selection

Medullary TEC attract positively selected thymocytes via expression of the chemokines Ccl21 and Ccl19, which are bound by Ccr7 on immature thymocytes following the engagement of their TCR with Peptide-MHC complexes expressed by cTEC (Ueno et al., 2004). The medulla is the primary site for the next selectional screening of the chosen TCR specificities known as negative selection. This process ensures that only thymocytes that express a TCR that binds self-peptide-antigen complexes with a low affinity can continue their maturation whereas all others undergo either lineage deviation (Derbinski et al., 2001) or apoptosis. To evaluate TCR affinity for self-peptides, positively selected thymocytes are exposed to divers self-antigens presented by mTEC and dendritic cells (DC). To achieve an almost complete coverage of self-antigens, mTEC use a unique epigenetic mechanism, termed promiscuous gene expression. This phenomenon is in part regulated by the expression of the autoimmune regulator AIRE and results in the low expression of genes, including so-called tissue-restricted self-antigens (TRAs) (Derbinski et al., 2005). This expression facilitates the preemptive elimination of T-cells that express potentially harmful TCR specificities.

Remarkably, the same receptor that provided the survival signal for positive selection decides also whether a cell gets negatively selected. The current model explaining this apparent paradox is based on the assumption that the affinity of the TCR for the peptide-MHC complexes defines the ultimate fate of the T-cell (Palmer and Naeher, 2009). In this context, cells that express intermediate affinity TCR and hence display autoreactivity evade negative selection and subsequent deletions as these cells can develop into FoxP3^{pos} regulatory T-cells (T_{reg}) (Picca et al., 2009; Klein and Jovanovic, 2011).

An impressive example for the importance of negative selection by self-antigens is the observation that the absence of thymic expression of a single retinal antigen is sufficient to trigger spontaneous eye-specific autoimmunity (DeVoss et al., 2006).

Thymocyte egress

Thymocytes susceptible to undergo negative selection are typically marked by the concomitant expression of the early activation markers CD69 and CD24 (Kishimoto and Sprent, 1997). As soon as CD69 is downregulated, engagement of the TCR results in the induction of proliferation identical to that of $T_{\text{naïve}}$ cells. With the loss of CD69, the spingosine-1-phosphate receptor 1 (S1P1) appears on the surface. This receptor binds spingosine-1-phosphate (S1P). Using an intravascular procedure to label emigrating cells, Zachariah et al. could demonstrate that mature thymocytes exit the thymus via blood vessels at the corticomedullary junction and that neural crest-derived pericytes, which typically ensheath blood vessels, are a main source for S1P (Zachariah and Cyster, 2010). The significance of S1P1 in thymocyte egress was demonstrated in mice whose haematopoietic cells either lack S1P1, or in mice where a S1P1 transgene is constitutively expressed by developing thymocytes (Matloubian et al., 2004; Zachariah and Cyster, 2010). S1P1-deficiency precludes the emigration of T-cells to the periphery, whereas transgenic overexpression of S1P1 under the control of the Lck proximal promotor lead to the precocious appearance of DP in blood, lymph nodes and spleen. The molecular mechanisms that lead to the expression of S1P1 are closely linked to the cessation of TCR signalling, which results in the termination of Akt-mediated phosphorylation of the transcription factor forehead box O (FOXO). Unphosphorylated FOXO can translocate into the nucleus, where it initiates krüppel-like factor 2 (KLF2)-mediated S1P1 expression.

1.3 Immune system and Metabolism

The development of immunopathologies is often directly linked to defects in genes encoding relevant components of the immune system (Maródi and

Notarangelo, 2007). There are, however, exceptions, where immunodeficiencies are caused by a defective factor that shows no obvious link to the immune system. For example, the absence of the enzyme adenosine deaminase (ADA), which is part of the purine salvage pathway, is one of the causes of a severe combined immunodeficiency disease (SCID). As ADA is involved in the breakdown of adenosine from food and the turnover of nucleic acids in cells, the deficiency of ADA results in the accumulation of purine metabolites, such as deoxyadenosine and deoxyadenosine phosphate (dATP), which induce the activation of an apoptotic cascade. Consequently, many cells fail to develop properly and undergo programmed cell death. Although ADA is expressed virtually in every cell, most of the effects caused by the lack of this enzyme are focussed on the immune system. The selective involvement of the immune system can be partly ascribed to the high rate of cell death following T-cell selection, which provides a constantly high intrathymic source of DNA that needs to be degraded (Carson et al., 1977). Therefore, in ADA-deficient patients the thymus is one of the primary organs affected, compromising proper T-cell development and function. The causal relation between ADA-deficiency and SCID was a completely unexpected finding and provided first evidences for the relevance of a metabolic compound for the function of the immune system.

Obviously, one can argue that cellular metabolism in general plays an essential role for any cell, and it is clear that specialized cellular functions are dependent on the availability of energy and/or the absence of toxic substrates. However, evidence is nowadays accumulating that immune cells may use metabolic pathways to control fate decisions and function in ways that are different from other cells. This interplay between immunological and metabolic processes is permanent, and in contrast to ADA-deficiency completely independent of any genetic defects. In this context, the field of the so-called "immune metabolism" has emerged to dissect the molecular mechanisms of the immunological-metabolic crosstalk.

It has been observed that obesity affects the immune system and promotes inflammation (Lumeng et al., 2007; Ouchi et al., 2011). Investigation of the involved mechanisms revealed that some molecules which are primarily known for sensing and responding to cellular nutrients also control fate switches of immune cells. mTOR is one of those metabolic sensors, that turned out to play a crucial role in the development and function of immune cells.

The following chapters address the link between mTOR and the organization and maintenance of a functional immune system.

1.4 mTOR

The discovery of the mTOR pathway began in the 1970s with the isolation of the macrolide antibiotic rapamycin from a soil sample taken from Easter Island (in Polynesian: "Rapa Nui" or navel of the world) that contained of the bacterium streptomyces hygroscopius. The role of rapamycin as a potent immunosuppressant was established over many years (Sabatini et al., 1994; Brown et al., 1994; Sabers et al., 1995) and included in 1991 the identification of the drug's substrate known as "mammalian (subsequently mechanistic) target of Rapamycin" (mTOR) by M. Hall and colleagues at the Biocentre Basel (Heitman et al., 1991). In the following years, rapamycin and the mTOR controlled pathway have gained central attention especially in the domains of oncology and immunology (Zhang et al., 2011; Gupta et al., 2012).
The mTOR protein is an evolutionally highly conserved 289-kDa serine-threonine kinase, which belongs to the phosphoinositide 3-kinase (PI3K)-related kinase family. Structurally, it consists of multiple Huntingtin, Elongation factor 3, Protein phosphatase 2EA, TOR1 (HEAT)-repeats at its N-terminal half followed by the FKBP12-rapamycin-binding and serine-threonine protein kinase domains near its C-terminal end (Fig. 1.3). The kinase activity is presently the only known enzymatic functions of mTOR. The mTOR protein forms two distinct multi-protein-complexes, termed mTOR complex 1 (mTORC1) and mTORC2. They differ in their upstream regulators, their downstream targets and the biological processes they control (Laplante and Sabatini, 2009).

1.4.1 mTORC1 - structure and components

mTORC1 consists of five proteins, with mTOR serving as the catalytic subunit of the complex. Two of the five proteins are unique for mTORC1, namely the regulatory-associated protein of mammalian target of rapamycin (raptor) (Hara et al., 2002; Kim et al., 2002) and proline-rich Akt substrate 40 kDa (PRAS40) (Sancak et al., 2007; Wang et al., 2007; Vander Haar et al., 2007), whereas mTOR itself and three additional proteins are also components of mTORC2.

Raptor is a 150 kDa protein that contains a conserved region in its N-terminal half, three HEAT repeats and seven WD-40 repeats (characterized by two terminal amino acids Tryptophan and Aspartic acid) near the C-terminus. Both, HEAT- and WD-40 repeats form curlicue-like structures that serve either as flexible (HEAT), or as rigid scaffold (WD 40) on which proteins bind and interact. Due to its structure, raptor has been thought to function as an adaptor molecule, regulating mTORC1 activity by recruiting substrates. The association of raptor to mTOR is sensitive to the presence of rapamycin and the nutritional status (Kim et al., 2002).

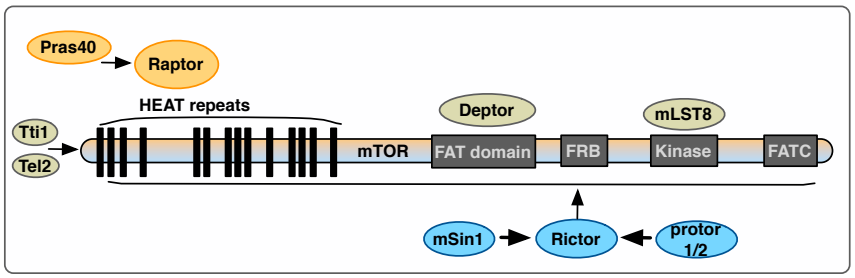

Figure 1.3: mTOR components; Scheme of mTORC1 and mTORC2 binding partners. In yellow: proteins unique for mTORC1, in blue: mTORC2-specific protein, in green: elements of both mTOR complexes. **The following abbreviations were used:** Pras40: proline-rich Akt substrate 40 kDa; Raptor: regulatory-associated protein of mammalian target of rapamycin; Deptor: DEP domain containing mTOR-interacting protein; mLST8: mammalian lethal with sec-13 protein 8; mSIN1: mamalian stress-activated protein kinase (SAPK)-interacting protein 1; Rictor: rapamycin insensitive companion of mTOR; Protor 1/2: protein observed with Rictor 1/2; HEAT repeats: Huntingtin, Elongation factor 3, Protein phosphatase 2 EA, TOR1 repeats; FAT domain: FRAP-ATM-TTRAP domain; FRB domain: FKBP12-rapamycin binding domain; FATC domain: FAT-C-terminal domain; *Adapted from Laplante and Sabatini, Cell 2012*

Raptor can be phosphorylated at multiple sites, by mTOR itself (Wang et al., 2009; Foster et al., 2010), the ribosomal S6 kinase (Rsk1/2) (Carrière et al., 2008; Roux et al., 2004), or the extracellular-signal-regulated kinase (ERK) (Foster et al., 2010; Langlais et al., 2011; Carriere et al., 2011), which typically enhances mTORC1 activity. During mitosis, raptor is hyperphosphorylated (Ramírez-Valle et al., 2010), promoting mRNA translation by internal ribosome entry sites (IRES). This hyperphosphorylation is blocked by inhibitors of the cell division control protein 2 homolog (Cdc2) or glycogen synthase kinase (GSK3) pathways. Other factors that negatively regulate mTORC1 signalling via modification of raptor are 5' AMP-activated protein kinase (AMPK) (Gwinn et al., 2008), and the autophagy associated Serine/threonine-protein kinase ULK1 (Dunlop et al., 2011). These examples show that mTORC1 activity can be modulated by several pathways, which all involve phosphorylation of raptor. Similar to the ablation of mTOR, the knockout of raptor is embryonic lethal (Guertin et al., 2006).

PRAS40 is a crucial mediator of Akt signalling towards mTOR (Vander Haar et al., 2007). PRAS40 interaction with mTOR is induced under conditions that inhibit mTOR signalling, such as nutrient or serum deprivation or mitochondrial metabolic inhibition (Vander Haar et al., 2007). PRAS40 binds the mTORC1 via raptor and regulates mTORC1 activity by functioning as a direct inhibitor of substrate binding. Following Akt activation by Insulin, PRAS40 is phosphorylated at Thr 246 which results in its dissociation from mTORC1 and the relieve of its constraints on mTORC1 activity (Sancak et al., 2007; Vander Haar et al., 2007). The components that are shared by mTORC1 and mTORC2 are mammalian lethal with sec-13 protein 8 (mLST8, also known as GβL) (Jacinto et al., 2004; Kim et al.,

2003), DEP domain containing mTOR-interacting protein (DEPTOR) (Peterson et al., 2009), and the Tti1/Tel2 complex (Kaizuka et al., 2010). Analysis of mLST8 domain organization has revealed that it consists of seven WD domains which form a β propeller. This structure is typically related to protein-protein interactions. Indeed, studies in mLST8 knockout mice have provided evidence that mLST8 is required to maintain the Rictor-mTOR interaction, but is dispensable for raptor-mTOR interaction (Guertin et al., 2006). The exact function of the other mTOR-interacting proteins is still not well defined and requires further investigations.

Upstream regulators of mTORC1

mTORC1 integrates a variety of upstream signals in order to coordinate the metabolic switches from a catabol to an anabol status and vice versa as a consequence of the respective nutritional conditions. To react to changing metabolic states, mTORC1 is receptive to divers intra- and extracellular cues, such as levels of growth factors, energy, oxygen, and amino acids (Fig. 1.4). The high number of upstream regulators provides diverse information input about the local and global energy availability in the organism. Based on these environmental leads, mTORC1 initiates central anabol metabolic processes including ribosomal biogenesis, initiation of translation or lipid synthesis whilst inhibiting at the same time catabol activities, such as autophagy. One of the key upstream regulators of mTORC1 is the heterodimer tuberous sclerosis 1 (TSC1, also known as harmatin) and TSC2 (also known as tuberin) which functions as GTPase-activating proteins (GAP) for the Ras homolog enriched in brain (Rheb) GTPase. When bound to GTP, Rheb positively regulates mTORC1 by stimulating its kinase activity (Long et al., 2005). However, functioning as GTPase, TSC1/TSC2 can convert Rheb into its inactive GDP-bound state, thus inhibiting mTORC1 activity (Inoki et al., 2003b).

Most of the mTORC1 upstream signals act on TSC1/TSC2, which consequently either inhibits or enables mTORC1 activity. Growth factors, such as Insulin and Insulin-like growth factor 1 (IGF1) induce the phosphorylation of TSC1 and TSC2 via activation of the PI3K and Ras controlled pathways and the subsequent release of effector kinases (e. g. kinase B (Akt/PKB), extracellular-signal-regulated kinase 1/2 (ERK1/2), and ribosomal S6 kinase (RSK1)). Phosphorylation of TSC1/TSC2 abrogates its capacity to inhibit mTOR (Inoki et al., 2002; Roux et al., 2004; Jaeschke et al., 2002). In a similar way, proinflammatory cytokines, e.g. tumor necrosis factor α (TNFα), initiate the phosphorylation of TSC1 and therefore trigger the inactivation of the TSC1/TSC2 complex (Lee et al., 2007). Stimulation of Akt activates mTORC1 through interaction with the TSC1/TSC2 complex and the mTORC1 inhibitor PRAS40 (Wang et al., 2007; Sancak et al., 2007; Vander Haar et al., 2007; Thedieck et al., 2007). Finally, also signalling via the

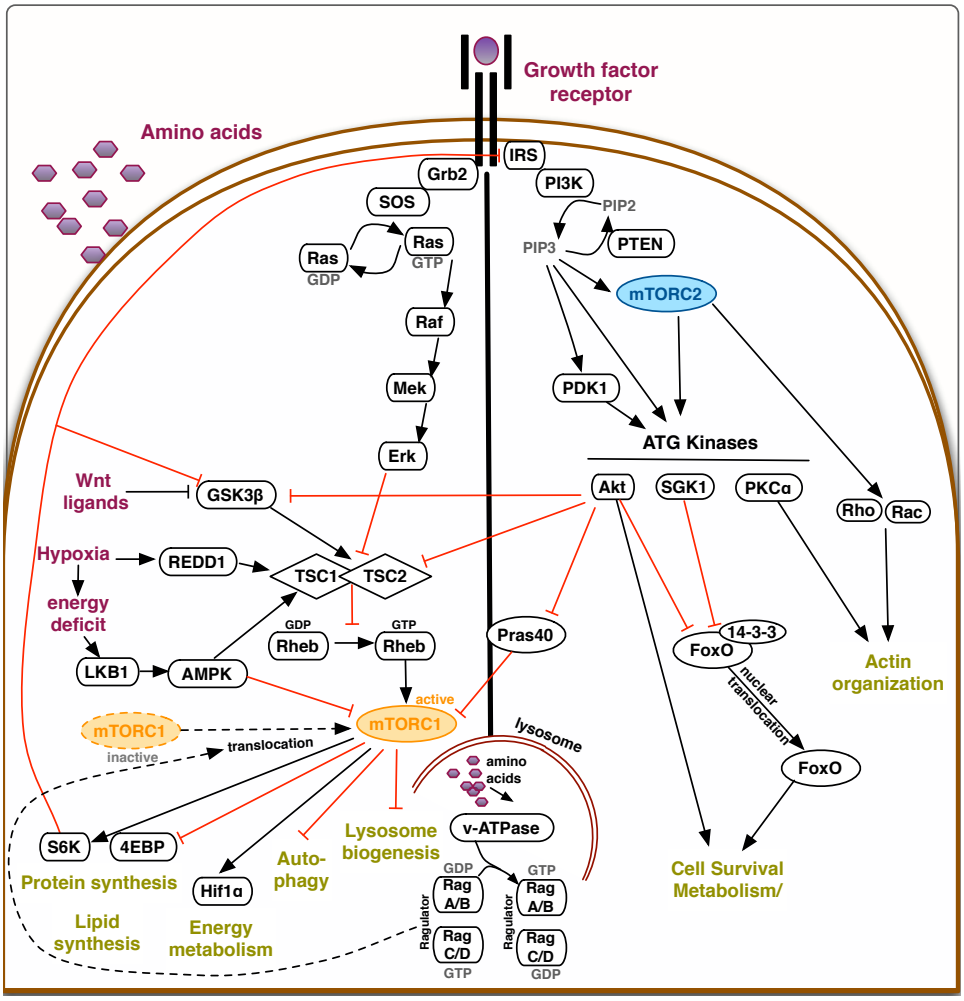

Figure 1.4: The mTOR Signalling Pathway; The main signalling nodes that regulate mTORC1 (on the right) and mTORC2 (on the left). Essential inputs regulating mTOR- signalling include amino acids, growth factors, energy, and oxygen. Active mTORC1 promotes protein synthesis, lipogenesis, and energy metabolism, whereas it inhibits autophagy and lysosome biogenesis. In contrast, mTORC2 is activated by growth factors and regulates actin organization and cell survival/metabolism. In this figure, environmental leads are depicted in violet, and the main downstream effects of mTOR signalling in green. **The following abbreviations are used:** Grb2: growth factor receptor-bound protein, SOS: son of sevenless, Ras: RAt Sarcoma, IRS: insulin receptor substrate, phosphoinositide 3-kinase, GDP: guanosin disphosphate; GTP: guanosin triphosphate, PIP2: phosphatidylinositol (4,5)-biphosphate PIP3: phosphatidylinositol (3,4,5)-triphosphate, PTEN: phosphatase and tensin homologue, Raf: rapidly accelerated Fibrosarcoma, Mek: mitogen-activated protein kinase kinase, Erk: extracellular signal-regulated kinases, GSK3β: glycogen synthase kinase 3β, TSC1/2: tuberous sclerosis complex 1/2, Rheb: Ras homolog enriched in brain, AMPK: AMP-activated protein kinase, Pras40: proline-rich Akt/PKB substrate 40kDa, PDK1: phosphoinositide-dependent kinase 1, SGK1: serum/glucocorticoid regulated kinase 1, PKCα: protein kinase Cα, FoxO: forkhead box O, S6K: ribosomal S6 kinase, 4EBP: 4E-binding protein, Hif1α: Hypoxia-inducible factor 1-α. *Adapted from Laplante and Sabatini, Cell 2012*

canonical Wnt pathway activates mTORC1 via inhibition of the glycogen synthase kinase 3β (GSKβ), which usually promotes TSC2-activity (Inoki et al., 2006).

The availability of energy to a cell is gauged by the level of Adenosine-monophosphate-activated protein kinase (AMPK) activity. Low energy levels or hypoxia activate AMPK by increasing intracellular AMP/ATP levels (Hardie et al., 1998). AMPK can directly phosphorylate TSC in a way that enhances its GAP activity towards Rheb and inhibits mTORC1 (Inoki et al., 2003a). AMPK also communicates directly with mTORC1 through phosphorylation of raptor, leading to the allosteric inhibition of mTORC1 (Gwinn et al., 2008).

The presence of amino acids — amongst them in particular leucin and arginin — play a very decisive role in the activation of mTORC1 signalling. Indeed, mTORC1 is activated by amino acids, which are a prerequisite for the responsiveness to any upstream signal (Blommaart et al., 1995; Hara et al., 1998).

The mechanism which guarantees that mTORC1 is only activated in the presence of amino acids, depends on TSC1/TSC2 and requires Rag GTPases, which are members of the Ras-family of GTP-binding proteins (Kim et al., 2008; Sancak et al., 2008) and a multisubunit complex, called Ragulator (Sancak et al., 2010). Mammals express four Rag proteins — RagA, RagB, RagC, and RagD — that form heterodimers consisting of RagA or RagB with RagC or RagD. RagA and RagB, like RagC and RagD, are highly similar to each other and are functionally redundant (Schürmann et al., 1995; Hirose et al., 1998; Sekiguchi et al., 2001). Under amino acid-rich conditions, RagA and RagB form GTP-loaded heterodimers, which are able to interact with raptor. This interaction results in the translocation of mTORC1 from a yet not well-defined position within the cytoplasm to the lysosomal surface, where the complete complex is then activated. A current model explaining the correlation between mTORC1 translocation and activation indicates that mTORC1 binds to and interacts with lysosomal membrane-bound Rheb (Sancak et al., 2010). However, it remains unknown why mTORC1 translocates specifically to lysosomes, since Rheb is also found on other endomembranes.

Downstream effects of mTORC1

mTORC1 is a positive regulator of cellular proliferation and growth as it promotes various anabolic processes that result in the biogenesis of proteins, lipids and organelles but at the same time limits catabolic processes.

The best described mTORC1 targets are the eukaryotic initiation factor 4E (eIF4E)-binding protein 1 (4E-BP1) and the p70 ribosomal S6 kinase 1 (S6K1) (Ma and Blenis, 2009). Both are involved in protein synthesis. Through phosphorylation of 4E-BP1, mTORC1 prevents its binding

to the cap-binding protein elongation factor 4E (elF4E). Unbound elF4E associates with elF4G to form the elF4E complex, which in turn is required for the initiation of cap-dependent translation (Hay and Sonenberg, 2004). Phosphorylated S6K also acts on the formation of the translation initiation complex by phosphorylating eIF4B and the ribosomal protein S6 (Raught et al., 2004), resulting in increased mRNA biogenesis and translational initiation and elongation. Raptor plays an important role for the interactions of mTORC1 with S6K and 4E-BP1, as it mediates via a so-called TOR signalling (TOS) motif the efficient and specific binding to a conserved 5 amino acid sequence in the N-terminal region of S6K and the C-terminal region of 4E-BP1(Nojima et al., 2003).

mTORC1 is also involved in the synthesis of lipids (reviewed in Laplante and Sabatini (2009)). For example, mTORC1 positively regulates the activity of the two transcription factors sterol regulatory elementbinding protein 1 (SREBP1) (Porstmann et al., 2009) and peroxisome proliferator-activated receptor-γ (PPARγ), which control the expression of factors that play a major role in the homeostasis of lipids and cholesterol (Kim and Chen, 2004).

Mitochondrial gene expression and oxygen consumption are also regulated by mTORC1 via (i) the transcriptional activity of the nuclear cofactor PPARγ coactivator 1(PGC1-α) and (ii) the association with the transcription factor yin-yang 1 (YY1) (Cunningham et al., 2007).

mTORC1 also inhibits autophagy to promote growth via the phosphorylation and hence suppression of ULK1/Atg13/FIP200 complex (unc-51-like kinase 1/mammalian autophagy- related gene 13/focal adhesion kinase family-interacting protein of 200 kDa) (Ganley et al., 2009; Hosokawa et al., 2009; Jung et al., 2009).

Moreover, mTORC1 negatively regulates the formation of lysosomes, which further contributes to the impairment of autophagy as their fusion to autophagosomes is hindered. This inhibition is effected via phosphorylation of the transcription factor EB (TFEB), which is then prevented to translocate to the nucleus and to control transcription of key factors in lysosomal function (Settembre et al., 2012). Furthermore, the use of quantitative phosphoproteomics revealed that mTORC1 stimulates de novo synthesis of pyrimidines and the progression through the S phase of cell cycle (Robitaille et al., 2013).

Together, these findings underscore the significance of mTORC1 signalling, as it controls a remarkably high number of major cellular processes.

1.4.2 mTORC2 — structure and components

The mTORC2 pathway is in contrast to mTORC1 less well described. Initially it was thought that mTORC2 was insensitive to exposure to rapamycin, as acute treatment with the macrolid failed to perturb mTORC2 signalling. However, long term exposure to rapamycin reduces nonetheless

mTORC2 signalling in some cell types via the suppression of its assembly (Sarbassov et al., 2006), though it still remains unclear why this longterm effect is cell type specific.

As already mentioned, mTORC1 and mTORC2 share mTOR, mLST8, DEPTOR and the Tti1/Tel2 complex (Fig. 1.3). The complex's unique components are the rapamycin insensitive companion of mTOR (rictor) (Sarbassov et al., 2004; Jacinto et al., 2004), mammalian stress-activated map-kinase interacting protein 1 (mSin1) (Jacinto et al., 2006; Frias et al., 2006) and protein observed with rictor 1 and 2 (protor 1 and 2) (Thedieck et al., 2007; Pearce et al., 2011).

Rictor has the ability to physically interact with the two other mTORC2-specific components, mSin 1 and Protor 1, to form a stable structure (Jacinto et al., 2006). Rictor lacks known common motifs but contains a C-terminus that is conserved among vertebrates. Functionally, rictor may act as a scaffold protein to mediate integrin-linked kinase activities (McDonald et al., 2008). The rictor-mTOR complex directly phosphorylates Akt/PKB on Ser 473 *in vitro* and facilitates Thr 308 phosphorylation by PDK1(Sarbassov et al., 2004). Furthermore, insulin signalling to FoxO requires rictor and mLST8 (Guertin et al., 2006). Via the mTORC1/S6K1-dependent phosphorylation of rictor at threonine 1135, mTORC2 and Akt signalling can be inhibited (Julien et al., 2010).

mSin1 contains a Ras binding domain (RBD), and a pleckstrin homology (PH) domain that is likely to interact with phospholipids. It functions as a scaffold protein, which regulates the assembly of mTORC2 and its interaction with the serum/glucocorticoid-induced protein kinase 1 (SGK 1), which is a key regulator of ion and solute transport processes in mammalian epithelia (Lu et al., 2011). Similarly, protor 1 also increases the mTORC2 mediated activation of SGK 1 (Pearce et al., 2007).

Together, Rictor and mSin1 are responsible for the integrity of mTORC2 and play a key role in Akt phosphorylation and signalling (Jacinto et al., 2006; Frias et al., 2006; Guertin et al., 2006).

Upstream regulators of mTORC2

Several regulators have been identified that are positioned upstream of mTORC2 and control its activity (Fig. 1.4). mTORC2 is activated by growth factors such as insulin, but is insensitive to amino acids. Activated mTORC2 binds to ribosomes in a fashion that is promoted by insulin-stimulated PI3K signalling (Zinzalla et al., 2011). Since ribosomal biogenesis is regulated by mTORC1, both mTOR complexes cooperate in the context of protein synthesis.

Downstream effects of mTORC2

mTORC2 controls cell survival, metabolism and cytoskeletal organization by phosphorylation of protein kinases belonging to the protein kinase A, C and G families (summarized as ACG kinases), including Akt, SGK1, and the protein kinase C α (PKCα) (Yan et al., 2008; Zoncu et al., 2011). Akt is a vital controller of survival, apoptosis, proliferation and growth through its capacity to phosphorylate divers targets. To be completely activated, Akt requires the phosphorylation of its Thr308, mediated by PDK1 and Ser473 by mTORC2. However ablation of several mTORC2 components showed that lack of Akt phosphorylation at Ser473 did not impair the phosphorylation of several Akt targets, such as TSC2 and Glykogen synthase kinase 3 β (GSK3β), suggesting that defective Ser473 phosphorylation determines rather the specificity of Akt than its activity (Guertin et al., 2006; Jacinto et al., 2006). The only target affected by Akt bearing an impaired Ser473 phosphorylation was the forkhead box O1/3a (FoxO1/3a), a transcription factor that is negatively regulated by this kinase. FoxO1/3a controls in a tissue-dependent manner various target genes involved in metabolism, cell cycle arrest, apoptosis and cell death.

SGK1 is another downstream target of mTORC2 important for the activation of ion channels (Alessi et al., 2009), and is implicated in cancer cell growth and survival (Dehner et al., 2008; Yan et al., 2008). SGK 1 shows overlap in substrate specificities with Akt.

Selective deletion of mTORC2 elements in cultured cells also revealed its involvement in actin cytoskeleton organization, through impaired activation of PKCα and Rho-GTPases (Sarbassov et al., 2004; Jacinto et al., 2004). Thus, actin polymerization and cell spreading are disturbed following the inhibition of mTORC2.

1.4.3 The role of mTOR in the Immunesystem

mTOR regulates immune cell proliferation

In medicine, mTOR has first gained attention as a target for immunosupression, since its allosteric inhibition through rapamycin was found to decrease IgE production and to protect against experimental autoimmune encephalitis and adjuvant arthritis (Martel et al., 1977). However, rapamycin only received serious consideration as an immunosuppressive drug years later, when its ability to efficiently prevent T- and B-cell proliferation was discovered (Kay et al., 1991). Similar to the structurally related macrolid FK506, rapamycin forms a complex with FK506 binding protein (FKBP12), an immunophilin, and thus exerts its immunosuppressive potential. Whereas FK506 modulates immune responses via the inhibition of calcineurin-induced IL-2 production, rapamycin-FKBP12 interferes with the IL2-stimulated activation of mTOR. Consequently, cell cycle progres-

sion of T-cells is blocked at the transition from G1 to S phase precluding the biological effect of IL-2. (Kuo et al., 1992; Abraham, 1998).

mTOR influences immune function

mTOR plays a critical role as a regulator of immune function and in T-cell differentiation, because of its ability to sense and integrate cues from the immune environment, such as the presence of IL-2, PD-1, CTL-4 or skewing cytokines (reviewed in Delgoffe and Powell (2009)). The differentiation of T- and B-cells into specialized effector and memory cells each requires specific metabolic conditions in keeping with the individual lymphocyte functions expected to be exercised. Thus, it is conducive to have a mechanism in place that senses the availability of nutrients and immune-costimulatory molecules to direct lymphocyte's fate.

Under physiological conditions, the presence of nutrients, energy and oxygen direct T-cell differentiation via facilitating mTOR signalling (Frauwirth and Thompson, 2004). Naive T-cells reside typically in a catabolic state with low levels of mTOR activity. Upon TCR activation, their metabolism is switched from a cata- to anabolic state to meet the high metabolic requirements of an effector T-cell. This switch is controlled by active mTOR, and is a prerequisite for correct T-cell differentiation.

Indeed, studies in mice with T-cell-specific deletions of the central mTOR complex components have revealed the importance of this complex in the regulation of T helper cell differentiation. For example, T-cells lacking the expression of the mTOR activator Rheb are not able to differentiate into Th1 or Th17 cells under polarizing conditions (Delgoffe et al., 2011). This failure is closely linked to a decrease in signal transducer and activator of transcription (STAT) 3 and STAT 4 activation as well as in the expression of the lineage-specific transcriptions factors T-bet (for Th1 cells) and RORγt (for Th17 cells). In contrast, studies on T-cells lacking mTORC2 signalling secondary to the ablation of rictor revealed a limited Protein kinase C 3 (PKC 3) activity as well as a reduced Trans-acting T-cell-specific transcription factor 3 (GATA-3) expression, which rendered the cells incapable of differentiating into Th2 cells under appropriate polarizing conditions (Delgoffe et al., 2011; Lee et al., 2010). Finally, T-cell-specific inhibition of both mTORC1 and mTORC2 increases SMAD3 following T-cell stimulation, leading to the upregulation of the transcription factor FoxP3 and subsequently to the generation of regulatory T-cells.(Delgoffe et al., 2011; Sauer et al., 2008; Merkenschlager and von Boehmer, 2010; Haxhinasto et al., 2008; Delgoffe et al., 2009). Moreover, the absence of mTOR promotes the differentiation of CD8 ^{pos} memory T-cells (Araki et al., 2009). Finally, mTORC1 regulates cell migration by suppressing the synthesis of both chemokines and cell-adhesion molecules, such as Ccr7 and CD62L (Sinclair et al., 2008), and by promoting the effector function of CD8^{pos} T-cells by in turn facilitat-

ing the expression of the pro-inflammatory cytokine receptor C-X-C motif receptor 3 (CXCR3) (Rao et al., 2010).

In summary, these data do not only underscore the general importance of mTOR in directing T-cell fate but also reflect the individual impact of mTORC1 and mTORC2 on the immune system.

In addition to its impact on T-cells, mTOR also influences B-cell differentiation and function. In mTOR hypomorph mice (Zhang et al., 2011), a partial block in the transition of large pre-B to small pre-B-cell stages is manifest. For cells that reached the periphery, however, an increased frequency in mature B cells and a concomitant decrease in transitional and marginal zone cells was observed.

mTOR is also involved in the cellular maturation and homeostasis of dendritic cells (DC) via engagement of Flt3-singaling (Sathaliyawala et al., 2010).

Finally, mTOR signalling has also been associated with the regulation of the innate immune response. Rapamycin-mediated mTOR inhibition promotes the release of pro-inflammatory cytokines, such as IL-12, IL-23, and IL6 in phagocytes following bacterial infection or exposure to lipopolysaccharide (LPS) and leads to reduced synthesis of IL-10 and other anti-inflammatory cytokines (Weichhart et al., 2008). In contrast, functional mTOR signalling limits the production of pro-inflammatory cytokines by inhibition of nuclear factor κ B (NFκB), whereas IL-10 production is promoted via the activation of STAT3.

Although the significance of the mTOR pathway has been well characterized for primary immune cells of the innate and the adaptive immune system, like phagocytes, T-cells, B-cells or dendritic cells, no study has focussed yet on the role of the mTOR pathway for the function of a primary lymphoid organ, such as the thymus.

1.5 Aim of the study

The mTOR pathway has gained increasing importance in biology and medicine since its discovery in the 1980s. Being target of the macrolid antibiotic rapamycin, its significance for the immune system became evident already very early. Initially, mTOR's immun-modulating properties have been ascribed to the fact that mTOR functions as a key regulator of cellular proliferation — and thus immune cell proliferation —, but later it became apparent that mTOR is involved in a much broader context in the physiology of every cell. Functioning as a link between metabolic demands and cellular function, mTOR senses environmental cues, and regulates cellular differentiation and homeostasis. However, most studies performed so far focussed on the role of the mTOR pathway or its inhibition in primary immune cells. To extend this focus to cells which are not of lymphoid origin themselves but

responsible for the maturation of competent immune cells, I investigated the immunological role of mTOR for the thymic epithelium. This study seeks to determine mTOR's relevance for the development and maintenance of TEC and to interrogate its influence on the distinct functions of cTEC and mTEC during precursor attraction and thymocyte selection and maturation. Through the generation of mice that are deficient for selective components of the mTOR pathway in the thymic epithelium, it has been possible to analyse the direct consequences of mTOR inhibition on the thymic epithelium as well as the indirect effects on the development and maturation of functional T-cells.

Chapter 2

Materials and Methods

2.1 Mouse model and manipulations

2.1.1 Mice

Mice homozygous for LoxP-sites flanking either Raptor exon 6 (Raptor$^{lox/lox}$), Rictor exon 4 and 5 (Rictor$^{lox/lox}$), or Raptor and Rictor (Raptor$^{lox/lox}$ Rictor$^{lox/lox}$) have been bred to transgenic mice expressing Cre recombinase under the control of Foxn1 regulatory elements as described in the sections 3.1 -3.1.3 . Unless otherwise noted, mice were used between 4 and 15 weeks of age. To define embryonic age, the day of the vaginal plug was designated as E0. Mice were housed at the Center for Biomedicines animal facility and at RCC Laboratory Animal Service, Füllinsdorf. Mice were kept and handled according to cantonal and federal regulations and permissions.

2.1.2 Time mating

For timed pregnancies one male and two females were separated in the same cage for 2 days using a grid to prevent uncontrolled mating. After 48h the grid was removed at 17h00. After 15h males were separated and females were checked for vaginal plugs. Plug positive females were assumed to be at gestational age 0 days.

2.1.3 Genotyping

Isolation of DNA

For isolation of genomic DNA, biopsies were digested in 500ml lysis buffer supplemented with Proteinase K (con$_{final}$): 100μg/ml) and incubated for at least 2 hours at 55C°.

Reaction Mix

Per reaction the following mix was used:
10ng DNA
2.5 μl 10X buffer (Sigma-Aldrich)
0.5 μl Primer (fw) at 5 μM
0.5 μl Primer (rv) at 5 μM
2.5 μl dNTPs at 10 μM (Sigma-Aldrich)
0.1 μl Taq Polymerase (5 U/μl) (Sigma-Aldrich)
add H_2O to 25 μl (5 Prime)

Primer

The following primer pairs were used on genomic DNA:
Foxn1Cre:
(fw) TCTGATGAAGTCAGGAAGAACC;
(rv) GAGATGTCCTTCACTCTGATTC
Raptor deletion on gDNA:
(fw) ATGGTAGCAGGCACACTCTTCATG;
(rv) CTCAGAGAACTGCAGTGCTGAAGG

Primer used for qPCR are listed in section 2.5.2.

Cycle conditions for PCR amplification

PCR amplification was performed on Mastercycler (Eppendorf)
94°C 5 min initially, followed by 33 cycles of:
94°C 30 s
58°C 45 s
72°C 1 min
72°C 10 min
hold at 12°C

Agarose gel electrophoresis

10μl of PCR product were mixed with 1μl of loading dye including RedSafe (Biotium) and loaded on a 2% agarose gel, prepared with TAE buffer to run for 30 min at 75V. 2μl of a ready-load 1Kb plus DNA ladder (Invitrogen) was used as a standard to determine the size of the PCR product. Pictures were captured on Gel Doc XR (bioRad) and analysed with Quality One 4.6.2 software from Bio-Rad.

2.2 Reagents

2.2.1 Buffer/Media

PBS sterile

Mili-Q Water + Dulbeco's phosphate buffered saline powder (Sigma) without $CaCl_2$ and $MgCl_2$. Filter sterilized (0.22μm cellulose acetate, bottle top filtered, Coroning, NY, USA)

HBSS

500 ml (Gibco-BRL) without $CaCl_2$ and $MgCl_2$

FACS buffer

PBS (Sigma-Aldrich) +2% FCS (Perbio)

IMDM medium

IMDM (Gibco-BRL, Gaithersburg, USA) + 10% FCS (Perbio) + 0.5 ml β Mercaptoethanol (50MM, Gibco-BRL) + 5 ml Kanamycin sulfate (Gibco-BRL)

Digest solution

FACS buffer + Collagenase/Dispase (of 1mg/ml con_{final}; Roche Diagnostics) + DNasae (20 μg/ml con_{final}; Roche).

Tail lysis buffer

10 ml 1M Tris pH 8.5 (100 mM con_{final})
1 ml 0.5M Na EDTA (5 mM con_{final})
1 ml 20% SDS (0.2% con_{final})
4 ml 5M NaCl (200 mM con_{final})
add 100 ml H_2O

6x Loading buffer

0.25% Bromophenol blue (Fluka, Buchs, Switzerland)
0.25% Xylene cynol FF (Fluka)
15% Ficoll (Type 400; Sigma)
add 50 ml ddH2O

DNA ladder

Ready-load 1Kb Plus DNA ladder (Invitrogen)

50x TAE

242 g Trizmabase (Sigma)
57.1 ml Glacial Acetic Acid (Fluka)
100 ml EDTA (0.5 M, pH 8.0; Sigma)
add ddH_2O up to 1 l

2.2.2 Antibodies used for flow cytometry

Antibodies used for immunohistochemistry are listed in section 2.4.6. The following antibodies were used for flow cytometric detection of intra- and extracellular antigens:
FITC: CD24 (M1/69; BioLegend), CD25 (PC61; BioLegend), CD4 (GK 1.5; BioLegend), CD45 (30-F11; BioLegend), CD62L (Mel-14; BioLegend), CD8 α (53-6.7; BioLegend), TCR Vβ TCR KIT (Becton Dickinson, Pharmingen), Ulex Europaeus Agglutinin (Vector Laboratories), CD40 (HM40-3; ebioscience), β-catenin (Becton Dickinson, Pharmingen)
PE: CD24 (M1/69; ebioscience), CD4 (GK 1.5; BioLegend), TCR α/β(H57-597; BioLegend), Ly51 (6C3; BioLegend), CD45 5.1 (A20; BioLegend), CD44 (IM7; BioLegend), FoxP3 (FJK-16s; ebioscience)
PECy7: CD62L (Mel-114; BioLegend), CD69 (H1.2F3; BioLegend), Nk1.1 (PK136 ; BioLegend), EpCAM (G8.8; BioLegend)
Cy5: UEA1 (Lectin; selfmade by K. Hafen), AIRE (5H11; selfmade by K. Hafen)
APC: CD117 (c-kit) (2B8; BioLegend), CD103 (2E7; BioLegend)
Alexa647: EpCAM (G8.8; BioLegend), CD3 (KT3; selfmade by K. Hafen)
APCCy7: CD4 (W3/25 ;BioLegend), I-A/I-E (M5/114.1; BD Biosciences)
Alexa700: CD8 α (53-6.7; BioLegend), CD45 (30-F11; BioLegend)
Biotin: CD3 (KT3; selfmade by K. Hafen), CD4 (GK 1.5; selfmade by K. Hafen), CD8α (53-6.7; BioLegend), CD11b (M1/70; BioLegend), CD11c (N418; BioLegend), B220 (Ra3-6B2; BioLegend), CD19 (ID3; selfmade by K. Hafen), CD45 (M1/9.3.4.HL2; selfmade by K. Hafen), EpCAM (G8.8; selfmade by K. Hafen), TCR gamma/delta; (GL3; ebioscience), F4/80 (BM4; BioLegend)
Strepavidin: APCCy7 (BioLegend), PerCPCy5.5 (BioLegend), PE-Texas Red (Molecular Probes), PECy7 (BioLegend)
PerCPcy5.5: CD25 (PC61; BioLegend), CD45 (A20; BioLegend)
PE-Texas Red: CD19 (6D5; Molecular Probes)
Unlabelled: Rat monoclonal α-mouse EDG (S1P1) IgG, Rabbit polyclonal α-human Raptor IgG A300-506 A (Bethyl Laboratories, Inc), Rabbit polyclonal α-human Raptor IgG A300-553 A (Bethyl Laboratories, Inc), Rabbit polyclonal α-mouse Raptor IgG (Abcam plc), Mouse monoclonal α-mouse Raptor IgG (Merck Millipore), Rabbit monoclonal α-human Raptor IgG (OriGene)

2.3 Cell isolation and flow cytometry

Characterization of cells by flow cytometry required the application of different isolation procedures, depending on the cellular size and the intended staining.

2.3.1 Isolation of thymocytes

To obtain thymocytes, thymi were roughly cleaned from adherent fat and connective tissue and placed between a folded piece of 40 μm gauze mesh. The fully covered thymus was subsequently gently squeezed between both mesh layers with the help of bent forceps until all thymocytes were released. Residues of cells were cleaned from the meshes through several rinsing steps using PBS 2% FCS.

2.3.2 Isolation of lymphocytes and splenocytes

Lymphocytes and splenocytes were isolated similarly as described in section 2.3.1. Unless otherwise stated, the following lymphnodes were used: axillary, brachial, inguinal, mesenteric, para-aortic, iliacal.

2.3.3 Isolation of thymic stromal cells

Due to their cell size a different technique for the isolation of TEC was performed. After removing the thymus from the thorax and cleaning of the residues of fat and connective tissue, thymi were incubated 3 times for 15 min at 37°C in HBSS containing 2% (w/v) FCS (Perbio), 100 mg/ml Collagenase/Dispase (Roche Diagnostics), and 40 ng/ml DNase I (Roche) for sequential digestion. The thymi were gently resuspended through a 1ml pipette tip after each step of incubation and allowed to settle before collecting the supernatant. For the last digestion step, the remaining thymic organoids were resuspended through a double pipette tip, built up of a 1ml and a 10 μl pipette tip until a homogenous cell suspension was achieved. Cells were counted with a Z1 Coulter particle counter from Beckman Coulter. Therefore three drops of zap-oglobin II lytic reagent from Beckman Coulter and 20 μl of cell suspension (Beckman Coulter, Inc., Fullerton, CA, USA) were added into 10 ml Isoton II.

2.3.4 Intracellular Staining

For intracellular staining, TEC were marked for cell-surface molecules, fixed, permeabilized (Cytofix/Cytoperm; BD Biosciences according to the manufacture's recommendation or in case of FoxP3 with fixatives and permeabilization buffer from ebioscience), and stained with BrdU, β-catenin, Foxp3

or Aire-specific antibodies. Unspecific staining was blocked using normal mouse serum and 2.4G.2 supernatant, prepared in our laboratory.

2.3.5 Immunomagnetic Separation techniques

TEC were enriched using automated cell separation (AutoMACS; Miltenyi Biotec). Depending on the individual experiment, TEC were either enriched through positive selection of TEC or depletion of CD45 expressing cells. To positively select TEC, cell concentration was adjusted to 100 x 10^6cells/ml and incubated with biotinylated α-EpCAM antibodies for 15 min on ice. After washing, cells were incubated with α-Biotin beads (10 x 10^6 μl/ 10 x 10^6 cells) for 15 min at 4°. Subsequently, the cells were washed and filtered twice (through a 70 μm and 40 μm). Before running "possel", Dnase I (Roche) was added (100 μg/ml). Alternatively, to deplete CD45 expressing cells, cell concentration was adjusted to 100 x 10^6cells/ml and incubated with α- CD45 beads (5 x 10^6 μl/ 10 x 10^6 cells) for 15 min at 4°C. Cells were subsequently washed and filtered twice (through a 70 μm and 40 μm). Before running "deplete", Dnase I (Roche) was added (100 μg/ml).

2.3.6 Flow Cytometry

Measurement of autophagy

To measure of autophagy the Cyto-ID Autophagy Detection Kit (Roche) was used. To prepare CytoID Green detection solution, 1 μl of CytoID Green was added reagent to 4 ml FACS buffer. A maximum of 1 x 10^6 pre-enriched thymic cells/ml were resuspended in 0.5ml of freshly diluted Cyto ID detection reagent and incubated for 30 min at 37° in the dark. After incubation, cells were filtered through a 40 μm mesh and and directly analysed on FACS-Aria II without prior washing.

Measurement of cleaved caspases

To measure apoptosis, the the CaspACE^{TM} FITC-VAD-FMK In Situ Marker (Promega) was used. The CaspACE^{TM} FITC-VAD-FMK In Situ Marker is a labeled derivative of the cell-permeable irreversible pan-caspase inhibitor, Z-VAD-FMK, which binds to cleaved caspases and label them fluorescently. For detection, the TEC-enriched and surface-stained thymic cell suspension was adjusted to 0.6 x 10^6 cells/ml, pelleted and resuspended in 500 μl FACS buffer including CaspACE^{TM} FITC-VAD-FMK In Situ Marker at a final concentration of 10 μM. Cells were subsequently incubated for 30 min at 37°C protected from light. After washing, cells were filtered through a 40 μm mesh and analysed on FACS-Aria II.

Measurement TUNEL

Cell death was measured using the In Situ Cell Death Detection Kit, Fluorescein (Roche).

To measure cell death, the positively selected TEC were surface-stained. The cell concentration was adjusted to 2×10^7 cells/ml. Next, 100 μl cell suspension was transferred into a V-bottomed 96-well microplate and mixed with 100 μl/well of a freshly prepared fixation solution (final concentration 2% PFA). Cells were subsequently incubated for 60 min at 15-25°C on a shaker, protected from light. After washing the sample three times with PBS, cells were resuspended in 100 μl permeabilisation solution and kept for 2 min on ice. Cell were washed twice with PBS and resuspended in 50 μl TUNEL reaction mixture and incubated for 60 min at 37°C in a humidified atmosphere in the dark. After washing the samples twice with PBS, cells were resuspended in FACS buffer, filtered through a 40 μm mesh and analysed on FACS-Aria II.

BrdU labelling and detection

For cell cycle analysis, mice were injected with BrdU (BD Pharmingen) (1 mg/mouse i.p.) and analysed at the time points indicated. Detection of cell-labeling was performed using the BrdU Flow Kit (BD Pharmingen), according to the manufactor's recommendations. For BrdU detection, TEC were enriched using AutoMACS program: "possel".

Cell sorting

The cells were sorted on a FACS Aria II (BD) into collection tubes, which were pre-wetted and coated using FACS buffer. Sort purity was evaluated for each sorted population, using between 200-1000 cells (depending on the cell number sorted).

2.4 Imaging-techniques

2.4.1 Tissue embedding

Freshly isolated organs were cleaned from connective tissue and embedded in OCT compound (Medite, Switzerland) in Tissue-Tek Cryomolds (Miles Inc., Elkhart, USA). Tissues were frozen in methyl-butane cooled with dry ice and then stored at -80°C.

2.4.2 Sectioning and Fixation of Tissues

Sectioning of OCT embedded organs was performed at a cryostat Leica 3050 (Leica Biosystems). Tissue sections were recovered on microscope slides, pre

cleaned/ready-to-use from Thermo Fisher Scientific Inc.

2.4.3 Preparation of cytospins

Cytospins were prepared from sorted TEC and respective control cells, using a Cytospin device composed of Cytospin filter cards for cyto-centrifugation (Thermo, 3424) and Cytospin microtubes 0.75 ml, with 0.5 mm bottom hole (Thermo, 1153). The cells were resuspended in 150 μl PBS + 2%, and transferred to the cytospin microtube positioned in the assembled cytospin device. The device was placed in a centrifuge equipped with a swing out rotor and spun at 100g for 1 min. Subsequently the cytospin device was carefully disassembled. Depending on the respective staining slides were processes as described in sections 2.4.4 and 2.4.5.

2.4.4 Hematoxylin and Eosin (HE) staining

OCT (Tissue-Tek, Sakura Finetec, Netherlands) embedded tissues were cut at 8 μm thickness. Tissues were air dried over night at RT, then either frozen at 80°C or processed directly. Sections were fixed in Delaunay's fixation solution for 1 min, then rehydrated in a series of ethanol dilutions for 1 min each: 100% ethanol, 96% ethanol, 70% ethanol, 50% ethanol and water. Tissues were then stained with Meyer's Hämalaun for 2 min. Afterwards the slides were washed with luke warm water 3 times 1 min before staining with 1% Erythrosin. After washing with water for 1 min, sections were dehydrated in a series of ethanol solutions: 50% ethanol, 70% ethanol, 96% ethanol for 1 min each, then ethanol 100% for 2 min. Slides were then air dried before cover slips were mounted with Pertex (Histolab, Products AB). Images were acquired using a Nikon Eclipse E600.

2.4.5 Immunohistochemistry

For immunohistochemistry tissue sections were prepared as described for the HE staining. Sections were fixed in acetone at RT for 10 min and briefly air dried. Samples were circled with a pap-pen (Sigma-Aldrich). Tissues were then washed 3×5 min in PBS. Slides were then transferred to a wet chamber and overlayed with 5% goat serum (Gibco) to cover each sample and left at RT for 15 min – 30 min. After blocking, tissues were stained with primary antibodies and incubated for a min of 1h in a wet chamber at RT. After washing the slides 3×5 min in PBS, secondary antibodies were applied and incubated for 30 min in the dark at RT. Sections were then again washed 3×5 min in PBS and stained with DAPI for 2 min. After washing 1×5 min, tissues were embedded in Hydromount (National Diagnostics). Primary and secondary antibodies were prepared 5% goat serum (Gibco) diluted in PBS.

2.4.6 Antibodies used for immunohistochemistry

Antibodies used for flow cytometry are listed in section 2.2.2.
CK5 (Covance), CK8 (Progen), MTS10 (a gift from R. Boyd, Melbourne, Australia), ERTR7 (provided by W. van Ewijk, Utrecht, The Netherlands), Aire (5H12; provided by S. Hamish, Adelaide, Australia), Ng2 (Abcam plc), CD31-FITC (390; ebiosciene), Rat monoclonal α-mouse EDG (S1P1) IgG, Rabbit polyclonal α-human Raptor IgG A300-506 A (Bethyl Laboratories, Inc), Rabbit polyclonal α-human Raptor IgG A300-553 A (Bethyl Laboratories, Inc), Rabbit polyclonal α-mouse Raptor IgG (Abcam plc), Mouse monoclonal α-mouse Raptor IgG (Merck Millipore), Rabbit monoclonal α-human Raptor IgG (OriGene), and reactivity to lectin UEA-1 (Reactolab).

Alexa Fluor-conjugated anti-IgG antibodies (Invitrogen) were used as secondary reagents. Images were acquired using a Zeiss LSM510 (Carl Zeiss).

2.5 Molecular biology

2.5.1 PCR

Primer pairs and PCR conditions are described in the section 2.1.3.

RNA isolation from cells

Total RNA was isolated from sorted TEC (or control populations) using the RNeasy micro Kit (Quiagen GmbH) according to the manufacturers recommendations. The isolated RNA was stored at -80°C until further processing. The quality and quantity of the isolated RNA was measured on a NanoDrop 1000 (Thermo Fisher Scientific).

cDNA synthesis

cDNA was synthesized by reverse transcription using Superscript III RT (Invitrogen). Reaction mix 1 contained:
10 μl total RNA
1 μl dNTP(10 μM)
1 μl dT20 (1 μM, Microsynt)
1 μl Random Hexamer (500 ng/μl Sigma)

Mix 1 was denatured for 5 min at 65°C in a Mastercycler gradient (Eppendorf) and kept for 1 min on ice before adding:
4.5 μl 5x first strand buffer
1 μl DTT (0.1 M, Invitrogen)
1 μl RNaseOUT (40 U/μl, Invitrogen; added in case of low material)
1 μl Superscript III RT (200 U/μl, Invitrogen)

cDNA synthesis was performed on Mastercycler gradient (Eppendorf) using the following conditions:
Incubation: 25°C 5 min
Incubation: 50°C 60 min
Activation of the reaction: 70°C 15 min
Inactivation of the reaction: 16°C 5 min HOLD
The samples were either directly used or stored at -20°C.

2.5.2 qPCR

qPCR was performed using SensiMix dT Kit (Quantace Ltd). The reaction mix was prepared in 0.1 ml strip tubes from Corbett Research (Corbett Research). The reaction was performed on Rotor-Gene 3000A (Corbett Research).
6.25 μl Sensimix 2x (Quantace)
0.375 μl forward primer (10 μM)
0.375 μl reverse primer (10 μm)
0.25 μl 50x SYBR Green I solution (Quantace)
4.25 μl distilled water
2.75 μl cDNA (20 ng/μl)

The cycle threshold (CT) was set at 0.1. CT values were used for the calculation of the relative expression difference between control and target samples assuming an amplification efficiency of 100%. Calculation was based on the comparative CT Method, known as the $2^{(\Delta\Delta CT)}$ method, whereby the CT values of both the calibrator and the samples of interest were normalized to GAPDH.

Primer

The following primer pairs were used on cDNA:
Raptor deletion on cDNA:
(fw) CTTCAACAAGAACTACACTCAG;
(rv) TGGATGGTTTGGGTTAATCG
Rictor deletion:
(fw) TTATTAACTGTGTGTGGGTTG;
(rv) CAGATTCAAGCATGTCCTAAGC
Ccl19:
(fw) CCTGGGTGGATCGCATCATCCG;
(rv) AGAGCATCAGGAGGCCTGGTCCT
Ccl21:
(fw) TTATTAACTGTGTGTGGGTTG;
(rv) TTCCAGACTTAGAGGTTCCCCG

Ccl25:
(fw) GTTACCAGCACAGGATCAAAT;
(rv) GGAAGTAGAATCTCACAGCA
Cxcl12:
(fw) AAATCCTCAACACTCCAAAC;
(rv) GCTTTCTCCAGGTACTCTTG
IL-7:
(fw) ATTATGGGTGGTGAGAGCCG;
(rv) GTTCATTATTCGGGCAATTACTATCA
GADPH:
(fw)GGTGAAGGTCGGTGTGAACG;
(rv) ACCATGTAGTTGAGGTCAATGAAGG

Primer pairs used for genotyping are listed in section 2.1.3.

2.5.3 GeneChip Array

TEC were sorted in biological triplicates from three wild type and three mutant mice at E16 and at 2 weeks. TEC of 2 week old mice were further separated into cTEC and mTEC. Sorted cells constituted only DAPI^{neg} TEC. Sort purity was greater than 95%. Total mRNA was isolated from sorted cells using the RNeasy micro Kit (Quiagen GmbH) according to the manufacturer's recommendations. The Ambion WT Expression kit was used for target preparation on GeneChip 1.0 ST Array System (Affymetrix).

2.6 *In vitro* experiments

2.6.1 T-cell activation assay

In vitro competence of T-cells was assessed with (1 x 10^5) sorted $T_{naïve}$ CD4^{pos}CD25^{neg}CD44^{neg} or CD8^{pos}CD44^{neg} T-cells from Raptor$^{lox/lox}$ and Raptor$^{lox/lox;Foxn1Cre}$ mice. If possible, cells were plated in triplicates of one individual mouse. To assess cell proliferation, the sorted naïve T-cells were resuspended in PBS and labelled with carboxyfluorescein diacetate succinimidyl ester (CFSE; Molecular Probes). Cells were cultured in 96-well plates in IMDM culture medium in the presence of the indicated α-CD3 mAB concentrations and lethally irradiated splenocytes (1 x 10^5) from RAG 2 deficient mice. Plates were covered with foil to avoid evaporation and kept at 37°C. After three days, the cells were carefully harvested, stained, filtered and analysed on FACS ARIA II. Proliferation was measured using the "Expansion Index" calculated by FlowJo Software (TriStar).

2.6.2 T_{reg}-suppression assay

The potency T_{reg} was assessed in an T_{reg}-suppression assay. $CD4^{pos}CD25^{neg}$ $CD44^{neg}$ T-cells ("responder"-cells) of C57BL/6 5.1 mice were isolated from lymphnodes, sorted and labelled with CFSE. Additionally, $CD4^{pos}CD25^{pos}$ from $Raptor^{lox/lox}$ and $Raptor^{lox/lox;Foxn1Cre}$ mice were isolated from lymphnodes and sorted. 2 - 5 x 10^4 responder cells were transferred into a 96-well plate and cultured together with regulatory T-cells in different dilutions in IMDM culture medium in the presence of α-CD3 (1μg/ml). Plates were covered with foil to avoid evaporation and kept at 37°C. After three days, the cells were carefully harvested, stained, filtered and analysed on FACS ARIA II. Proliferation was measured using the "Expansion Index" calculated by FlowJo Software (TriStar).

2.7 *In vivo* experiments

2.7.1 Colitis induction by adoptive transfer of naive $CD4^{pos}$ T-cells

In vivo competence of T-cells was assessed by adoptive transfer of sorted naïve T-cells ($CD4^{pos}$ $CD25^{neg}$ $CD44^{neg}$) from wild type and mutant mice to RAG 2 -/- mice. The sorted cells were resuspended in Hank's Buffered Salt Solution (HBSS) and injected intravenously into the tail of Rag 2 deficient mice (250μl/mouse). Mice were monitored for clinical signs of disease (diarrhea, fur, hunched back) and weight every other day. Endpoint of the experiment was determined as 20% weight loss of the maximum weight of each individual mouse.

2.8 Statistics

The statistical calculations were carried out using Graphpad Prism6 and Numbers 09. The probability values were calculated with student's t-test (unpaired, two-tailed). $p > .05$ were considered as non-significant, $^*p < .05$; $^{**}p < .01$; $^{***}p < .005$).

Chapter 3

Results

3.1 Mouse models of TEC-targeted loss of mTOR function

Three different mouse models have been established to investigate separately the role of either signalling pathway on mouse thymic epithelium, and to evaluate their respective contribution to the overall block of mTOR signalling. The comparison of the different mouse models also allowed us to interrogate whether the combined loss of mTORC1 and mTORC2 function could result in a phenotype that would be the sum of each of the defects of a singular loss of signalling engaging these complexes. Alternatively, the double mutant may reveal that concomitant loss of mTORC1 and mTORC2 results in a much stronger phenotype compared to their individual deletion.

3.1.1 mTORC1 inhibition in Raptor$^{lox/lox;Foxn1Cre}$ mice

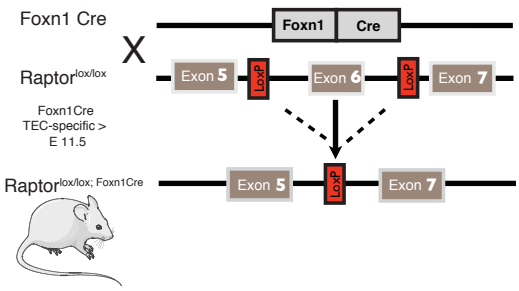

Figure 3.1: Conditional deletion of raptor in Raptor$^{lox/lox;Foxn1Cre}$ mice; To obtain a TEC-targeted deletion of raptor, mice homozygous for exon 6 flanked by loxP sequences were crossed to Foxn1 Cre mice. Cre-mediated recombination deletes exon 6 and leads to a frameshift-induced translational stop.

To study the consequences of mTORC1 inhibition in TEC, conditional knockout mice were generated that lack the expression of the mTORC1-specific component Raptor in these cells. For this purpose, we crossed mice homozygous for LoxP flanked raptor exon 6 (Cybulski et al., 2009) to Foxn1Cre mice, i.e. animals that express the recombinase in all thymic epithelia (Fig. 3.1). As LoxP sites function as target sites for the Cre re-

combinase, the gene(s) flanked by the LoxP sites are deleted in each cell expressing Cre. In Raptor$^{lox/lox;Foxn1Cre}$ mice, Cre-mediated recombination deletes exon 6 of the raptor gene, leading to a frameshift induced stop of translation and therefore to a lack of Raptor protein in Foxn1 expressing cells. Cre-specific recombination in Foxn1 Cre mice can be detected as early as E11.5 (Zuklys et al., 2009).

To characterize the mouse model, DNA and RNA were isolated from sorted embryonic TEC (E14) and analysed for the presence of the recombined locus as well as for raptor specific transcripts (Fig. 3.2). Detection of raptor protein was assessed by FACS, immunohistochemistry and cytochemistry. Five different commercially available antibodies designed for the detection of either murine and/or human Raptor protein were tested on thymic tissue sections and/or isolated cells (cytospins). As Raptor is ubiquitously expressed in the cytoplasm of all cells (Sancak et al., 2008), including thymocytes and non-TEC stromal cells, antibodies directed against epithelial keratins were added to the staining to identify the cell type that has lost its Raptor expression in the thymus. Stainings of tissue sections of 1w old thymi, revealed areas, where the signal for both, Raptor protein and epithelial-specific keratin overlapped in control Raptor$^{lox/lox}$ mice. In contrast, such overlap of staining signals were not observed in Raptor$^{lox/lox;Foxn1Cre}$ mice. (Fig. 3.3).

The vicinity to developing thymocytes and non-epithelial stromal cells complicated a clear allocation of the cellular source of Raptor, therefore we also tested all antibodies for their potential to detect Raptor protein using FACS. Unfortunately, none of the five antibodies tested revealed a believable (i.e sharp) signal in wild type TEC, precluding the detection of raptor by flow cytometry (data not shown).

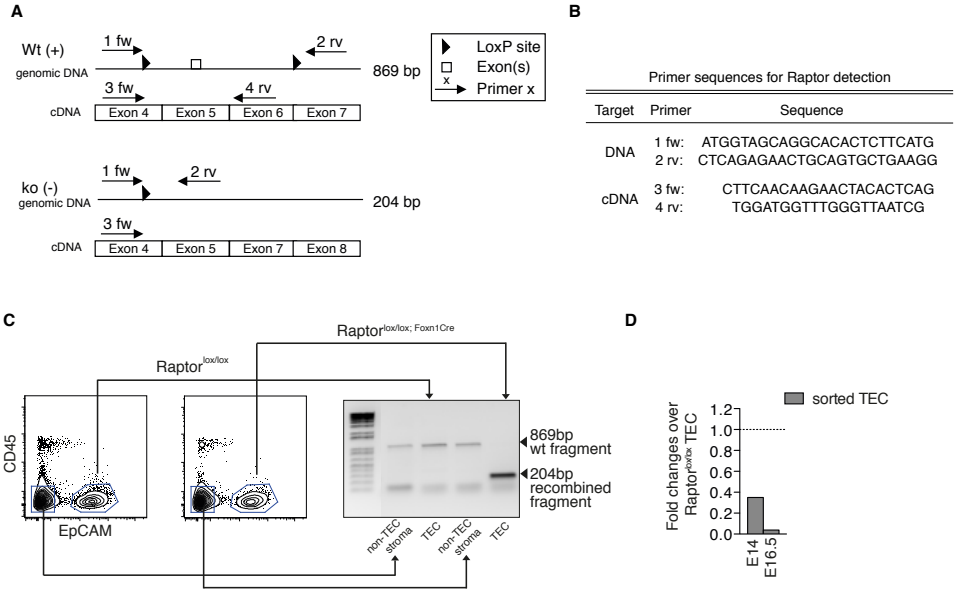

Figure 3.2: Confirmation of raptor deletion; (A) Extract of the raptor gene on genomic DNA and cDNA depicted for Raptor$^{lox/lox}$ mice (upper panel) and Raptor$^{lox/lox;Foxn1Cre}$ mice (lower panel). Labelled arrows are representative for the different primers that were used for raptor detection. **(B)** Primer pairs and sequences. **(C)** Genomic deletion of exon 6 was verified on sorted non-TEC (CD45^{neg} EpCAM^{neg}) and TEC (CD45^{neg} EpCAM^{pos}) stromal cells from E14 thymic tissue. Rectangles on FACS plots are displaying sorting gates for both cell populations. Deletion was confirmed by genomic PCR using primer pair 1 and 2. The recombined locus provides an amplification product of 204bp, while its wild type counterpart generates a product of 869bp size. **(D)** Absence of raptor transcript was confirmed by rtPCR of sorted TEC of embyros at day 14 and 16.5 using primers 3 and 4. As primer 4 was designed to recognize a sequence from exon 6, a product will not be generated once successful deletion of exon 6 has occurred. Expression levels for Raptor mRNA were normalized to GAPDH mRNA levels in the same sample and are shown as fold increase relative to wild type TEC.

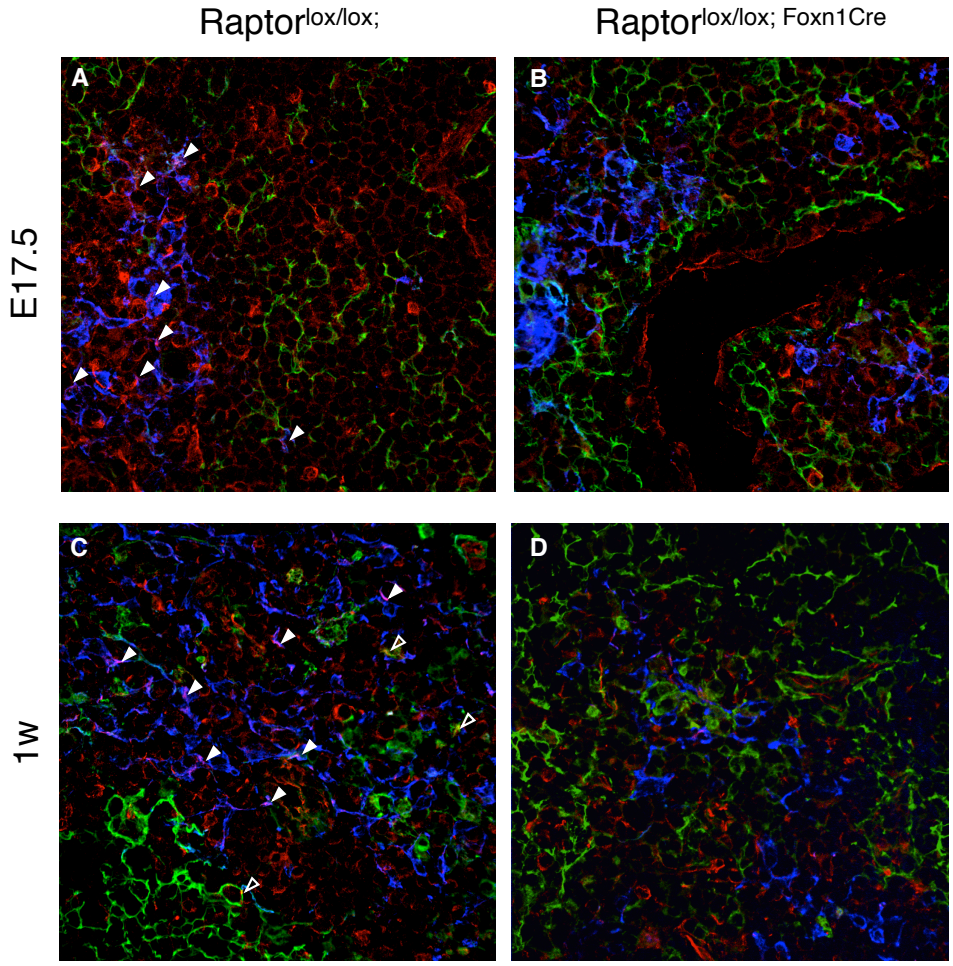

Figure 3.3: Raptor protein detection; Thymic tissue sections (8 µm) of gestational day 17.5 (**(A/B)** and (1w) **(C/D)** old Raptor$^{lox/lox}$ control mice *(left)* and Raptor$^{lox/lox;Foxn1Cre}$ mice *(right)* were stained for Cytokeratin (K)-8 (green), K5 (blue) and raptor (red). Filled white rectangles indicate colocalization of raptor protein in medullary (K5 positive) TEC; empty white rectangles highlight raptor-detection in cortical (K8 positive) TEC. Figures have been taken at 60x magnification.

3.1.2 mTORC2 inhibition in Rictor$^{lox/lox;Foxn1Cre}$ mice

To investigate the role of mTORC2 signalling for TEC biology, conditional knockout mice were generated lacking the expression of Rictor in these cells (Fig. 3.4). Similar to the generation of Raptor$^{lox/lox;Foxn1Cre}$ mice, the Cre/LoxP system was used to generate the tissue-conditional deletion. Mice harboring rictor gene-targeted alleles with LoxP sites flanking exon 4 and 5 have been crossed to transgenic mice expressing Cre recombinase under the control of the Foxn1 promotor. The resultant mice are designated in this thesis as Rictor$^{lox/lox;Foxn1Cre}$ mice.

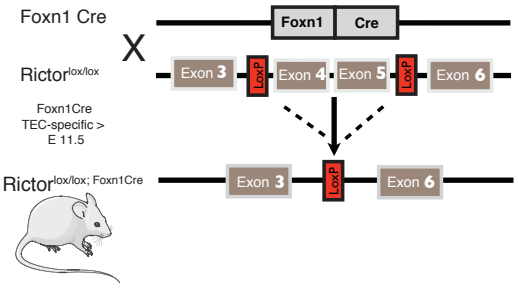

Figure 3.4: Conditional deletion of rictor in Rictor$^{lox/lox;Foxn1Cre}$ mice; Mice homozygous for LoxP flanked exons 4 and 5 were crossed to Foxn1 Cre mice. Following Cre mediated recombination exons 4 and 5 of the rictor gene are deleted leading subsequently to a frameshift-induced stop of translation.

3.1.3 Block of mTOR in Raptor$^{lox/lox}$Rictor$^{lox/lox;Foxn1Cre}$ mice

Combining the two already existing mouse models with a selective blockade of either mTORC1 or mTORC2 signalling in the thymic epithelium, a third conditional knockout mouse — the Raptor$^{lox/lox}$Rictor$^{lox/lox;Foxn1Cre}$ mouse (Fig. 3.5) — was created. Again, transcription of Cre was targeted to TEC using the Foxn1 locus to drive the recombinase. LoxP-mediated recombination of the targeted Raptor and Rictor loci results in a complete loss of mTOR signalling within TEC. The resultant mice are designated Raptor$^{lox/lox}$Rictor$^{lox/lox;Foxn1Cre}$ mice.

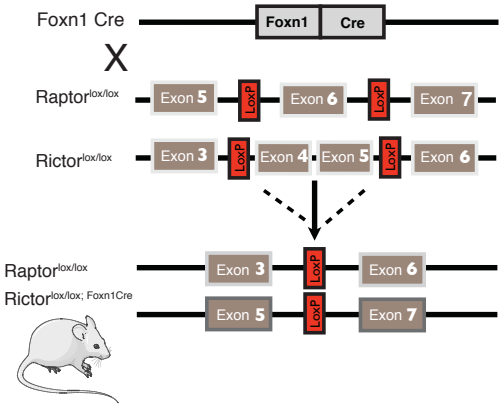

Figure 3.5: Conditional deletion of raptor and rictor in Raptor$^{lox/lox}$ Rictor$^{lox/lox;Foxn1Cre}$ mice; TEC-restricted Rictor-Raptor double knockouts were generated by crossing mice individually homozygous for LoxP flanked raptor exon 6 or rictor exons 4 and 5, respectively. This cross resulted in mice homozygous for Rictor and Raptor knock-in alleles. Further breeding with transgenic mice expressing the Cre recombinase under the control of Foxn1 regulatory elements, resulted in the deletion of Raptor and Rictor protein in TEC.

3.2 Comparative analysis of mice with a loss of mTOR function in TEC

The generation of three different mouse lines with either a single conditional loss of mTORC1 or mTORC2 function via the deletion of *raptor* and *rictor*, respectively, or a combined loss of these regulatory components of the mTOR pathway allowed a comparison of the deficiencies.

Analysis of thymi from newborn mice, bearing a deficiency for either Rictor, Raptor or both proteins showed, that both the single absence of Rictor and the combined absence of Rictor and Raptor in TEC results in a significant reduction of thymic size already in neonatal thymi ($14.6 \times 10^6 \pm 2.7 \times 10^6$ in wild type mice vs. $5.9 \times 10^6 \pm 1.9 \times 10^6$ ($^{***}p < .005$) in Rictor$^{lox/lox;Foxn1Cre}$ mice and $1.6 \times 10^6 \pm 0.5 \times 10^6$ ($^{***}p < .005$) in Rictor$^{lox/lox}$Raptor$^{lox/lox;Foxn1Cre}$mice) (Fig. 3.6 A, B). The selective deletion of Raptor, however, did not result in significant changes in total thymic cellularity when compared to thymi of age-matched wild type littermates ($12.4 \times 10^6 \pm 0.5 \times 10^6$ in Raptor$^{lox/lox;Foxn1Cre}$ mice).

Further analysis of thymi from 2 week old wild type and mutant mice revealed, however, the importance of both single mTOR complexes for the thymic epithelia. In comparison to their age-matched wild type littermates, each conditional knockout mouse displayed a significant albeit different decrease in total thymic cellularity. TEC-restricted Rictor-deletion showed on inspection the least, total blockade of mTOR signalling the most impact on organ size (Fig. 3.7 A). These changes were mirrored by quantification of total thymic cellularity (Fig. 3.7 C). Thymi from Rictor$^{lox/lox;Foxn1Cre}$ mice had only half of the total cellularity observed in wild type mice, whereas Raptor$^{lox/lox;Foxn1Cre}$ mice displayed a reduction of 65% when compared to wild type mice. The most pronounced impact on total thymic cellularity was observed in mice without any mTOR signalling in their TEC. Instead of $328 \times 10^6 \pm 17 \times 10^6$ total thymic cells, the double mutant mice had only

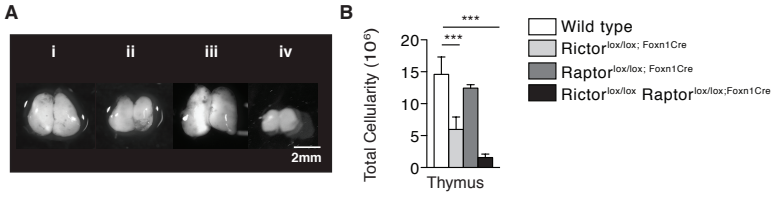

Figure 3.6: Inhibition of mTORC2 and mTOR signalling in TEC impaires normal neonatal thymic development; (A i-iv) Representative photographs from neonatal thymi of different selective conditional knockout mice and their respective wild type littermates; **(A i)** from wild type mice ; **(A ii)** from Rictor$^{lox/lox;Foxn1Cre}$ mice **(A iii)** from Raptor$^{lox/lox;Foxn1Cre}$mice and **(A iv)** from Rictor$^{lox/lox}$Raptor$^{lox/lox;Foxn1Cre}$mice. **(B)** Absolute numbers of total thymic cells after flow cytometric analysis of thymi. Values represent the mean plus SD. Per experiment a minimum of 3 mice were used. p values were determined by Student's t test with $^{*}p < .05$; $^{**}p < .01$; $^{***}p < .005$)

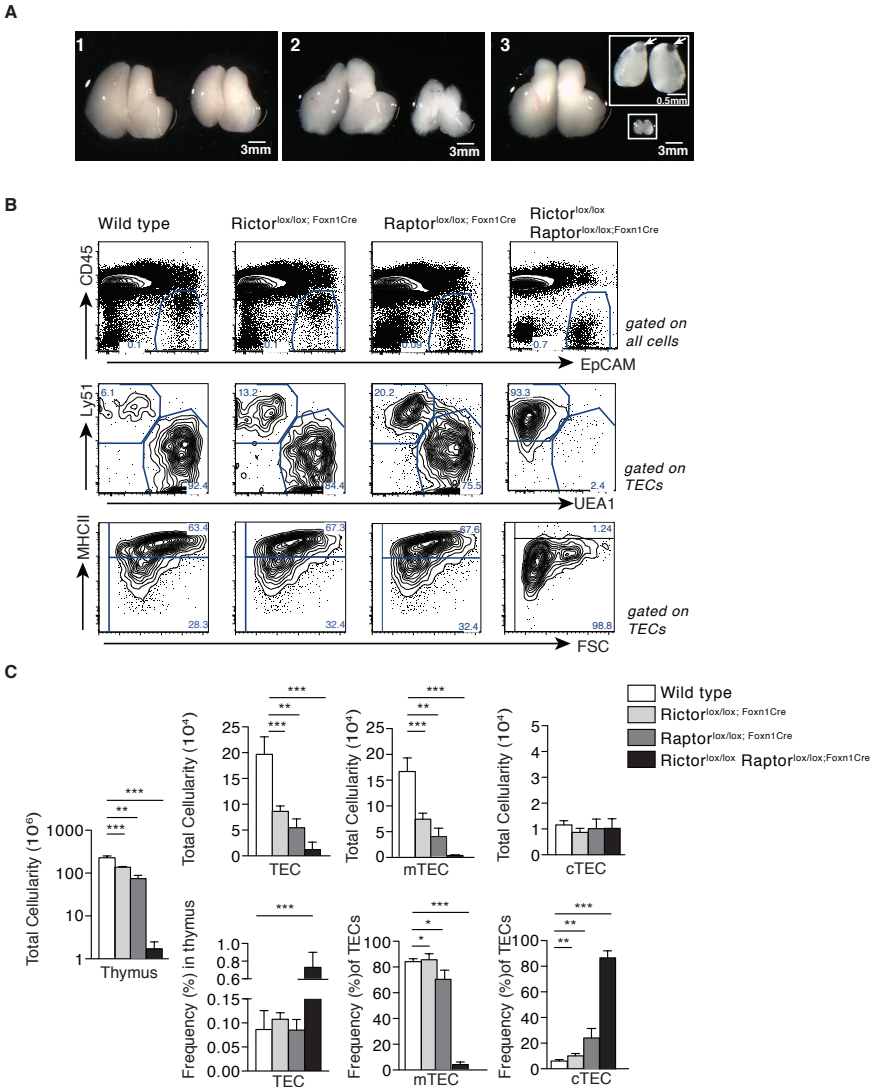

Figure 3.7: Inhibition of mTOR signalling in TEC leads to thymic hypoplasia and a loss of mTEC; (A1-3) Representative photographs from 2 week old thymi of different selective conditional knockout mice and their respective wild type littermates; **(A1)** Rictor$^{lox/lox}$ mice (*left*); Rictor$^{lox/lox;Foxn1Cre}$ mice (*right*) **(A2)** Raptor$^{lox/lox}$ mice (*left*); Raptor$^{lox/lox;Foxn1Cre}$ mice (*right*) **(A3)** Rictor$^{lox/lox}$Raptor$^{lox/lox}$mice (*left*); Rictor$^{lox/lox}$Raptor$^{lox/lox;Foxn1Cre}$mice (*right*). Boxed area is shown in higher magnification to point out cysts (*arrows*) present in Rictor$^{lox/lox}$Raptor$^{lox/lox;Foxn1Cre}$mice.**(B)** Flow cytometric analysis of TEC from the indicated mouse lines. TEC were defined as CD45^{neg} EpCAM^{pos} cells *(gates in upper panels)*. To further subdivide TEC into cTEC and mTEC, cells have been stained for UAE1 reactivity and Ly51 expression *(middle panels)*. Gates are highlighting cTEC (Ly51^{pos} and UEA1^{neg}) and mTEC (Ly51^{neg} and UEA1^{pos}). MHCII expression has been used to distinguish MHCII^{low} TEC and MHCII^{high} TEC *(lower panels)*. The relative frequency of the distinct subpopulations is provided as a percentage. **(C)** Absolute numbers of total thymic cells, TEC as well as TEC subpopulations *(upper line)* of thymi from 2 week old wild type mice as indicated. Relative numbers of TEC per thymus and proportion of cTEC and mTEC among TEC are shown at the lower line. Values represent the mean plus SD. (The number of mice analysed per experiment is $n = 10$ for Rictor$^{lox/lox}$mice; $n = 8$ for Raptor$^{lox/lox}$mice and $n = 6$ for Rictor$^{lox/lox}$Raptor$^{lox/lox}$mice; p values were determined by Student's t test with $*p < .05$; $**p < .01$; $***p < .005$)

$1.7 \times 10^6 \pm 0.7 \times 10^6$ total cells per thymus. In addition, large cysts were present in thymi of Raptor$^{lox/lox}$Rictor$^{lox/lox;Foxn1Cre}$ mice (Fig. 3.7 A3) but not in the other mutant mice. FACS analysis of mutant and wild type thymi revealed also distinct consequences of partial or general inhibition of mTOR signalling for the cellular composition of the thymus. Although the relative frequency of TEC within the thymus of single knockouts was not significantly changed, Raptor$^{lox/lox}$Rictor$^{lox/lox;Foxn1Cre}$ mice displayed a 7-fold higher TEC to thymocyte ratio in comparison to wild type mice (Fig. 3.7 C). All three mouse models showed progressive changes in the representation of specific TEC subsets when analysing the TEC compartment in further detail (Fig. 3.7 B). Thymi deficient for Rictor protein expression in TEC showed a mild but significant reduction in the frequency of medullary TEC (e.i. UEA1^{pos}, Ly51^{neg}) (90.3% ± 1.7% in wild type vs. 85.1% ± 1.7% in Rictor$^{lox/lox;Foxn1Cre}$ mice; (***$p < .005$)). The frequency of mTEC was more profoundly reduced in Raptor$^{lox/lox;Foxn1Cre}$ mice (95.4% ± 0.7% in wild type vs. 69.7% ± 6.8% in Raptor$^{lox/lox;Foxn1Cre}$ mice; (***$p < .005$)). In sharp contrast, in Rictor$^{lox/lox}$Raptor$^{lox/lox;Foxn1Cre}$ mice only a marginal population of 3.7% ± 1.7% of all TEC were mTEC. In absolute numbers, the reduction of both total thymic cellularity and mTEC frequency resulted in a decrease in total mTEC. Changes in mTOR signalling did not affect the absolute numbers of cTEC, though it affected their relative frequency due to the overall decrease in thymic cellularity. Remarkably, partial or total inhibition of mTOR did not lead to any significant quantitative changes within the cTEC compartment, even though total thymus cellularity was particularly reduced in Raptor$^{lox/lox}$Rictor$^{lox/lox;Foxn1Cre}$ mice. Comparison of MHCII expression on TEC isolated from mutant mice revealed a normal MHC phenotype for the Raptor- and Rictor-deficient cells. However, a total block in mTOR signalling resulted in a complete loss of the MHCII^{high} TEC population (Fig. 3.7 B). This finding suggests that mTOR mediated signals are essential for MHCII^{high} cell surface expression.

To evaluate whether the observed changes in TEC number and quality had functional consequences in particular for thymopoiesis, T-cell development was next analysed by flow cytometry (Fig. 3.8 B). Thymi from the three different mouse lines, and wild type littermates at 2 weeks of age were investigated for the frequency of specific thymocyte subpopulations within the TCR α/β lineage. Similar to the differential impact on thymic size and TEC quality, the deletion of single mTOR signalling components had a differential impact on intrathymic T-cell maturation. In mice deficient for Rictor expression in TEC, the frequencies of DN, DP and SP thymocytes were almost unperturbed, except for a minor reduction in the frequency of SP CD8^{pos} T-cells (1.1% ± 0.2% in wild type vs. 0.7% ± 0.1%; (*$p <$ .05) in Rictor-deficient mice). Lack of Raptor led to a slight but significant change in the relative amount of DP (82% ± 1.6% in wild type vs. 87% ± 1.6%; (*$p < .05$) in Raptor-deficient mice) and CD4^{pos} T-cells (10.2% ±

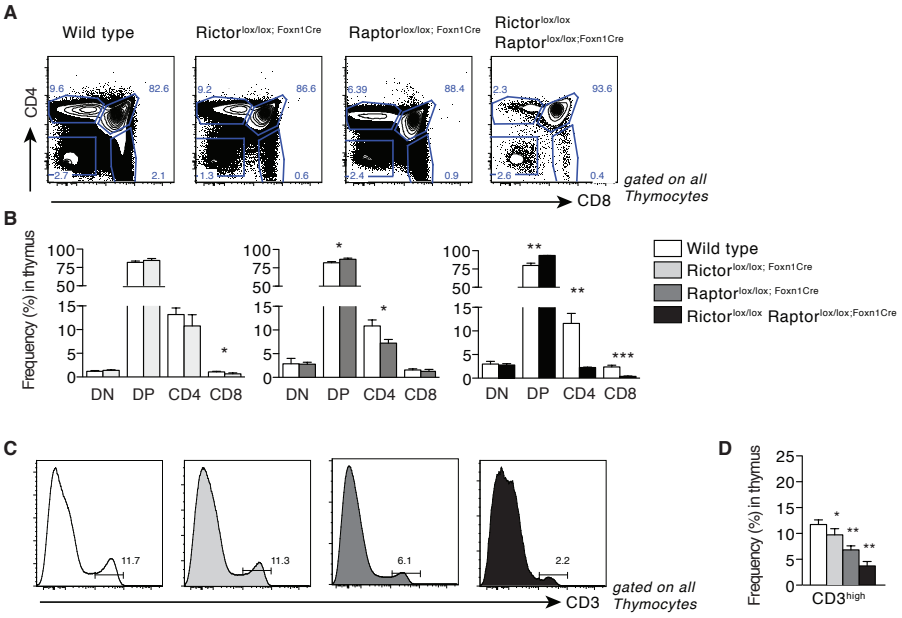

Figure 3.8: Inhibition of mTOR signalling in TEC impaires normal thymocyte development; Thymic cell suspensions of two week old mice lacking expression of either rictor, raptor or both proteins in TEC were stained for CD4 and CD8 cell surface expression and analysed by flow cytometry. Cell suspension of wild type littermates served as controls. **(A)** Representative FACS plots of total thymocytes. DAPI^{pos} cells and doublets have been excluded prior to analysis. Frequencies of the respective thymocyte subpopulation are indicated next to each gate. **(B)** Frequencies of DN, DP, as well as CD4 and CD8 single positive thymocytes are calculated and compared to values of age-matched wild type littermates. Values represent the mean plus SD. **(C)** Flow cytometric profile of CD3 surface expression on thymocytes; the gate indicates the percentage of cells expressing high CD3 concentrations. **(D)** Statistical analysis of CD3^{high} frequencies in thymi of the mice indicated. Values represent mean frequencies plus SD. (The number of mice analysed per experiment is $n = 10$ for Rictor$^{lox/lox}$mice; $n = 8$ for Raptor$^{lox/lox}$mice and $n = 6$ for Rictor$^{lox/lox}$Raptor$^{lox/lox}$mice; p values were determined by Student's t test with $*p < .05$; $**p < .01$; $***p < .005$)

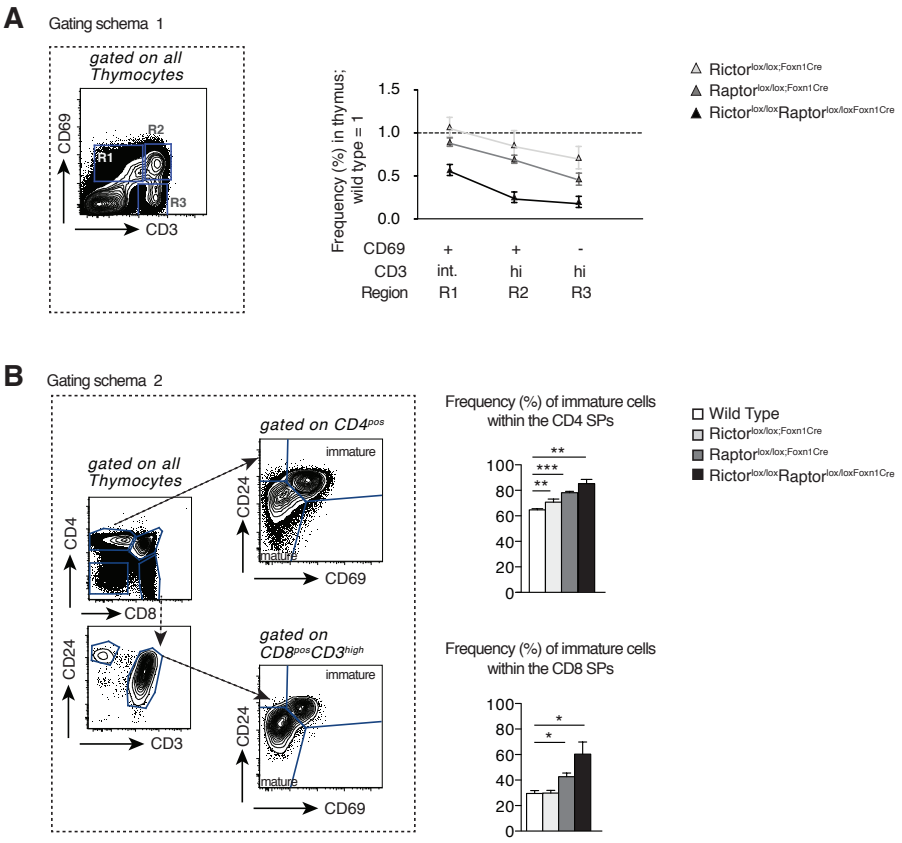

Figure 3.9: Selective mTOR inhibition impaires thymocyte maturation; (A) Representative FACS plot of thymocytes stained for surface expression of CD69 and CD3. Gates R1-R3 drawn in the plot are defining distinct thymocyte subpopulations that have undergone positive selection. Mean frequencies of thymocytes within gate R1-R3 have been normalized to mean wild type frequencies and are depicted as colored triangles (light grey for Rictor$^{lox/lox;Foxn1Cre}$ mice; grey for Raptor$^{lox/lox;Foxn1Cre}$ mice and black for Rictor$^{lox/lox}$Raptor$^{lox/lox;Foxn1Cre}$mice.) **(B)** Gating scheme illustrates characterization of immature and mature CD4 and CD8 T-cells for comparative analysis of their relative amount in the thymus. Immature CD4 thymocytes are characterized by high expression of CD24 and CD69, whereas mature CD4 positive cells express lower amounts of CD69 and are negative for CD24. In order to restrict the analysis to post-selection thymocytes, CD8 positive cells that do not express CD3 on their surface were excluded from further analysis in a first step. The remaining CD8 SP cells were subsequently further subdivided into immature and mature cells, according to their surface expression of CD69 and CD24 similarly to CD4 T-cells. Values are indicated as means plus SD. (The number of mice analysed per experiment is $n = 10$ for Rictor$^{lox/lox}$mice, $n = 8$ for Raptor$^{lox/lox}$mice and $n = 6$ for Rictor$^{lox/lox}$Raptor$^{lox/lox}$mice; p values were determined by Student's t test with $^{*}p < .05$; $^{**}p < .01$; $^{***}p < .005$)

1.2% in wild type vs. 7.3% ± 0.8% in raptor-deficient mice). In contrast, Raptor$^{lox/lox}$Rictor$^{lox/lox;Foxn1Cre}$ mice demonstrated large changes in the frequency of DP and SP thymocytes. The frequency of DP cells was increased from 79.3% ± 3.2% in wild type to 93.5% ± 0.1% (***$p < .005$) in the mTOR double mutant mouse. In parallel, the relative frequency of CD4 and CD8 SP thymocytes was strongly decreased in comparison to controls; instead of the observed frequencies of 11.9% ± 2.1% CD4^{pos} cells and 2.5% ± 0.4% CD8^{pos} cells in wild type, thymi of mTOR double mutant mice contained only 2.3% ± 0.1% CD4^{pos} cells (**$p < .01$) and 0.4% ± 0.1% CD8^{pos} cells (***$p < .005$). These results suggested changes in positive thymocyte selection; a contention further underscored by a significantly lower relative frequency of CD3^{high} cells (Fig. 3.8 C and D) in the mTOR double mutant mice (3.7% ± 0.9%) in comparison to wild type mice (12% ± 2.5%; **$p <$ .01).

The observed reductions in the frequencies of mature thymocytes were suggestive of an impaired potential of the genetically modified TEC to support positive selection. It was therefore of interest to investigate differences in thymocyte maturation between the three mouse models using phenotyping and quantification by FACS analyses (Fig. 3.9 A). Thymocytes follow well-defined changes in CD69 and CD3 expression during their development from DN to SPs. Early immature thymocytes are CD3^{low} and do not yet undergo positive selection. Concurrent with an upregulation on the cell surface of the TCR/CD3 complex, positive selection of DP thymocytes is enabled. Successful positive selection results in the up-regulation of CD69. This sequence of phenotypic changes allows a close monitoring of the efficiency of thymocyte positive selection without the need to define the specificity of the TCRs engaged. In Fig. 3.9 A, thymocytes with an early positive selection phenotype, (i.e. CD69^{pos} CD3^{int}) are defined in gate "R1". Next, thymocytes upregulate concomittantly the expression of CD3 and CD69, resulting in a thymocyte population that is CD69^{pos} and CD3^{high} ("R2" in Fig. 3.9 A). Finally, mature thymocytes tune down CD69 expression while maintaining a high cell surface density of the CD3/TCR complex ("R3" in Fig. 3.9 A). The mean frequencies of thymocytes within the gates "R1", "R2", and "R3" were then compared for the three strains of mice to assess the severity of changes in positive thymocyte selection. All knockout values were normalized to those obtained in wild-type animals (Fig. 3.9 A). Except for early postselection-thymocytes in gate "R1" and "R2" derived from Rictor-deficient thymi, thymocytes of each genetically modified mouse were less frequent in each of the defined gates ("R1–R3") than in wild type. The extent of the impairment correlated with the other changes observed and was again most prominent in mice with a complete lack of mTOR signalling.

An additional approach to measure post-selectional maturation focuses more on the maturational state of CD4 and CD8 SP thymocytes and quantifies CD24 and CD69 surface-expression of SP (Fig. 3.9 B). CD4^{pos} and

$CD8^{pos}$ thymocytes can be classified as "immature" and "mature" depending on the pattern of CD69 and CD24 expression. Immature SP thymocytes are positive for both markers, whereas mature cells lose CD24 expression. Due to asymmetric up-regulation of CD4 and CD8 during the transition from DN to DP thymocytes, the population of $CD8^{pos}$ cells consists of two distinct subpopulations. The so-called immature single positive (ISP) cells have not yet undergone positive selection and were therefore excluded from the analysis on the basis of their low CD3 expression (Fig. 3.9 B gating scheme). Two thirds of CD4 and one third of CD8 SP thymocytes in wild type mice are immature according to the phenotypic staging. These proportions were significantly altered in mutant mice. 70% ±2.3% of all $CD4^{pos}$ cells in $\text{Rictor}^{lox/lox;Foxn1Cre}$ mice, 78% ± 1.1% in $\text{Raptor}^{lox/lox;Foxn1Cre}$ mice and 84% ± 2.9% $\text{Rictor}^{lox/lox}\text{Raptor}^{lox/lox;Foxn1Cre}$ mice were immature. The frequencies of immature $CD8^{pos}$ thymocytes were also significantly increased in the Raptor and double mutant mice. Instead of 33% immature SP among the $CD8^{pos}$ cells, TEC-directed loss of Raptor led to 42% ± 2.9% ($^*p < .05$) and the combined inhibition of mTORC1 and mTORC2 in $\text{Rictor}^{lox/lox}\text{Raptor}^{lox/lox;Foxn1Cre}$ mice led to 60% ± 3.8% ($^*p < .05$) immature CD8 SP thymocytes.

Given the changes in thymocyte cellularity and maturation in mTOR mutant mice, I next investigated the peripheral T-cell compartment of these animals. FACS analysis of splenic cell suspensions of 2 week old mice revealed no significant changes in total splenocyte cellularity (Fig. 3.10). However, the frequencies of T-cells (marked by the surface expression of CD3 and the absence of CD19) were significantly diminished (Table in Fig. 3.10 B (iii)). The ratio of $CD4^{pos}$ to $CD8^{pos}$ remained unchanged in each of the mutant mice. A closer look at the CD4 T-cell compartment revealed, however, that the distribution of naïve T-cells ($T_{\text{naïve}}$), memory T-cells (T_{mem}) and regulatory T-cells (T_{reg}) was differentially affected in the mutant mice. To distinguish $T_{\text{naïve}}$ and T_{mem} from T_{reg}, $CD4^{pos}$ splenocytes were subdivided according to their CD25 expression (Fig. 3.10 A) and $CD25^{neg}$ cells were further differentiated as either naïve ($CD62L^{pos}$) or memory T-cells ($CD44^{pos}$). In contrast, T_{reg} were characterized based on their expression of CD4, CD25, and intracellular FoxP3.

The frequency of $T_{\text{naïve}}$ and T_{mem} was only decreased in Rictor and Raptor double mutant mice. Here, fewer naïve T-cells could be discovered from the spleen (34.2% ± 3.3% vs 88.1% ± 3.1% in wild type mice). In parallel, the frequency of T_{mem} increased 7-fold (7.2% ± 2.4% in wild type to 51.8% ± 0.8%) and that of T_{reg} approximately 3-fold (6.8 % ± 0.4% in wild type mice, 19.4% ± 1.9% in mutant mice). Thus, the pronounced peripheral lymphopenia observed in $\text{Rictor}^{lox/lox}\text{Raptor}^{lox/lox;Foxn1Cre}$ mice can be ascribed to a substantial decrease in naïve T-cells. Mice deficient either in Raptor or Rictor expression in TEC had also fewer T_{reg}, though this decrease was less striking but still significant. The increase in T_{reg}

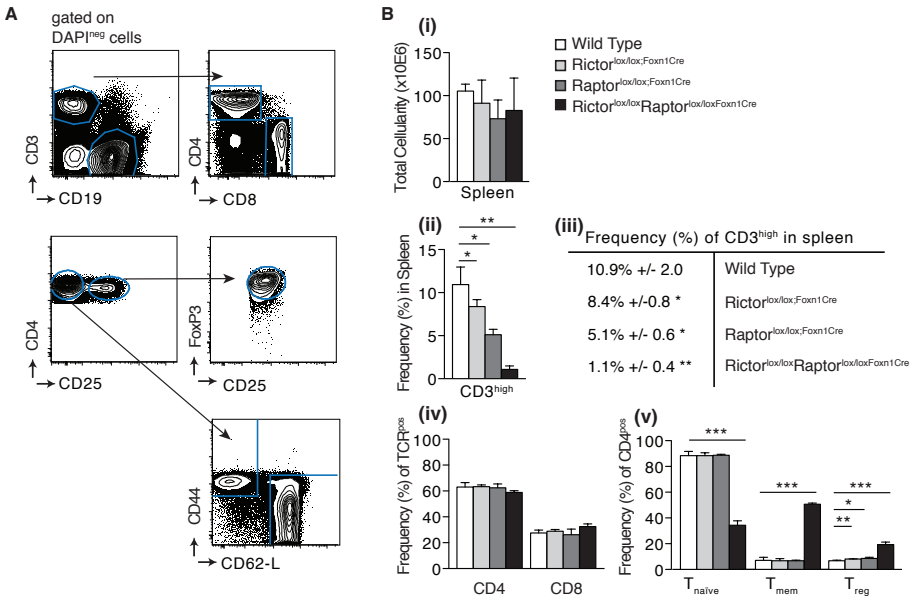

Figure 3.10: mTOR-deficiency in TEC leads to peripheral lymphopenia and to a shift in the representation of peripheral T-cell subpopulations; (A) Gating scheme: representative FACS plots from 2 week old wild type mice illustrate the gating strategy for the characterization of splenic cells. $DAPI^{pos}$ cells and doublets have been excluded prior to analysis. T-cells were characterized among total splenocytes by high surface-expression of CD3 and lack of CD19. $CD3^{pos}$ cells were further subdivided according to the expression of either CD4 or CD8. To discriminate naïve ($T_{\text{naïve}}$) and memory T-cells (T_{mem}) from regulatory T-cells (T_{reg}), $CD4^{pos}$ splenocytes were further split based on the expression of CD25. $CD25^{neg}$ cells expressing CD62L were classified as $T_{\text{naïve}}$, whereas $CD25^{neg}$ cells positive for CD44 were grouped as T_{mem}. To identify T_{reg}, $CD4^{pos}CD25^{pos}$ splenocytes were selected and analysed for Foxp3 expression. In all mice analysed, the percentage of FoxP3 expressing cells among the $CD4^{pos}CD25^{pos}$ subset was close to 100%. **(B)** Quantification of total splenic cells **(i)**, frequencies of $CD3^{hi}$ cells presented in bar graphs **(ii)** and in a table **(iii)**, and frequencies of T-cell subpopulations ($CD4^{pos}$ and $CD8^{pos}$ **(iv)**;T_{reg}, $T_{\text{naïve}}$ and T^{men} **(v)**); Values are indicated as means plus SD. (The number of mice analysed per experiment is $n = 10$ for $\text{Rictor}^{lox/lox}$ mice, $n = 8$ for $\text{Raptor}^{lox/lox}$ mice, and $n = 6$ for $\text{Rictor}^{lox/lox}\text{Raptor}^{lox/lox}$ mice; p values were determined by Student's t test with $*p < .05$; $**p < .01$; $***p < .005$)

intensified with age and was proportional to the degree of lymphopenia. Indeed, aged $\text{Raptor}^{lox/lox;Foxn1Cre}$mice showed a significant lymphopenia due to a reduction in $T_{\text{naïve}}$ cells (Fig. 3.27).

3.3 Detailed analysis of TEC and thymocyte development in the absence of Raptor expression in TEC

Next, Raptor$^{lox/lox;Foxn1Cre}$ mice were analysed in detail, as these animals display a clear phenotype but still have sufficient thymic tissue for an in-depth cellular and molecular analysis.

3.3.1 Thymic cellularity and architecture

First, I investigated thymi from Raptor$^{lox/lox;Foxn1Cre}$ mice and as controls Raptor$^{lox/lox}$ mice at ages from one week to 35 weeks. Total thymic cellularity was significantly diminished with age in Raptor$^{lox/lox;Foxn1Cre}$ mice, reaching 30%–50% of the cellularity measured in wild type thymi (Fig. 3.11 A and B). This hypoplasia was accompanied by a reduced TEC cell count, which was apparent as early as two weeks of age. TEC followed typical age-dependent variations in cellularity, with increasing cell numbers from postnatal stages until puberty and adulthood and a subsequent decrease at advanced age. However, thymic hypoplasia in Raptor$^{lox/lox;Foxn1Cre}$ mice of 1 week of age was not correlating with a reduction in total TEC. Within the TEC compartment, impaired mTORC1 signalling had a different impact on cTEC and mTEC. The absolute number of mTEC decreased substantially in mice of two weeks and older, coinciding with the decrease in total TEC. In contrast, the absolute number of cTEC remained unchanged in the mutant mice when compared to age-matched controls. cTEC cellularity in one and two week old mutant mice was even higher than that in wild type animals. However, these changes in TEC numbers only became apparent in the second week of life. Indeed, total thymic cellularity and TEC frequency for both groups of animals were equal at embryonic day 15 and at birth (Fig. 3.11).

The changes observed in the thymic epithelium were confirmed by immunohistology (Fig. 3.12). Although a distinct separation of the cTEC- and mTEC-compartments was still appreciated in hematoxylin and eosin stained sections of 7 week old female Raptor$^{lox/lox}$ and Raptor$^{lox/lox;Foxn1Cre}$ mice, immunofluorescence staining of tissue sections showed distinct changes within the thymi of mutant mice in comparison to wild type mice. A combined staining for cytokeratin 5 (K5, typical for mTEC), cytokeratin 8 (K8, a characteristic of cTEC) and the fibroblast-specific marker ERTR7 revealed a loss in mTEC and a concomitant remodeling of the thymic stroma with fibroblasts (Fig. 3.12 B). To ensure that the lack of K5-positive staining was indeed the consequence of a loss of mTEC, we used in addition the mTEC-specific marker MTS10. Both, MTS10 and K5 positive cells were strongly reduced in Raptor$^{lox/lox;Foxn1Cre}$ mice, leaving only a few well demarcated

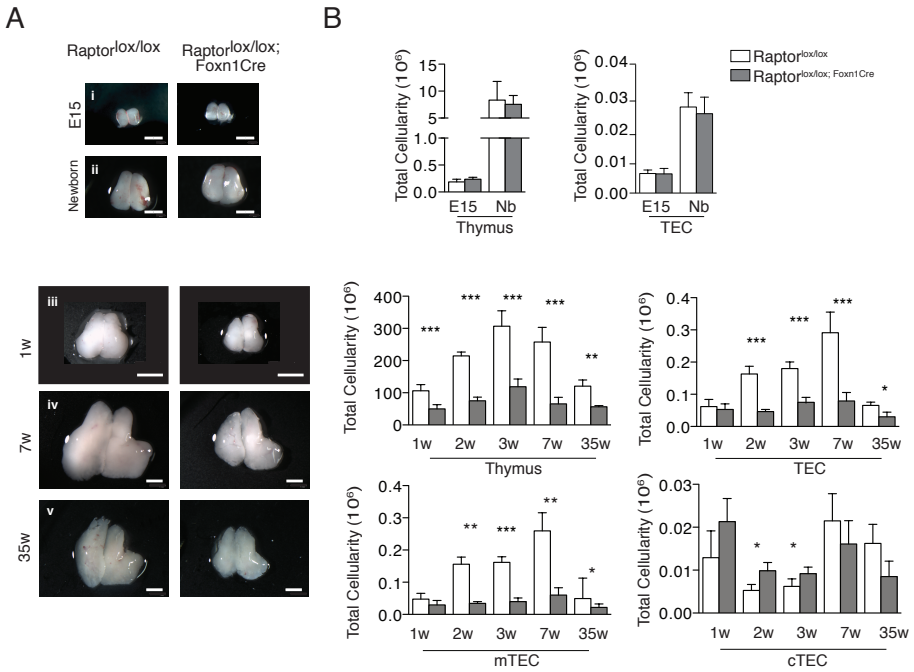

Figure 3.11: Loss of mTORC1 in TEC results postnatally in thymic hypoplasia with an absolute decrease of mTEC; (A) Representative photographs of thymi from E15 (i), newborn (ii), 1 weeks (iii), 7 weeks (iv) and 35 weeks (v) of Raptor$^{lox/lox}$ mice (left) and Raptor$^{lox/lox;Foxn1Cre}$ mice (right). Scale bar represents 100 µm. **(B)** Thymus cellularity, TEC cell count and total amount of cTEC and mTEC of Raptor$^{lox/lox}$ and Raptor$^{lox/lox;Foxn1Cre}$ mice of different ages. Values are indicated as means plus SD. (For all experiments a minimum of three mice per group were analysed. p values were determined by Student's t test with $*p < .05$; $**p < .01$; $***p < .005$)

medullary islets in the thymic tissue of Raptor-deficient mice. Despite this considerable reduction of mTEC, a distinct population of mature mTEC, characterized by reactivity with Ulex europaeus agglutinin I (UEA1) and the expression of the autoimmune regulator (AIRE), were detected in the medulla (Fig. 3.12 B). Taken together, these data are suggestive of a redundancy in mTORC1 mediated signalling during the prenatal stages of development, and possibly the first week of life. They also demonstrate that mTEC but not cTEC are susceptible to a loss of Raptor.

3.3.2 Early thymocyte development

Interactions between blood-borne precursor cells and thymic epithelia are essential for the development of thymocytes. In view of the considerable impact of mTORC1 inhibition on TEC numbers and phenotype, I next investigated the function of TEC in the absence of mTORC1. To exclude the possibility that an altered thymocyte compartment in Raptor$^{lox/lox;Foxn1Cre}$ mice was the result of changes in the bone marrow and thus in the generation of haematopoietic T-cell precursors, mutant and wild type mice were inves-

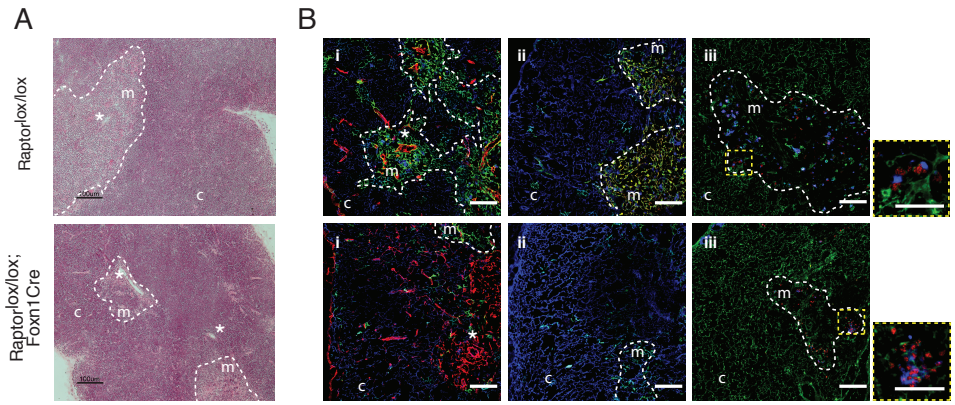

Figure 3.12: Alterations in the thymic microenvironment of Raptor$^{lox/lox;Foxn1Cre}$ mice; (A) Hematoxylin and Eosin staining of thymic tissue sections (8 µm) of 7 week old female Raptor$^{lox/lox}$ mice (*upper panel*) and Raptor$^{lox/lox;Foxn1Cre}$ mice (*lower panel*). Scalebar indicates 50µm. **(B)** Confocal microscopy of thymic tissue sections (8 µm) stained either for (i) cytokeratin 8 (blue), cytokeratin 5 (green) and ERTR7 (red) or (ii) cytokeratin 8 (blue), cytokeratin 5 (green) and MTS10 (red) or (iii) cytokeratin 8 (green), UEA1 (blue) and AIRE (red). "c" denotes cortex, "m" denotes medulla, white star marks large vessels. Dashed white line encircles thymic medulla. Yellow boxed area within the medulla is shown in higher magnification. Scalebar indicates 50µm.

tigated for the presence and frequency of these cells in the bone marrow (Fig. 3.13). Lineage^{neg} Sca1^{pos} c-kit^{high} (LSK) cells expressing the lectin CD62L, are the immediate pre-thymic T-cell precursor (Perry et al., 2004). These cells were detected in Raptor$^{lox/lox;Foxn1Cre}$ mice at a normal frequency. As expected, the loss of Raptor expression in TEC did thus not exert any notable impact on the compartment of extrathymic T-cell precursors.

Next, I analysed thymocyte development in Raptor$^{lox/lox;Foxn1Cre}$ mice at one week, two weeks and seven weeks of age. Maturation-specific surface markers were used to quantify thymocyte subpopulations of well-defined developmental stages. For this purpose, single cell suspensions from mutant and wildtype thymi were stained for the expression of markers, expressed after commitment to a specific cell lineage (CD3, CD4, CD8, CD11b, CD11c, CD19, B220, Gr1, Ter119, Nk1.1, Dx5, TCRα/β, TCRγ/δ and F4/80). Cells, negative for any of these markers are typically termed "Lineage^{neg}" and comprise the earliest thymocyte stages. Lineage^{neg} cells were subsequently analysed for the cell surface expression of CD44 and CD25, which allows a further differentiation of these cells into four subpopulations, designated DN1–DN4 (Fig. 3.14 A). Their frequencies were largely identical at one week, two weeks and seven weeks of age. Although small differences in the frequency of DN4 cells (at one week) and of DN2 cell (at seven weeks) could be detected in the thymi of Raptor$^{lox/lox;Foxn1Cre}$ mice, these changes were minimal and inconsistent over time (Fig. 3.14 B). The quantification of the frequencies at all time points investigated did not reveal a block in

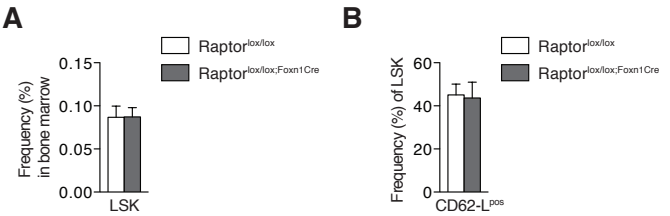

Figure 3.13: Unperturbed frequencies of thymocyte progenitors in the bone marrow of Raptor$^{lox/lox;Foxn1Cre}$ mice; Thymocyte progenitors within the bone marrow were analysed by FACS and quantified. **(A)** Frequencies of Lineage^{neg} Sca1^{pos} c-kit^{high} (LSK) in the bone marrow of Raptor$^{lox/lox}$ and Raptor$^{lox/lox;Foxn1Cre}$ mice. **(B)** Frequencies of CD62L^{pos} among LSK in the bone marrow of Raptor$^{lox/lox}$ and Raptor$^{lox/lox;Foxn1Cre}$ mice. Values were indicated as mean plus SD. Each experimental group consisted of 3 mice.

the maturational transition. To compare the maturational kinetics between DN1–DN4 cells in Raptor$^{lox/lox}$ and Raptor$^{lox/lox;Foxn1Cre}$ thymi, mice were injected with BrdU (1mg/mouse i.p.) and the label was "chased" after 4 hours. Similar frequencies of BrdU-labelled cells were recovered for the four DN subsets of mutant and wild type mice, revealing identical kinetics in the progression from one DN stage to the next (Fig. 3.14 C). These data demonstrate that the loss of mTORC1 signalling in TEC did not impair the earliest stages of intrathymic T-cell development.

3.3.3 Late thymocyte development

The transition from DP to SP cells depends on a close interaction between the thymic epithelium and thymocytes, where only those cell are selected to advance to a SP stage that express a TCR with a moderate affinity for the self-complexes, presented usually by the medullary epithelia. Comparative analysis of thymocytes from 1, 2 and 7 weeks old Raptor$^{lox/lox}$ mice and Raptor$^{lox/lox;Foxn1Cre}$ mice, respectively, revealed also normal progression of intrathymic T-cell differentiation for the later stages of development (Fig. 3.15). Although minimal differences in the relative frequency of the different thymocyte subpopulations occur, these changes were not consistent over time and limited in extent that their biological relevance has to be questioned. (1week: CD8 0.6% ±0.08% in wild type vs. 0.4% ±0.04% in Raptor-deficient mice, at 2 weeks DP 83.2% ±1.5% vs. 87.7% ±1.6% and CD4 9.8% ±1.1% vs. 6.4% ±0.7%) However, Raptor$^{lox/lox;Foxn1Cre}$ mice had significantly fewer thymocytes at any time point investigated.

A careful analysis of the post-selectional maturation of SP thymocytes revealed a significant and continuous difference in the progression of T-cells to full maturity, based on the cell surface expression of CD24 and CD69 (Fig. 3.16 A). SP CD4^{pos} and CD8^{pos} thymocytes are initially positive for CD24 and CD69 and only downregulate their expression within a few days of residency in the medulla (Yamashita et al., 1993). At the age of 1 week, a mild, however not statistically significant increase in the relative repre-

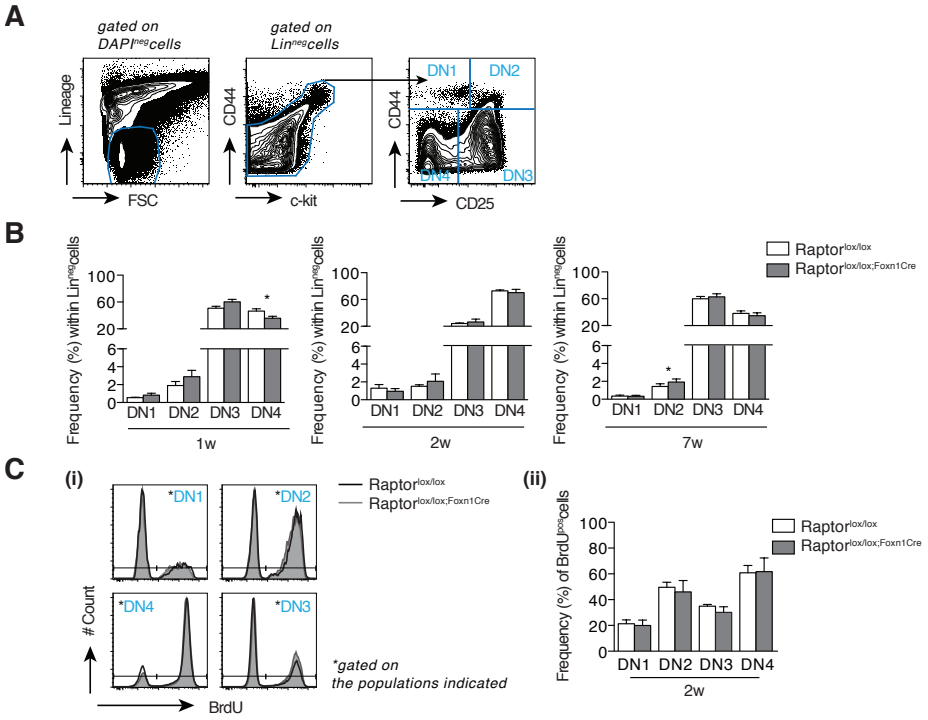

Figure 3.14: Unaltered early thymocyte development in Raptor$^{lox/lox;Foxn1Cre}$ mice; (A) FACS plot of wild type mice illustrate gating strategy and definition of thymocyte subsets, based on the absence of Lineage markers (CD3, CD4, CD8, CD11b, CD11c, CD19, B220, Dx5, Nk1.1, Gr1, Ter119, F4/80, TCRα/β, TCRγ/δ), and the expression of c-kit, CD44 and CD25. **(B)** Frequencies of double negative (DN) subpopulations DN1–DN4 among the Lineage^{neg} cells in the thymus of Raptor$^{lox/lox}$ and Raptor$^{lox/lox;Foxn1Cre}$ mice of the age indicated. Values represent mean plus SD. The number of mice analysed per experiment is $n = 4$ (Raptor$^{lox/lox}$ mice) and $n = 4$ (Raptor$^{lox/lox;Foxn1Cre}$ mice) at 1 week, $n = 3$ (Raptor$^{lox/lox;}$ mice) and $n = 5$ (Raptor$^{lox/lox;Foxn1Cre}$ mice) at 2 weeks, and $n = 4$ (Raptor$^{lox/lox}$ mice) and $n = 4$ (Raptor$^{lox/lox;Foxn1Cre}$ mice) at 7 weeks. **(C)** Incorporation of BrdU after a 4 hours chase (1mg/mouse i.p.). (i) Histograms for BrdU signal within the DN1–DN4 subset of 2 week old Raptor$^{lox/lox}$ (black line) and Raptor$^{lox/lox;Foxn1Cre}$ mice (grey area). (ii) Frequencies of BrdU^{pos} thymocytes of the individual DN subsets shown as mean plus SD. (Per experimental group. 4 mice have been analysed; p values were determined by Student's t test with $*p < .05$; $**p < .01$; $***p < .005$)

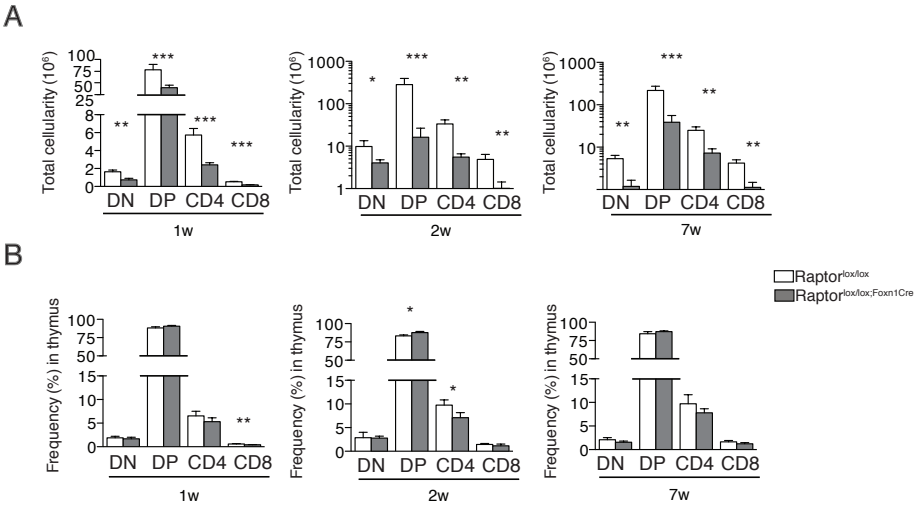

Figure 3.15: No block in the transition of DN to SP thymocytes in Raptor$^{lox/lox;Foxn1Cre}$ mice; (A) Absolute number of thymocytes (DN–SP) within thymi of Raptor$^{lox/lox}$ and Raptor$^{lox/lox;Foxn1Cre}$ mice of 1, 2 and 7 weeks of age determined by flow cytometric analysis of surface expression of CD4 and CD8. **(B)** Relative frequencies of DN, DP, CD4 SP and CD8 SP thymocytes at 1, 2, and 7 weeks of age. Values were indicated as mean plus SD. The number of mice analysed per experiment is $n = 4$ (Raptor$^{lox/lox}$ mice) and $n = 4$ (Raptor$^{lox/lox;Foxn1Cre}$ mice) at 1week, $n = 3$ (Raptor$^{lox/lox;}$ mice) and $n = 5$ (Raptor$^{lox/lox;Foxn1Cre}$ mice) at 2 weeks, and $n = 4$ (Raptor$^{lox/lox}$ mice) and $n = 4$ (Raptor$^{lox/lox;Foxn1Cre}$ mice) at 7 weeks.

sentation of immature CD4^{pos} and CD8^{pos} thymocytes was observed with 69.5 % ±1.2% immature cells within the CD4 lineage in wild type mice and 72.2 % ± 3.6% in mutant mice and 32.2% ±3.7% immature cells within the CD4 lineage in wild type and 37.0 % ±6.6% in Raptor$^{lox/lox;Foxn1Cre}$ mice. At 2 weeks, the proportion of immature CD4^{pos} thymocytes had significantly increased from 67.3 % ±1.6% in wild type mice to 78.2% ±1.1% (***$p < .005$) in mutant mice, and at 7 weeks from 64.0 % ±3.2% wild type mice to 75.1% ±4.3% (**$p < .01$) in age-matched mutant mice. The frequencies of immature SP cells within the CD8 lineage increased at 2 weeks from 32.9% ±3.4% in wild type to 42.6% ±2.9% (*$p < .05$) in mutant mice and from 30.2% ±2.1% in wild type mice to 41.1% ±3.2% (**$p < .01$) in Raptor$^{lox/lox;Foxn1Cre}$ mice at 7 weeks of age. Two possible explanations may account for this increased frequency of immature SP cell in Raptor$^{lox/lox;Foxn1Cre}$ mice. DP thymocytes undergo the transition to SP thymocytes in a shorter time in comparison to wild type mice, or, alternatively, fewer immature thymocytes get negatively selected before attaining a mature SP phenotype. To investigate whether the observed overrepresentation of immature SP thymocytes can be ascribed to a slower maturation kinetic in the mutant mice, Raptor$^{lox/lox}$ and Raptor$^{lox/lox;Foxn1Cre}$ mice were exposed to BrdU (1mg/mouse i.p.) and the labelling of SP thymocytes was tested 4 days later. The frequencies of BrdU^{pos} cells within the imma-

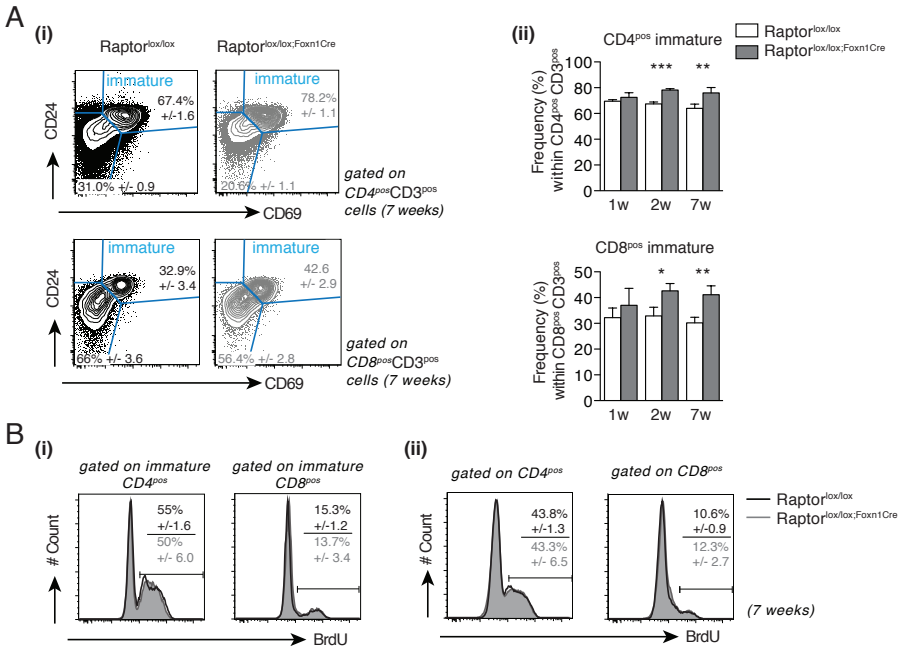

Figure 3.16: Overrepresentation of immature SP in Raptor$^{lox/lox;Foxn1Cre}$ mice; (A) (i) Flow cytometric analysis of CD4 (upper panel) and CD8 (lower panel) SP thymocytes based on the expression of CD24 and CD69 at 7 weeks. To include only thymocytes that have been positively selected, analysis included either CD4^{pos}CD3^{pos} or CD8^{pos}CD3^{pos} cells. Presence of CD24 and CD69 was indicative of an immature SP phenotype. The mean relative frequency and SD of the distinct subpopulations is provided on the respective gate. (ii) Comparison of the relative frequency of CD4^{pos}CD24^{pos}CD69^{high} (immature) thymocytes within the CD4 SP (upper graph) and CD8^{pos}CD24^{pos}CD69^{high} (immature) thymocytes within the CD8 SP cells (lower graph) in Raptor$^{lox/lox}$ and Raptor$^{lox/lox;Foxn1Cre}$ mice of 1, 2 and 7 weeks. **(B)** (i) Histogram displaying BrdU signal in CD4 and CD8 immature SP (i) or all CD4 and CD8 SP of Raptor$^{lox/lox}$ (black line) and Raptor$^{lox/lox;Foxn1Cre}$ mice (grey area) after a 4 days pulse of BrdU (2x 1mg/mouse within 4h). The mean relative frequency and SD of BrdU^{pos} cells within CD4 and CD8 SP is indicated on the respective histogram; Raptor$^{lox/lox}$ mice (black), Raptor$^{lox/lox;Foxn1Cre}$ (grey). Values were indicated as mean plus SD. Each experimental group consisted of at least 3 mice. p values were determined by Student's t test with $*p < .05$; $**p < .01$; $***p < .005$)

ture CD4 and CD8 SP cells of Raptor$^{lox/lox}$ and Raptor$^{lox/lox;Foxn1Cre}$ mice were identical for both strains of mice (Fig. 3.16 B (i), (ii)), thus excluded an altered maturation kinetic during positive selection. These data indicate that despite an altered microenvironment, thymi of Raptor$^{lox/lox;Foxn1Cre}$ mice support DP to SP transition accurately.

In contrast to mature SP cells, immature SP thymocytes are subjected to negative selection (Weinreich and Hogquist, 2008). Downregulation of CD69, and therefore the development from an immature to a mature state, represents a cell-intrinsic process within a defined time course of two to three days (Yamashita et al., 1993). Thus, it is likely that an increase in the frequency of immature SP thymocytes is caused by a less efficient elimination of immature SP during negative selection. To address this question, RTOC will be prepared from thymocyte-depleted E14 thymic lobes and mixed at similar ratio with sorted immature CD4^{pos} cells of Raptor$^{lox/lox;Foxn1Cre}$ and of wild type mice (with CD45.1 congenital marker). If, indeed, autoreactive T-cell clones contribute to the immature T-cell pool, the immuno-competent wild type stroma will eliminate these cells, which will be reflected in an altered ratio of wild-type to mutant-derived thymocytes.

3.3.4 Thymocyte egress

To examine a further explanation for the higher frequency of immature SP thymocytes, thymocyte exit was investigated next in wild type and mutant mice. Mature SP cells upregulate the expression of the sphingosine-1-phosphate receptor (S1P1) on their cell surface, which is a prerequisite for their egress. S1P1 binds to S1P released by neural crest-derived pericytes, which are specialized cells ensheathing blood vessels. Detection of S1P1 on mature thymocytes revealed that the relative frequency of S1P1 expressing mature CD4^{pos} and CD8^{pos} SP thymocytes was significantly reduced in Raptor$^{lox/lox;Foxn1Cre}$ thymi compared to wild type (Fig. 3.17 A (i), (ii)).

Immunohistology further illustrated that thymi of Raptor$^{lox/lox;Foxn1Cre}$ mice display a higher density of vasculature and an increased number of pericytes in the medulla (Fig. 3.17 B), providing an indirect evidence for an increased concentration of S1P in the medulla of mutant mice.

Together, these data suggest that an accelerated egress of mature SP thymocytes in Raptor$^{lox/lox;Foxn1Cre}$ mice accounts additionally for the decrease in mature SP cells observed in mutant mice.

3.3.5 TEC differentiation and maintenance

TEC subpopulations

The separation of cTEC and mTEC into distinct maturational stages can be further refined using additional cell surface and cytoplasmic markers. Major histocompatibility complex class II molecules (MHCII) are commonly

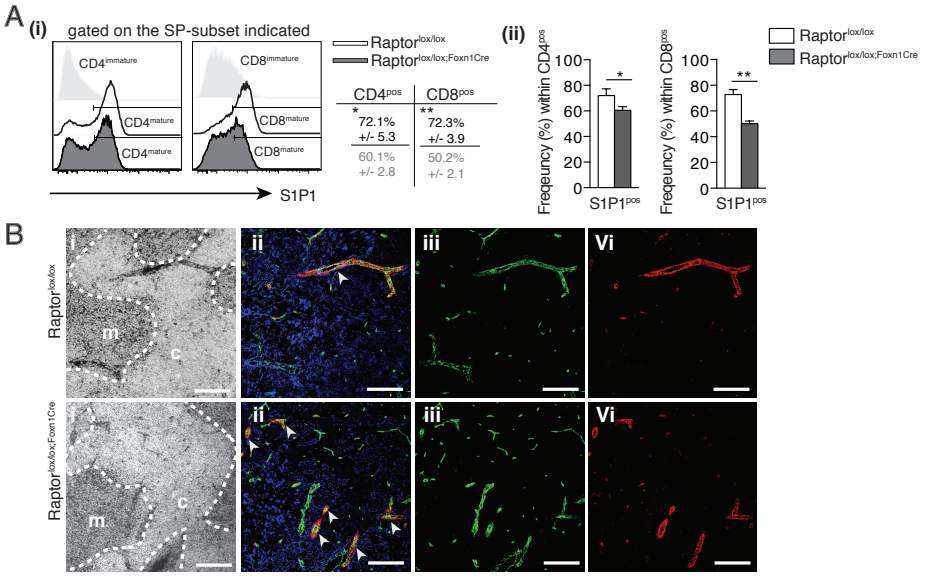

Figure 3.17: Mature SP thymocytes from Raptor$^{lox/lox;Foxn1Cre}$ express less S1P1; (A) (i-ii) Representative histograms depicting S1P1 expression on mature CD4^{pos} and CD8^{pos} thymocytes in wild type and mutant mice. S1P1 expression profile of immature SP thymocytes of wild type mice were included (grey) to compare S1P expression intensities. The mean relative frequencies and SD are indicated in a table and illustrated in bar graphs. p values were determined by Student's t test with $*p < .05$; $**p < .01$; $***p < .005$). **(B)** Confocal microscopy of thymic tissue sections (8 µm) stained for DAPI, panKeratin (blue), CD31 (green) and Ng2 (red). Stainings were shown separately for selective colors; DAPI *(I)*, merge of all colors (panKeratin, CD31 and Ng2) *(II)*, CD31 *(III)* and Ng2 *(IV)*. "c" denotes cortex, "m" denotes medulla, white arrow heads mark pericytes. Dashed white line encircles thymic medulla. Scalebar indicates 50µm.

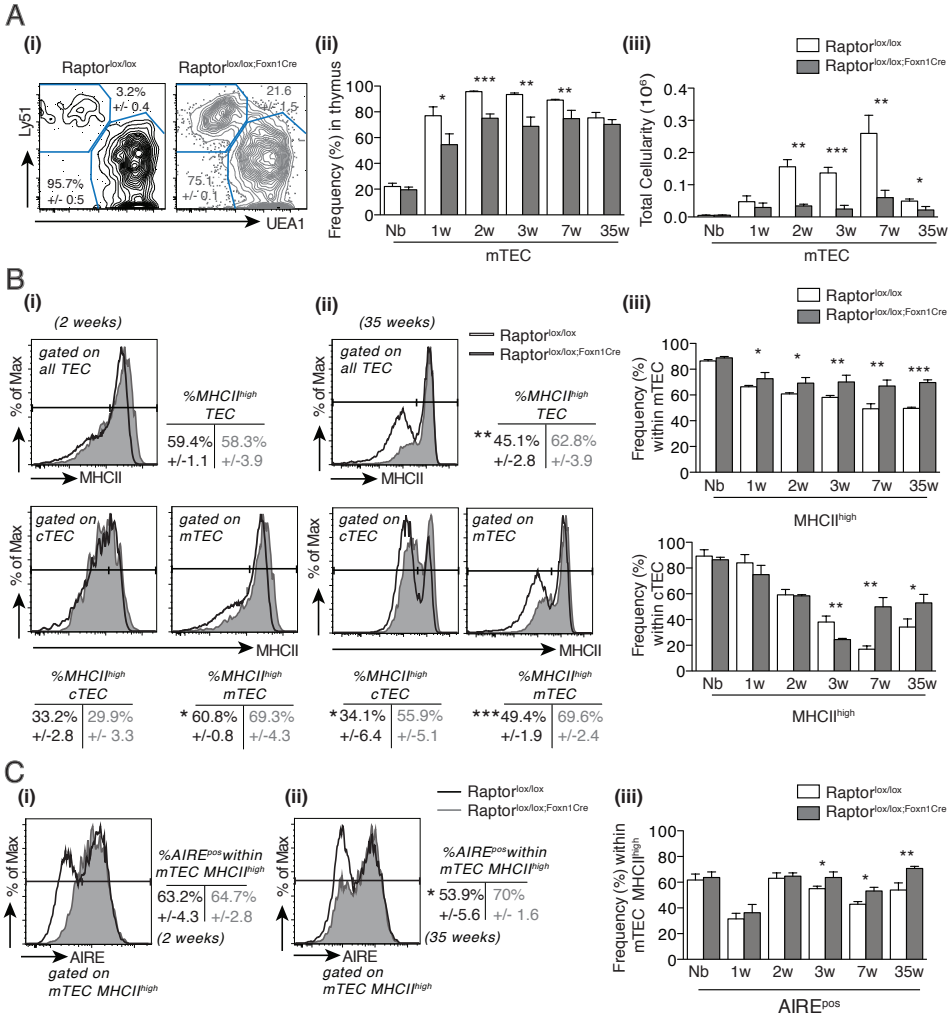

Figure 3.18: Phenotypical characterization of raptor-deficient TEC over time in comparison the wild type TEC; (A) (i) FACS plots of TEC ($CD45^{neg}EpCAM^{pos}$) of $Raptor^{lox/lox}$ (black) and $Raptor^{lox/lox;Foxn1Cre}$ mice (grey), showing the representation of cTEC ($CD45^{neg}EpCAM^{pos}Ly51^{pos}UEA1^{neg}$) and mTEC ($CD45^{neg}EpCAM^{pos}Ly51^{neg}UEA1^{pos}$) within the TEC compartment at 2 weeks of age. Percentages indicated on the plots are displaying the mean frequency of the TEC subpopulation (cTEC in the upper right and mTEC in the lower left corner) ± SD. Frequencies (i) and absolute number (ii) of mTEC in $Raptor^{lox/lox}$ and $Raptor^{lox/lox;Foxn1Cre}$ mice at the time points indicated. **(B)** Histogram overlays of TEC, or cTEC and mTEC, respectively from 2 weeks (i) or 35 weeks (ii) old $Raptor^{lox/lox}$ (black line) and $Raptor^{lox/lox;Foxn1Cre}$ mice (grey area). Values next to the histogram indicate the frequencies of $MHCII^{hi}$ cell as mean plus ± SD. (iii) Frequencies of $MHCII^{hi}$ expressing cells within mTEC (upper graph) and cTEC (lower graph) in $Raptor^{lox/lox}$ and $Raptor^{lox/lox;Foxn1Cre}$ mice of different ages. **(C)** Histogram overlays gated in $MHCII^{hi}$ mTEC of $Raptor^{lox/lox}$ (black line) and $Raptor^{lox/lox;Foxn1Cre}$ mice (grey area) at 2 weeks (i) and 35 weeks (ii) of age. Values next to the histogram indicate the frequencies of $AIRE^{pos}$ cells within the $MHCII^{hi}$ mTEC as mean plus ± SD. (iii) Frequency of $AIRE^{pos}$ cells within the $MHCII^{hi}$ mTEC observed in $Raptor^{lox/lox}$ and $Raptor^{lox/lox;Foxn1Cre}$ mice from newborn (Nb) to 35 weeks of age. Each experimental group consisted of at least 3 mice. p values were determined by Student's t test with $*p < .05$; $**p < .01$; $***p < .005$)

expressed on all TEC lineages, either to low or high degrees. mTEC that express low cell surface MHCII (designated mTEC^{lo}) are deemed immature, whereas MHCII high-expressing mTEC (mTEC^{hi}) are mature (Gray et al., 2007, 2006). To investigate whether the absence of Raptor reduced not only the relative and absolute number of mTEC (Fig. 3.18 A) but also impacted on their differentiation, I next determined the MHCII cell surface expression on TEC from Raptor-deficient and wild type mice of different ages (Fig. 3.18 B). There was a non-significant difference at 2 weeks and a significant change at 35 weeks of age. At the latter time point, MHCII^{hi} TEC made up for 62.8% ±3.9% of all TEC in the mutant mice in comparison to the controls (45.1% ±2.8%; $^{**}p < .01$) (Fig. 3.18 B(ii)). This regulation was next investigated separately for cTEC and mTEC. In 2 weeks old mutant mice, the frequency of MHCII^{hi} cTEC was similar to the values in wild type mice (33.2% ±2.8% in wild type mice vs. 29.9% ±3.3% in mutant mice)(Fig. 3.18 B(i)). In mice of this age, only mTEC with a MHCII^{hi} phenotype were significantly overrepresented in the Raptor-deficient animals when compared to age-matched wild type mice (60.8% ±0.8% in wild type mice vs. 69.3% ±4.3% in mutant mice; $^{*}p < .05$). In 35 week old mutant mice, the difference in the frequency of MHCII^{hi} mTEC in Raptor-deficient mice was even higher than at 2 weeks (49.4% ±1.9% in wild type mice vs. 69.5% ±2.4% in mutant mice; $^{***}p < .005$), and the increase in MHCII^{hi} cTEC in Raptor-deficient mice became significant (34.1% ±6.4% in wild type vs. 55.9% ±5.1% in mutant mice; $^{*}p < .05$). The comparison of the MHCII expression on cTEC and mTEC of wild type and mutant mice between newborn age and 35 weeks revealed that mTEC of Raptor$^{lox/lox;Foxn1Cre}$ mice displayed already from the age of 1 weeks a significant increase in MHCII^{hi} expressing cells. In contrast, MHCII^{hi} cTEC were significantly overrepresented from 3 weeks of age onwards (Fig. 3.18 B(iii)). These data suggest that the medullary expression of MHCII is much earlier affected in the absence of raptor than on cTEC.

Another marker attributed to maturity of mTEC is the Autoimmune regulator (AIRE), which has been found to be exclusively expressed in MHCII^{hi} mTEC (Gray et al., 2007; Derbinski et al., 2005) and was described to be associated with a post-mitotic, terminally differentiated TEC (Kyewski and Klein, 2006). The proportion of AIRE^{pos} mTEC was increased in mutant mice, a change which became significant at 3 weeks of age (58% ±1.6% in wild type mice vs. 70.2% ±5.3% in Raptor$^{lox/lox;Foxn1Cre}$ mice; $^{*}p < .05$)(Fig. 3.18 C (i), (ii, (iii)). This significant difference in AIRE^{pos} cells increased continuously (8.5% at 3weeks, 16.8% at 35 weeks).

A subclassification of cTEC subpopulations by FACS has recently been proposed (Shakib et al., 2009) and takes advantage of a differential CD40 expression with immature cTEC lacking this co-stimulatory ligand, whereas mature cTEC express this molecule. The comparison of Raptor$^{lox/lox}$ and Raptor$^{lox/lox;Foxn1Cre}$ mice 2 weeks and 35 weeks of age for the presence

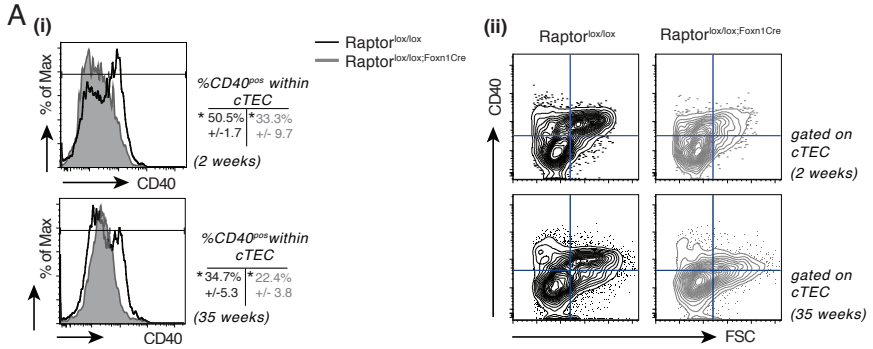

Figure 3.19: Lack of CD40 expression in cTEC of Raptor$^{lox/lox;Foxn1Cre}$ mice; (A) (i) histogram overlays depicting the expression of CD40 in cTEC of Raptor$^{lox/lox}$ and Raptor$^{lox/lox;Foxn1Cre}$ mice at 2 and 35 weeks. (ii) FACS plots illustrating the relation of CD40 expression and size (FSC) in cTEC of Raptor$^{lox/lox}$ and Raptor$^{lox/lox;Foxn1Cre}$ mice at 2 and 35 weeks. Each experimental group consisted of at least 3 mice. p values were determined by Student's t test with $*p < .05$; $**p < .01$; $***p < .005$)

of CD40 on cTEC demonstrated that these mature cortical epithelia were largely missing in the mutant mice at each time point investigated (Fig. 3.19 A (i)). Moreover, a correlation between TEC size and CD40 expression levels was observed (Fig. 3.19 A (ii)), which suggests that Raptor-deficiency impacts on one or both parameters.

Thymic nurse cells

Within the thymic microenvironment, specialized cTEC have been identified that completely embody various numbers of developing thymocytes. Termed "nurse cells" (Wekerle and Ketelsen, 1980; Kyewski et al., 1981; Hirokawa et al., 1986), these cells are thought to optimize the process of positive T-cell selection (Nakagawa et al., 2012). To visualize these nurse cells, TEC were sorted and subsequently placed on a glass slide (cytospin). Closed cell complexes were then detected by light microscopy (Fig. 3.20A). To characterize the cells captured by the nurse cells in more detail, the cell complexes were stained for DAPI, CD45, keratin 5 and 8 (Fig. 3.20 B). The analysis revealed numerous hematopoietic cells (CD45^{pos}, DAPI ^{pos}) captured by cortical TEC (K8^{pos}). At present, the specific stages of thymocytes nursed by cTEC have not yet been determined.

To investigate whether the lack of mTORC1 signalling in TEC has an impact on the ability of cTEC to form nurse cell complexes, thymic cell suspension of wild type and Raptor$^{lox/lox;Foxn1Cre}$ mice were quantified by FACS (Fig. 3.21 A). Wild type mice displayed 11.4% nurse cells within the cTEC compartment. In contrast, cTEC of Raptor$^{lox/lox;Foxn1Cre}$ mice displayed only about 4% nurse cells. The correct gating was confirmed by comparison of SSC/FSC profiles of nurse cells and TEC in both mouse strains (Fig. 3.21 B). From these data, it can be concluded that less thymic nurse

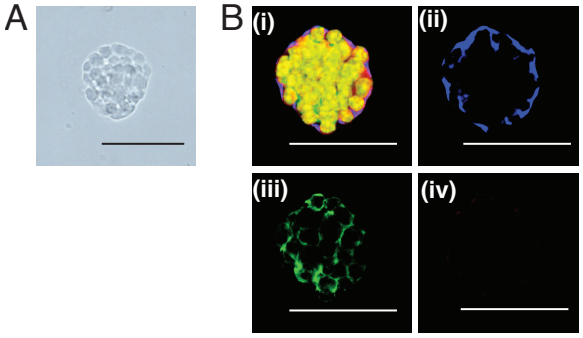

Figure 3.20: Characterization of thymic nurse cells; (A) Light microscopic picture of a thymic nurse cell, located on a cytospin of sorted TEC ($CD45^{neg}EpCAM^{pos}$) of a wild type mouse. Confocal microscopic picture **(B)** of thymic nurse cell, stained for DAPI **(i)**, K8 **(ii)**, CD45 **(iii)** and K5 **(iv)**. Scale-bar indicates 50μm.

cells can be found in thymi composed of raptor-deficient TEC compared to wild type.

3.3.6 Chemokinetic function of TEC

To orchestrate the complex process of T-cell precursor attraction, thymocyte maturation and emigration, signals are in place that emanate from the thymic stroma and control these processes. TEC represent the main source of chemo-attractants enabling heamatopoietic precursor cells to continuously colonize the thymus. There was a direct correlation between total thymic cellularity and the total number of early thymic precursors (ETP) within the thymi of $Raptor^{lox/lox;}$ and $Raptor^{lox/lox;Foxn1Cre}$ mice. This implies that the number of thymocyte precursors that enter the thymus is eventually shaping the size of the thymus (Fig. 3.22 A). Raptor-mutant mice had fewer ETP (vs. in wild type mice) both when compared to thymus cellularity and to the number of TEC (Fig. 3.22 B (i), (ii), (iii)), though the latter correlation was only observed in mice older than 2 weeks of age (Fig. 3.22 B (i)). Taken together, these data strongly indicate that the loss of Raptor expression in TEC results in a qualitative change that impairs the attraction of T-cell precursors.

Next, I assessed the expression of chemokines in TEC using qPCR. Previous analysis revealed the presence of nurse-cell-thymocyte complexes within the cTEC compartment. Therefore, chemokine-transcript levels of cTEC were normalized to EpCAM, whose expression was shown to be independent of Raptor (Fig. 3.22 C (i)).

In a first experiment, the main cellular source for chemoattractants was identified. For this purpose, chemokine transcript levels of sorted wild-type cTEC and mTEC were compared to transcript levels detected in unsorted total thymic cells. In wild type mice, Cxcl12 and Ccl25 were abundantly expressed in cTEC, whereas transcripts for Ccl19 and Ccl21 were typically detected in mTEC (Fig. 3.22 C (ii)). In the absence of Raptor expression, the levels of all chemokine transcripts were decreased in cTEC, with the exception of Ccl21. The identical analysis in mTEC demonstrated that

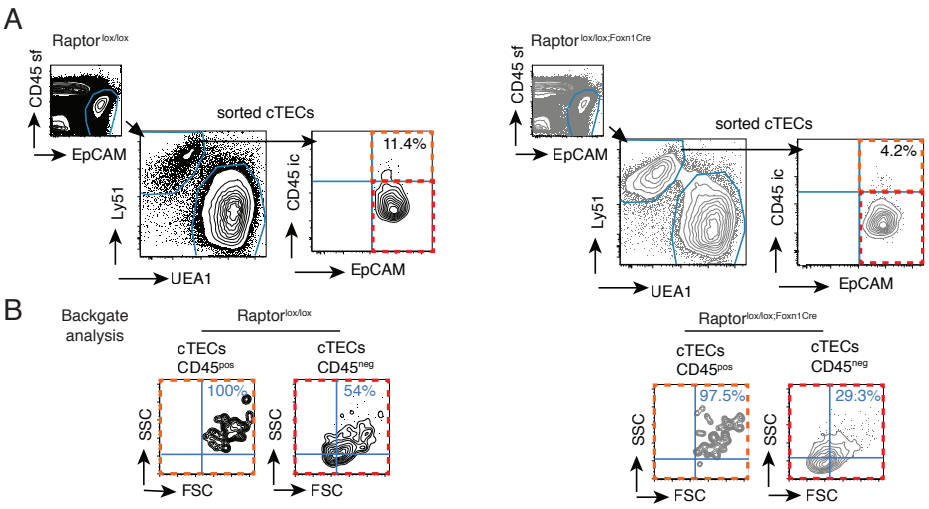

Figure 3.21: Raptor$^{lox/lox;Foxn1Cre}$ mice display less thymic nurse cells; (A) FACS plots of Raptor$^{lox/lox}$ mice (black) and Raptor$^{lox/lox;Foxn1Cre}$ mice (grey) illustrating gate- and staining strategy. cTEC, discriminated by surface staining for CD45, EpCAM, Ly51 and UEA1 as CD45^{neg}EpCAM^{pos}Ly51^{pos}UEA1^{neg}cells, were sorted and intracellularly stained for CD45. Using different dyes conjugated to CD45, cell surface and intracellular CD45 staining could be discriminated. The re-stained cTEC were re-analysed by FACS. The percentage of intracellular (ic) CD45^{pos}EpCAM^{pos} re-analysed cTEC is indicated as percentage in the upper right quadrant of then FACS plot. Orange and red boxed areas are referring to the backgate analysis depicted in **(B)**. Backgate analysis of Side Scatter (SSC) and Forward Scatter (FSC) illustrate the size of cTEC CD45^{pos} (orange box) and cTEC CD45^{neg} (red box) of Raptor$^{lox/lox}$ mice and Raptor$^{lox/lox;Foxn1Cre}$ mice.

the Ccl21 transcripts were unchanged, whereas those for Cxcl12 were significantly decreased, and those for Ccl19 and Ccl25 mildly increased. IL-7 transcripts were halved in cTEC from Raptor$^{lox/lox;Foxn1Cre}$ mice. Raptor-deficient mTEC produced about twice as many IL-7 transcripts compared to wild type mTEC. Taken together, mTORC1 signalling-deficient TEC are impaired in the transcription of factors necessary to attract T-cell precursors to the thymic microenvironment (Cxcl12, Ccl19, Ccl25) and to promote their survival *in situ* (IL-7).

3.3.7 TEC size

The size of an organ is regulated by two individual parameters, namely the number of cells and their size. A lack of mTORC1-signalling in TEC significantly reduced thymic size and this decrease correlated with an overall reduction in absolute cell number. An inhibition of mTORC1 has also been associated with a reduction of cell size. The precise mechanism remains, however, poorly understood (Fingar et al., 2004; Fumarola et al., 2005). In drosophila, the mTOR homolog dTOR is cell autonomously required for normal cell growth during larval development (Zhang et al., 2000). A loss-of-function mutant of dTOR results in substantial decrease in both, cell number and cell size. To investigate, whether the inhibition of mTORC1 signalling in TEC also influences cellular size, TEC were assessed by light microscopy and FACS for their size (Fig. 3.23 A, B). For this purpose, sorted TEC of Raptor$^{lox/lox}$ and Raptor$^{lox/lox;Foxn1Cre}$ mice were cytospun and stained for hematoxylin and eosin. Light microscopy revealed Raptor-deficient TEC to be smaller than TEC of wild type animals (Fig. 3.23 A). However, due to the exposure to fixatives and high centrifugal forces during spinning, preparation-associated artifacts could not be excluded as a cause for the observed differences. For an independent and likely more reliable measurement of sizes, the mean fluorescence intensities (MFI) of the TEC forward scatter (FSC) was determined, using flow cytometry (Fig. 3.23 B (i), (ii)). TEC size was identical for mutant and wild type TEC at prenatal stages. A decrease in TEC size was observed in postnatal TEC of Raptor$^{lox/lox;Foxn1Cre}$ mice (Fig. 3.23 B (i)). In view of the heterogenous composition of the TEC compartment in general and the genotype-related overrepresentation of specific TEC subpopulations in particular, the cell size of cTEC and mTEC from mutant mice were separately analysed (Fig. 3.23 B (ii)). To quantify the cell size reduction, cTEC and mTEC sizes of Raptor$^{lox/lox;Foxn1Cre}$ mice were compared to that of the respective TEC subpopulations in wild type mice. Statistical analysis revealed a reduction of TEC size of about 10% in the mutant mice of one week and older. This reduction was marginally more pronounced for cTEC. Because cell size varies during cell cycle, cell size of mTORC1-sufficient and -deficient TEC was determined in relation to the stage within the cell cycle. TEC size was reduced in all stages of the cell cycle

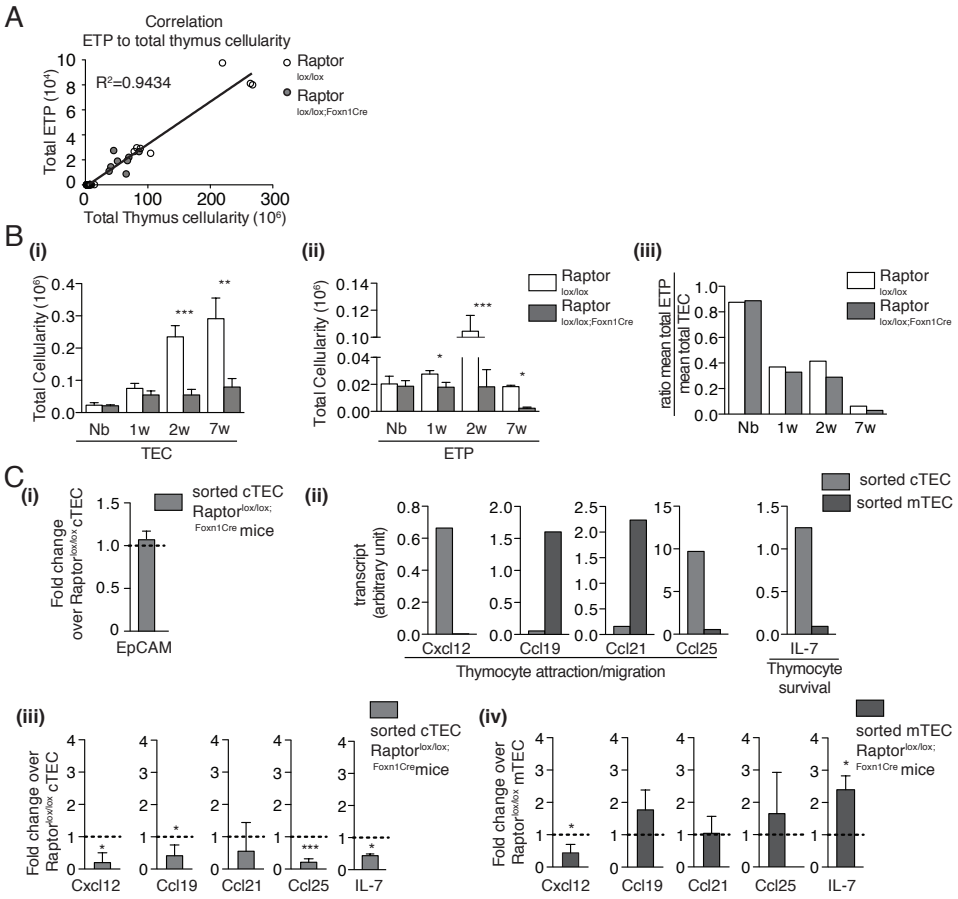

Figure 3.22: TEC of Raptor$^{lox/lox;Foxn1Cre}$ mice have impaired capacity of precursor attraction; (A) Correlation between number of total ETP and total thymic cellularity in Raptor$^{lox/lox;}$ (white circle) and Raptor$^{lox/lox;Foxn1Cre}$ mice (grey circle). **(B)** Total cellularity of TEC (i) and ETP (ii) in Raptor$^{lox/lox;}$ and Raptor$^{lox/lox;Foxn1Cre}$ mice. Values were indicated as mean plus SD. Each experimental group consisted of at least 3 mice. p values were determined by Student's t test with $*p < .05$; $**p < .01$; $***p < .005$) (iii) Ratio of the mean absolute number of ETPs to the mean absolute number of TEC in Raptor$^{lox/lox;}$ and Raptor$^{lox/lox;Foxn1Cre}$ mice. **(C)** Result of qPCR analysis of sorted cTEC and mTEC. (i) Amount of EpCAM transcript present in sorted cTEC of Raptor$^{lox/lox;Foxn1Cre}$ mice normalized to values found in sorted cTEC of Raptor$^{lox/lox;}$ mice. (ii) Fold change of various transcripts in sorted cTEC (light grey) and mTEC (dark grey) of Raptor$^{lox/lox;Foxn1Cre}$ mice compared to total wild type thymus. Fold change of transcripts in cTEC (iii) and mTEC (iv) of Raptor$^{lox/lox;Foxn1Cre}$ mice compared to Raptor$^{lox/lox;}$ mice. Values are means of at least three independent experiments; indicated plus SD. p values were determined by Student's t test with $*p < .05$; $**p < .01$; $***p < .005$)

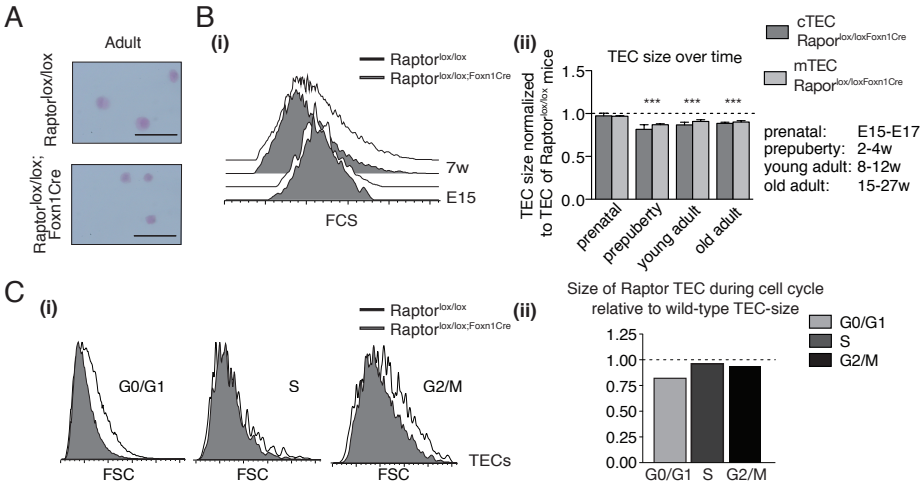

Figure 3.23: TEC of Raptor$^{lox/lox;Foxn1Cre}$ mice are smaller than wild type TEC; (A) Hematoxylin Eosin staining of sorted TEC (CD45^{neg}EpCAM$^{pos)}$ of adult Raptor$^{lox/lox}$ and Raptor$^{lox/lox;Foxn1Cre}$ mice. Scale bar indicates 50 μm. **(B)** (i) FACS histogram overlays, displaying the forwards scatter (FCS) of TEC at gestational day 15 and at 7 weeks of age in Raptor$^{lox/lox}$ (black line) and Raptor$^{lox/lox;Foxn1Cre}$ mice (grey area). (ii) Comparison of the mean fluorescence intensity (MFI) for the FCS of Raptor-sufficient and Raptor-deficient cTEC (dark grey) and mTEC (light grey) at the ages indicated. Mean values for the size of Raptor-deficient cTEC and mTEC were normalized to values evaluated from the respective TEC subpopulation in wild type TEC. **(C)** (i) FACS histogram overlays, comparing the sizes of TEC originating from Raptor$^{lox/lox}$ (black line) or Raptor$^{lox/lox;Foxn1Cre}$ mice (grey area) at different stages of the cell cycle. Cell cycle phases were determined by PI staining. (ii) Comparison of Raptor$^{lox/lox}$ and Raptor$^{lox/lox;Foxn1Cre}$ mice TEC cell size during cell cycle. Values of the FSC MFI of Raptor$^{lox/lox;Foxn1Cre}$ TEC were normalized to FSC MFI measured in Raptor$^{lox/lox}$ TEC. p values were determined by Student's t test with $^{*}p < .05$; $^{**}p < .01$; $^{***}p < .005$)

in the absence of Raptor with the largest impact observed for cells residing in G0/G1-phase and the smallest changes noted for the S-phase. This result is in agreement with in vitro studies analysing Jurkat cells treated with the mTOR-inhibitor Rapamycin (Fingar et al., 2004). Thus, Raptor expression in TEC determines cell size, and its absence correlates with a smaller cell volume at any stage of the cell cycle.

3.3.8 TEC cell cycle

The inhibition of mTOR-signalling impairs proliferation. Therefore, I next investigated, whether thymic hypoplasia observed in Raptor$^{lox/lox;Foxn1Cre}$ mice was related to reduced TEC proliferation. For this purpose, Raptor$^{lox/lox}$ and Raptor$^{lox/lox;Foxn1Cre}$ mice were injected with BrdU (1mg/mouse i.p.) and the incorporation of label was analysed 4 hours later. At the age of 2 days, the absolute number of BrdU^{pos} cTEC and mTEC were identical to that of age-matched controls (Fig. 3.24). However, a significant reduction in spontaneous cell proliferation was revealed in 1 and 3 week old mutant mTEC (Fig. 3.11 A and B). In contrast, the cell proliferation of cTEC was

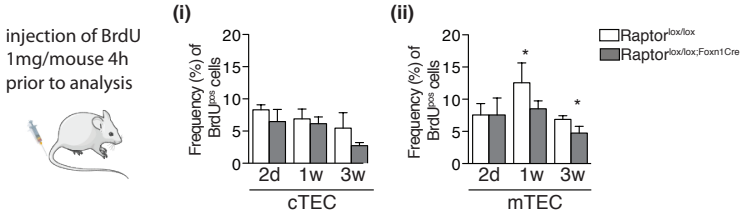

Figure 3.24: TEC of in Raptor$^{lox/lox;Foxn1Cre}$ mice proliferate less than TEC of age-matched Raptor$^{lox/lox}$ mice measured by incorporation of BrdU; Raptor$^{lox/lox}$ and Raptor$^{lox/lox;Foxn1Cre}$ mice of different ages were injected with 1mg BrdU/mouse 4h prior to analysis.**(A)** Frequency of BrdU^{pos} cTEC (i) and mTEC (ii) at the time points indicated. Values were indicated as mean plus SD. Each experimental group consisted of at least 3 mice. p values were determined by Student's t test with $*p < .05$; $**p < .01$; $***p < .005$)

not impaired due to the absence of Raptor. This latter finding is in line with the observation that cTEC in Raptor$^{lox/lox;Foxn1Cre}$ mice and Raptor$^{lox/lox}$ mice have identical cTEC numbers. Taken together, mTORC1 signalling is essential for the proliferation of mTEC, providing an explanation for the particular reduction of mTEC in Raptor$^{lox/lox;Foxn1Cre}$ mice.

3.3.9 TEC response to acute stress

Changes in organ cellularity can generally be attributed to differences in either cell proliferation and/or in cell death. To address changed susceptibility for programmed cell death between TEC with a functional or a non-functional mTORC1 signalling, respectively, the presence of cleaved caspases and Terminal deoxynucleotidyl transferase dUTP nick end labeling (TUNEL) were sought by flow cytometry. Since this analysis requires a cell isolation step, during which the TEC are exposed to enzymes and mechanical stress, the presence of activated caspases was reflective of the general capacity of TEC to cope with acute cell stress. First, the influence of mTOR signalling on TEC viability was assessed. For this purpose, TEC from 2 days old mice — representative for a time point before the ablation of Raptor results in a discernible phenotype — and 3 weeks old mice were analysed. The activation of caspases was indistinguishable between 1 week old mutant and wild type mice. However, a significant difference was observed in 3 weeks old animals as 62.5% ±4.2% CaspACE^{pos} cells were recovered in Raptor$^{lox/lox}$ mice and 42.6% ±1.9% CaspACE^{pos} TEC from Raptor$^{lox/lox;Foxn1Cre}$ mice ($*p < .05$) (Fig. 3.25) A (i), (ii)).

To exclude the possibility that differences in thymus size influenced the accessibility of TEC and therefore facilitated the digest procedure, an additional control experiment was carried out isolating TEC from a comparable thymus "cell mass" (i.e. one Raptor$^{lox/lox}$ thymus and a pool of three Raptor$^{lox/lox;Foxn1Cre}$ thymi were prepared in parallel). The differences seen in the previous experiments continued to be observed between Raptor$^{lox/lox}$ and Raptor$^{lox/lox;Foxn1Cre}$ mice, with TEC lacking Raptor dis-

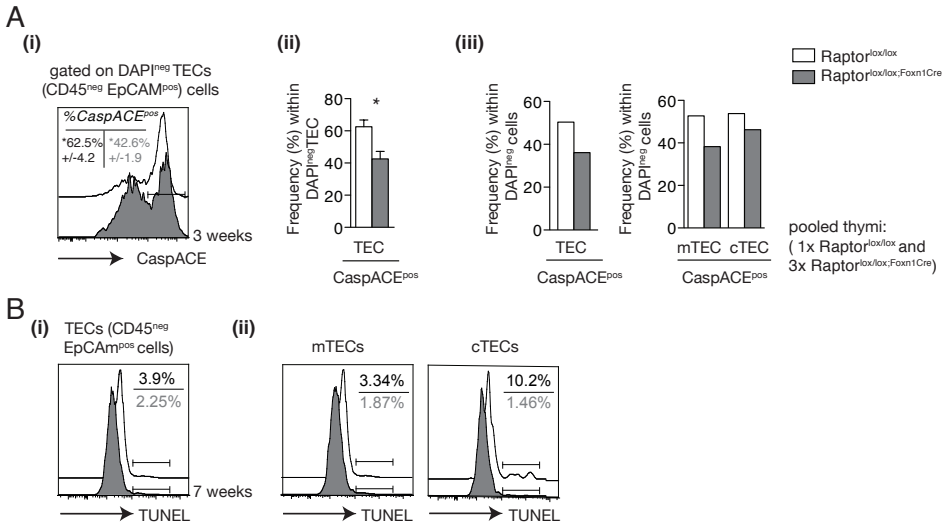

Figure 3.25: TEC of Raptor$^{lox/lox;Foxn1Cre}$ mice are less susceptible to stress-induced apoptosis than wild type TEC; (A) (i) Histogam overlay for CaspACE signal in TEC of 3 week old Raptor$^{lox/lox}$ (black line) and Raptor$^{lox/lox;Foxn1Cre}$ mice (grey area). To exclude dead cells from the analysis, only DAPI^{neg} cell were analysed. The percentages indicated on the FACS plot represent the mean values of CaspACE^{pos} cells within TEC ± SD. (ii) Comparison of the frequency of CaspACE^{pos} TEC among Raptor-sufficient and Raptor-deficient TEC after a routine TEC isolation procedure. Values were indicated as mean plus SD. Each experimental group consisted of at least 3 mice. p values were determined by Student's t test with $*p < .05$; $**p < .01$; $***p < .005$)(iii) Values were indicated as mean plus SD. (iii) Comparison of the frequency of CaspACE^{pos} TEC among Raptor-sufficient and Raptor-deficient TEC after a routine TEC isolation procedure starting with an approximately similar number of thymic cells for isolation. **(B)** Histogram overlay displaying TUNEL^{pos} cells among TEC (i), or cTEC and mTEC (ii) of Raptor$^{lox/lox}$ (black line) and Raptor$^{lox/lox;Foxn1Cre}$ mice (grey area). The percentages indicated on the FACS plot represent the mean values of TUNEL^{pos} cell within TEC ± SD.

playing a higher resistance to cell stress.

Next, a TUNEL-staining of mutant and wild type TEC was performed, in order to assess apoptosis and cell death not only by detection of activated caspases, which occur very early after cell damage, but also by analysis of substrates generated at the end of the apoptotic signalling cascade, like DNA fragments. TUNEL-positivity was observed in 3.9% of TEC from Raptor$^{lox/lox}$ and 2.2% TEC from Raptor$^{lox/lox;Foxn1Cre}$ mice (Fig. 3.25 B (i)). This difference held up when analysing cTEC and mTEC separately: (3.34% mTEC in wild type and 1.87% mTEC in Raptor$^{lox/lox;Foxn1Cre}$ mice were TUNEL positive, while 10.2% cTEC in wild type and 1.5% cTEC in Raptor$^{lox/lox;Foxn1Cre}$ mice were detected (Fig. 3.25) B (ii)).

These data have shown Raptor-deficient TEC to be less susceptible to acute stress and apoptosis than TEC of wild type littermates, arguing against the hypothesis that thymic hypoplasia might be attributed to an increase in TEC cell death (Fig. 3.25 A (iii)).

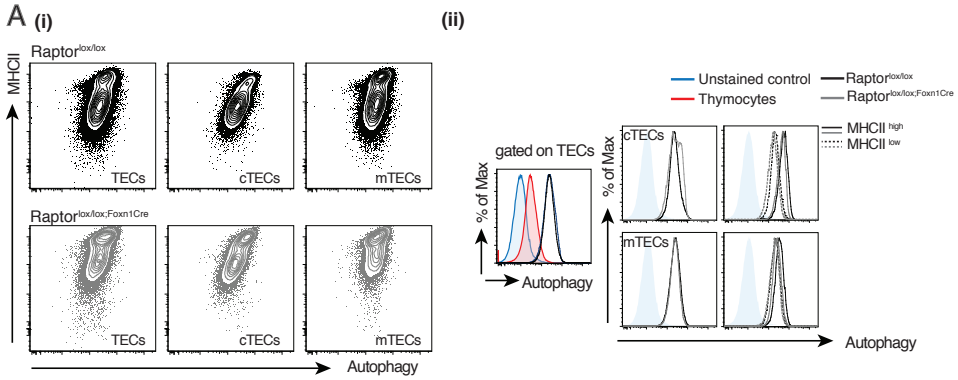

Figure 3.26: Autophagic activity is highest in MHCII^{high} cTEC, but unaltered in the presence or absence of Raptor protein in TEC; FACS analysis of autophagy in TEC and TEC subsets. **(A)** (i) FACS plots illustrating the relation between MHCII expression and autophagic activity in TEC (CD45^{neg}EpCAM^{pos}) cTEC (CD45^{neg}EpCAM^{pos}UEA1^{neg}Ly51^{pos}) and mTEC (CD45^{neg}EpCAM^{pos}UEA1^{pos}Ly51^{neg}) of adult (7w) Raptor$^{lox/lox}$ (black) and Raptor$^{lox/lox;Foxn1Cre}$ mice (grey). (ii) Histogram overlays for autophagic activity of TEC, or cTEC and mTEC, respectively of Raptor$^{lox/lox}$ (black) and Raptor$^{lox/lox;Foxn1Cre}$ mice (grey). Autophagic activity of MHCII^{high} or MHCII^{low} cTEC or mTEC is indicated as dotted line in either black (Raptor$^{lox/lox}$) or grey (Raptor$^{lox/lox;Foxn1Cre}$). Unstained control TEC are represented by a blue line, stained thymocytes by a red line.

3.3.10 Autophagy in TEC

mTOR is a negative regulator of cellular autophagy (Nazio et al., 2013). Therefore, the autophagic activity of Raptor-deficient and Raptor-proficient TEC was compared. Using a dye that selectively labels autophagic vacuoles, such as pre-autophagosomes, autophagosomes, and autolysosomes, the autophagic flux was measured.

To increase the number of cells and therefore the reliability of the analysis, thymi from 7 weeks old Raptor$^{lox/lox}$ and Raptor$^{lox/lox;Foxn1Cre}$ mice, respectively, were pooled for the following investigations.

In contrast to most cells, TEC display already very high basal activity of autophagy, which is linked to their generation of peptide/MHC class II ligands and their role as antigen presenting cells. The analysis included as controls unstained TEC and stained thymocytes to test the specificity and significance of the signals observed with staining of autophagic vacuoles in TEC. The autophagy signal was higher in mature TEC and more prounced in the cortial epithelia in comparison to medullary TEC (3.26 A (i)). Autophagy was increased in both, wild type and mutant TEC when compared to that in thymocytes, but did not differ between Raptor-sufficient and Raptor-deficient epithelia (3.26 A (ii)). On closer examination, a distinct “shoulder” in the histogram of cTEC from mutant mice was observed in comparison to corresponding epithelia from wild type mice, suggesting a possible higher autophagy in the former cells. Further analysis revealed, however, that both mature and immature cTEC displayed the same degree

of autophagy. Thus, the overrepresentation of MHCII^{hi} expressing cTEC in Raptor$^{lox/lox;Foxn1Cre}$ likely accounts for the mild difference in signal observed when analysing unseparated cTEC.

3.4 Peripheral T-cell function in mice deficient for Raptor expression in TEC

Thymi from Raptor$^{lox/lox;Foxn1Cre}$ mice older than 1 week of age are lymphopenic. To test how this influenced the peripheral T-cell compartment, the spleen and lymphnodes of mutant and control mice were next investigated. A significant decrease regarding the absolute number of CD4^{pos} and CD8 ^{pos} splenocytes was discernible in Raptor$^{lox/lox;Foxn1Cre}$ mice from 1 week onwards. In 35 weeks old mice, the total number of T-cells was comparable for both types of mice analysed (Fig. 3.27 A (i),(ii)). The frequencies of CD4^{pos} and CD8 ^{pos} splenocytes, however, were at all investigated time points identical in Raptor$^{lox/lox}$ and Raptor$^{lox/lox;Foxn1Cre}$ mice (Fig. 3.27 B (i),(ii)).

A closer look at the CD4^{pos} T-cell compartment revealed a shifted representation of the CD4^{pos} subpopulations in mutant mice when compared to wild type mice (Fig. 3.27 B (iii)–(v)). Raptor$^{lox/lox;Foxn1Cre}$ mice displayed a significant reduction in the frequency of naïve T-cells ($T_{\text{naïve}}$) at 7 weeks of age and older (78.3% ±3% in wild type mice and 58.1% ±9.3% in mutant mice; $***p < .005$). In contrast, regulatory T-cells (T_{reg}) and memory T-cells (T_{mem}) from mutant mice were overrepresented when compared to wild type mice at the age of 2 weeks or 7 weeks, respectively, and older (7.5% ±0.4% T_{reg} in 7 weeks old wild type mice vs. 10.4% ±0.7% in mutant mice ($***p < .005$); and 21.7% ±3.0% T_{mem} in 7 week old wild type mice vs. 41.8% ±9.3% in mutant mice; ($*p < .05$)). These data show that Raptor ablation in TEC influences the number and phenotype of peripheral T-cells.

3.4.1 V-beta repertoire

Changes in the selection of immature thymocytes and peripheral T-cell lymphopenia can influence TCR Vβ-usage. Therefore, the TCR repertoire of thymocytes and lymphocytes of Raptor$^{lox/lox}$ and Raptor$^{lox/lox;Foxn1Cre}$ mice was investigated. As the relative frequency of the individual T-cell subpopulations varied in wild type and mutant mice, the different T-cell subsets (CD4^{pos} T_{reg}, T_{mem}, $T_{\text{naïve}}$, and CD8^{pos} T-cells) were analysed separately. The frequencies for all 16 TCR Vβ families were comparable in all T-cell subsets (Fig. 3.28 A, B). Hence, Raptor-deficiency in TEC is compatible with the development of a polyclonal T-cell repertoire, though it remains to be determined whether this function is altered in older mice.

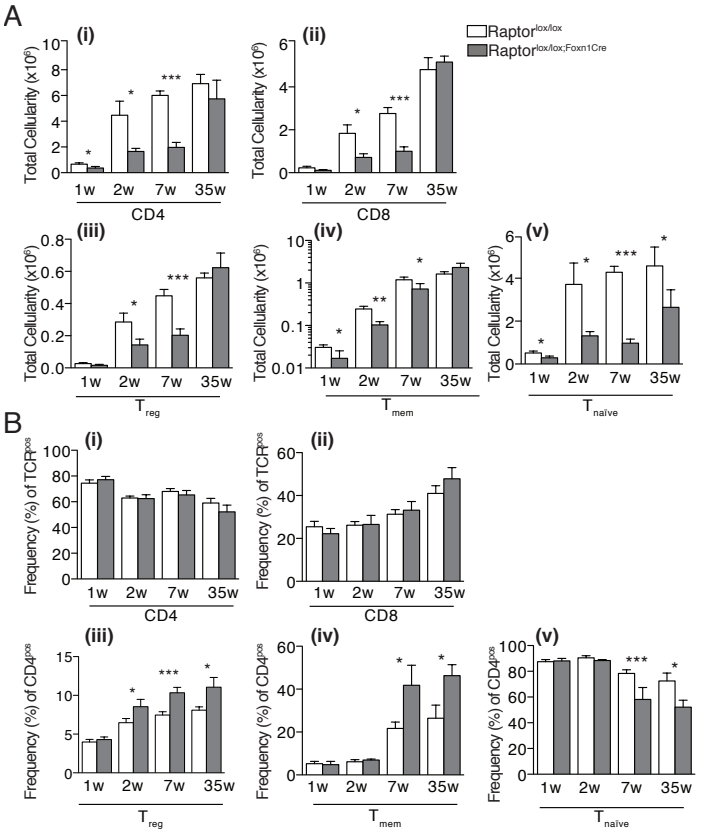

Figure 3.27: Peripheral lymphopenia in Raptor$^{lox/lox;Foxn1Cre}$ mice with alterations in the representation of T-cell subsets; (A) Absolute number of CD4^{pos} **(i)** and CD8^{pos} T-cells **(ii)**, T$_{reg}$ (CD4^{pos}, CD25^{pos}, FoxP3^{pos})**(iii)**, T$_{mem}$ (CD4^{pos}, CD44^{high}, CD62L^{neg}) **(iv)** and T$_{\text{naïve}}$ (CD4^{pos}, CD44^{low}, CD62L^{pos}) **(v)** in the spleen of 1–35 weeks old Raptor$^{lox/lox}$ mice and Raptor$^{lox/lox;Foxn1Cre}$ mice. **(B)** Frequencies of CD4^{pos} **(i)** and CD8^{pos} T-cells **(ii)**, T$_{reg}$ (CD4^{pos}, CD25^{pos}, FoxP3^{pos})**(iii)**, T$_{mem}$ (CD4^{pos}, CD44^{high}, CD62L^{neg}) **(iv)** and T$_{\text{naïve}}$ (CD4^{pos}, CD44^{low}, CD62L^{pos}) **(v)** in the spleen of 1–35 weeks old Raptor$^{lox/lox}$ mice and Raptor$^{lox/lox;Foxn1Cre}$ mice. Values were indicated as mean plus SD. Each experimental group consisted of at least 3 mice. p values were determined by Student's t test with $*p < .05$; $**p < .01$; $***p < .005$)

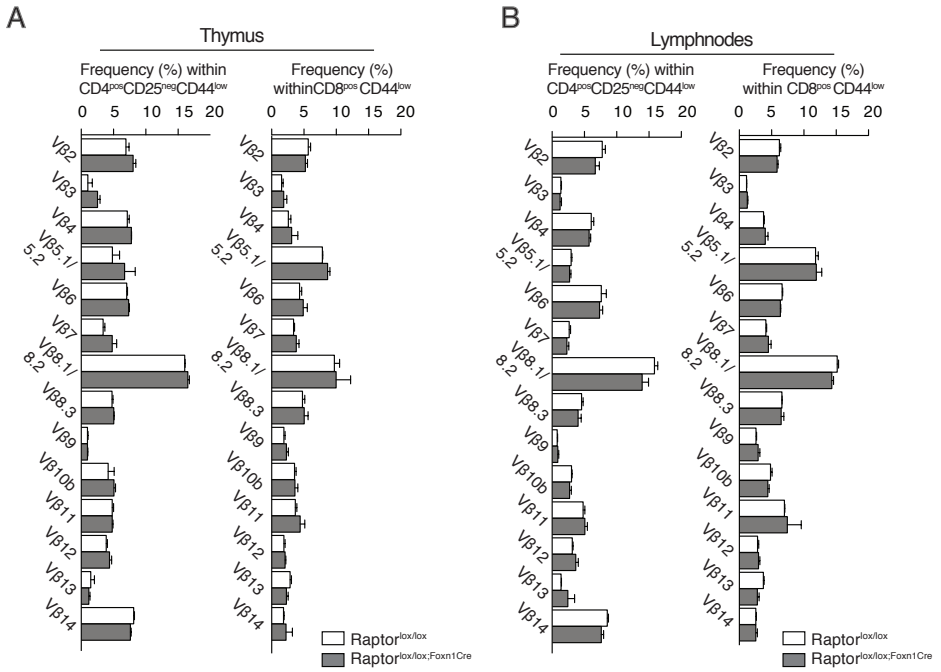

Figure 3.28: Equal frequencies of usage of the TCR vβ-chains of naïve CD4^{pos} and CD8^{pos} T-cells in Raptor$^{lox/lox}$ and Raptor$^{lox/lox;Foxn1Cre}$ mice; Usage of the TCR Vβ-chains of naïve CD4^{pos} and CD8^{pos} in thymus **(A)** and lymphnodes **(B)**. Values were indicated as mean plus SD. Each experimental group consisted of at least 3 mice. p values were determined by Student's t test with $*p < .05$; $**p < .01$; $***p < .005$)

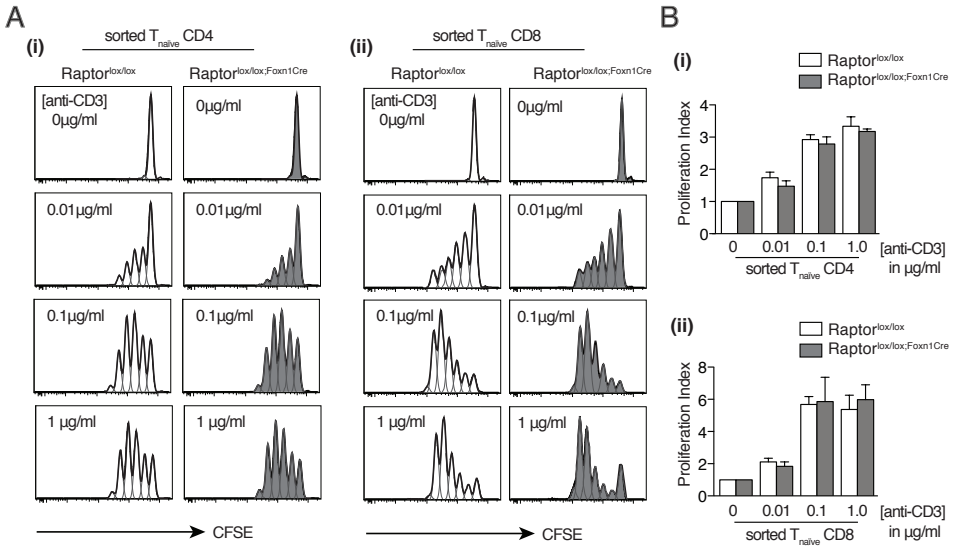

Figure 3.29: T-cells derived from Raptor$^{lox/lox;Foxn1Cre}$ mice show identical capability to proliferate secondary to TCR- stimulation *in vitro* **as wild type T-cells; (A)** CFSE profiles illustrating the proliferation of sorted naïve CD4 (i) and CD8 (ii) lymphocytes from wild type and mutant mice after three days in culture in the presence of α-CD3 at the concentrations indicated. Co-stimulation was provided from irradiated RAG-/- splenocytes. **(B)** Bar graphs displaying the proliferative index of sorted naïve CD4 (i) and CD8 (ii) lymphocytes after stimulation calculated by FlowJo Software. Values were indicated as mean plus SD. Each experimental group consisted of at least 3 mice. p values were determined by Student's t test with $^{*}p < .05$; $^{**}p < .01$; $^{***}p < .005$)

3.4.2 *In vitro* activation of naïve T-cells

The function of the T-cells selected in the thymus of Raptor$^{lox/lox;Foxn1Cre}$ mice was next investigated. For this purpose, purified $T_{\text{naïve}}$ CD4^{pos} or CD8^{pos} T-cells from Raptor$^{lox/lox}$ and Raptor$^{lox/lox;Foxn1Cre}$ mice were cultured for 3 days in the presence of different α-CD3 concentrations (0 to 1μg/ml) and lethally irradiated splenocytes from recombination activating gene 2 (RAG2) deficient mice as a source of co-stimulatory molecules. The cell proliferation was determined by labeling the sorted naïve T cells with carboxyfluorescein succinimidylester (CFSE). With rising α-CD3 concentrations, both CD4^{pos} and CD8^{pos} naïve T cells from Raptor-deficient and -proficient mice showed similar increased proliferative responses (Fig. 3.29 A and B). Thus, naïve T-cells generated in the thymus in the presence of TEC lacking Raptor react normally to CD3 stimuli when compared to wild type controls, as reflected by identical CFSE profiles and proliferative indices.

3.4.3 *In vivo* activation of naïve T-cells

To finally assess the *in vivo* competence of T-cells generated in either wild type or Raptor$^{lox/lox;Foxn1Cre}$ mice, sorted $_{\text{naïve}}$ CD4^{pos} T-cells were adoptively transferred to RAG2 -/- mice. The ability of transferred $_{\text{naïve}}$ T-cells

to mount an immune reaction against the gut flora in lymphocyte-deficient mice RAG2-/- mice can be used to gauge their competence to react to antigens. The induction of wasting disease was defined as end point of the experiment. With an average survival of 35 days ±19 days in wild type and 30 days ±8 days in mutant mice, no obvious difference in the potential to react *in vivo* against antigens could be observed between $T_{naïve}$ cells originating from a wild type thymus or a thymus that lacked mTOCR1 signalling in its epithelium (Fig. 3.29 A (i)). To evaluate the reliability of this outcome, the experimental setup was repeated, however this time not with 2 x 10^5 but 4 x 10^5 $T_{naïve}$ cells transplanted. With an average survival of 50 days ±18 days in wild type mice and 44.5 days ± 9 days in RAG-/- mice, the induction was less efficient but revealed no difference in the survival of RAG-/- mice according to the origin of the cells transferred (Fig. 3.29 A (ii)).

This finding indicates that $T_{naïve}$ cells generated in a thymus composed of Raptor-deficient TEC show an identical potential to mount an immune-response as $T_{naïve}$ cells of wild type mice.

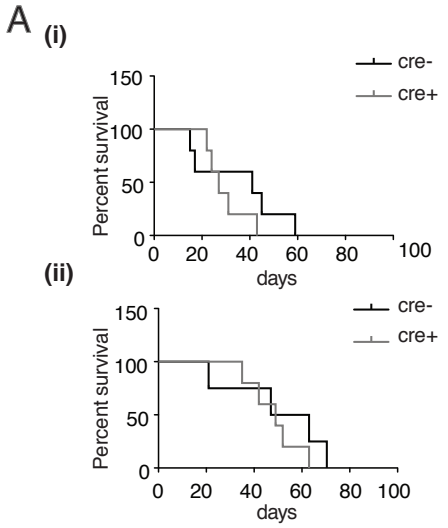

Figure 3.30: Induction of wasting disease in RAG2-/-; Evaluation of T-cells to induce wasting disease after adoptive transfer into RAG2-/- recipients. **(A)** Survival curve after transplantation of 200,000 (i) or 400,000 (ii) sorted $T_{naïve}$ cells ($CD4^{pos}CD44^{neg}CD62L^{pos}$) of $Raptor^{lox/lox}$ (black line) and $Raptor^{lox/lox;Foxn1Cre}$(*greyline*) mice into RAG2 -/- recipients. Induction of wasting disease represented the end point of the experiment and was defined by a weight loss of 20% of the maximum body weight. Per experimental group 5 RAG2 -/- mice were used. In the group of 400,000 transplanted $T_{naïve}$ cells generated in $Raptor^{lox/lox}$ mice, one RAG2 -/- mouse died unexpectedly without previous weight loss at day 38.

3.4.4 Suppressive potential of T_{reg}

Next, the ability of $Raptor^{lox/lox;Foxn1Cre}$ mice to generate T_{reg} cells was investigated. The absolute number of peripheral T_{reg} cells in $Raptor^{lox/lox;Foxn1Cre}$ mice was significantly lower when compared to the number of regulatory T-cells in wild type animals. This decrease may reflect a reduced T-cell production in $Raptor^{lox/lox;Foxn1Cre}$ mice or, alternatively, may be caused by a diminished intrathymic *de novo* generation. To address these possibilities T_{reg} were analysed in the thymi of wild type and mutant mice. In 7 week old mice, the frequency of regulatory T-cells within the $CD4^{pos}$ thymocytes

was 2% ±0.2% in comparison to 0.6% ±0.1% (***$p < .005$) in mutant mice (Fig. 3.31 A (i) and (ii)). To assess the functionality of the regulatory T-cells generated in Raptor$^{lox/lox;Foxn1Cre}$ mice, a T_{reg} suppression assay was performed. Sorted CD4^{pos} effector T-cells (expressing a CD45.1 congenital marker) were sorted and cultured for 3 days in the presence of α-CD3 (1μg/ml) and different cell numbers of T_{reg} isolated from wild type and mutant were added. T_{reg} isolated from mutant mice displayed a better *in vitro* suppressive potential than wild type T_{reg} when tested at a ratio of 2:1 and higher in comparison to cells from wild type mice (Fig. 3.31 B (i) and (ii)). To further investigate this finding, T_{reg} subsets expressing CD103 and/or CD278 (i.e. ICOS, Inducible T-cell COStimulator) were investigated as the use of these cell surface markers identifies four separate but interrelated groups of cells. CD103/ICOS double positive T_{reg} best suppress the *in vitro* proliferation of activated CD4^{pos} effectors cells and their relative frequency increases with the degree of peripheral lymphopenia (Barthlott et al., manuscript in preparation). This T_{reg} subpopulations was over-represented in mutant mice (33.3% ±2.8% in mutant mice in comparison to 13.6% ±3.5% in wild type mice (***$p < .005$)). This result provides a possible explanation for the absence of spontaneous autoimmunity in Raptor$^{lox/lox;Foxn1Cre}$ mice (Fig. 3.31 B). To further verify the function of T-cells selected in a thymic microenvironment devoid of Raptor expression by TEC, experiments are now underway in wild type and mutant mice to deplete their T_{reg} *in vivo* and to monitor the incidence and the kinetics of autoimmunity.

3.4.5 Incidence of autoimmunity

To investigate whether T-cell development in the context of epithelia devoid of mTORC1-signalling leads to an increased incidence of autoimmunity, possible target organs of such a response against self-antigens were isolated from 13 weeks old wild type and Raptor$^{lox/lox;Foxn1Cre}$ mice, and screened for the presence of lymphoid infiltrates using hematoxylin and eosin staining (Fig. 3.32).

The selected organs represent some of the most frequently targeted organs in autoimmune pathologies; eye and optic nerve (rheumatoid arthritis, multiple sclerosis), pancreas (autoimmune pancreatitis), salivary glands (Sjögren's syndrome) and thyroid (Hashimoto's thyroiditis).

Cellular infiltrates could not be detected in any of the tissues analysed. Together with the observation that the lifespan of Raptor$^{lox/lox;Foxn1Cre}$ mice is identical to the one of wild type littermates, this data suggests that lack of Raptor in TEC is not linked to an increased risk of developing autoimmune pathologies.

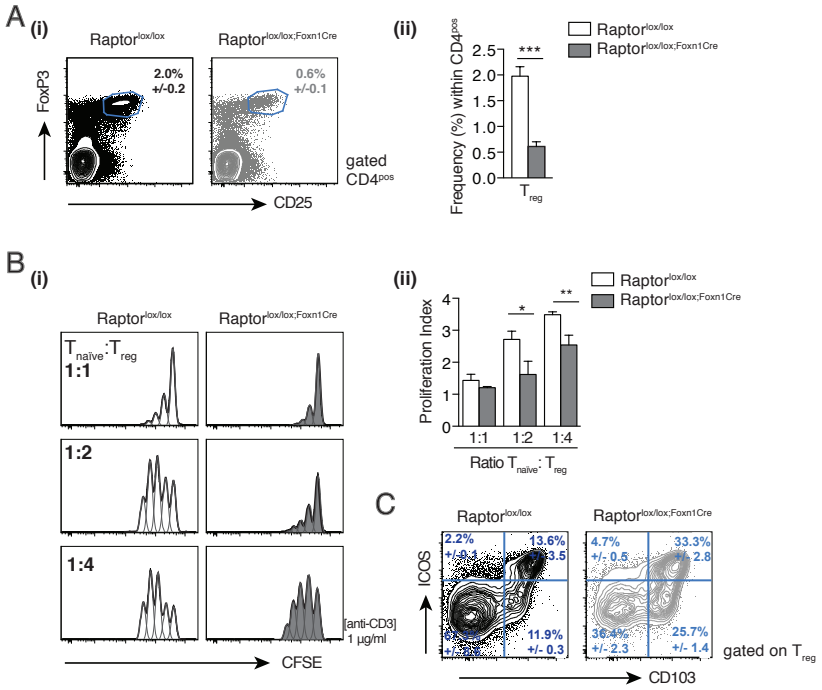

Figure 3.31: Raptor$^{lox/lox;Foxn1Cre}$ mice generate fewer but more potent T$_{reg}$ in comparison to wild type; (A) (i) Flow cytometric detection of regulatory T-cells in thymi of 7 week old Raptor$^{lox/lox}$ and Raptor$^{lox/lox;Foxn1Cre}$ mice. T$_{reg}$ were identified based on the expression of CD4, CD25 and FoxP3. Cells were gated on CD4^{pos} thymocytes **(ii)**. Frequencies of T$_{reg}$ within CD4^{pos} cells in mutant and wild type mice. **(B) (i)** T$_{reg}$ suppression assay displaying Carboxyfluorescein succinimidyl ester (CFSE) proliferation profiles of sorted wild type (CD45.1) T$_{\text{naïve}}$ CD4^{pos} cells cultured with α-CD3 (1μg/ml) and sorted T$_{reg}$ of Raptor$^{lox/lox}$ (white) or Raptor$^{lox/lox;Foxn1Cre}$ mice (grey) mice in the dilutions indicated (ratios are T$_{\text{naïve}}$: T$_{reg}$). Analysis was performed after 3 days in culture. **(B) (ii)** Suppressive potential of T$_{reg}$ at different dilutions illustrated in bar graph. **(C)** Representative FACS plots of T$_{reg}$ subpopulations, distinguished by the cell surface expression of Inducible T-cell COStimulator (ICOS) and CD103. Cells were isolated from lymph nodes of 7 weeks old Raptor$^{lox/lox}$ and Raptor$^{lox/lox;Foxn1Cre}$ mice. Values were indicated as mean plus SD. Each experimental group consisted of at least 3 mice. p values were determined by Student's t test with $^{*}p < .05$; $^{**}p < .01$; $^{***}p < .005$)

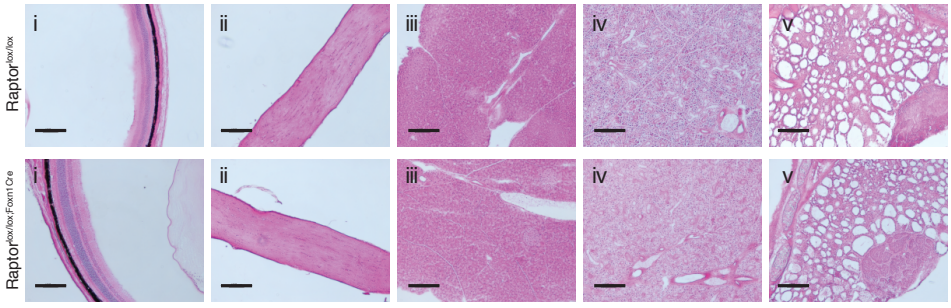

Figure 3.32: Organ sections of aged Raptor$^{lox/lox;Foxn1Cre}$ mice show no signs of autoimmunity; Hematoxylin and Eosin staining of divers organ sections (8 µm) of 13 weeks old female Raptor$^{lox/lox}$ mice (*upper panel*) and Raptor$^{lox/lox;Foxn1Cre}$ mice (*lower panel*). The following organs were used: eyes **(i)**, optic nerve **(ii)**, pancreas **(iii)**, salivary gland **(iv)**, and thyroid **(v)**. Scalebar indicates 200µm.

3.5 Gene expression profiling in Raptor-sufficient and -deficient TEC

To address the perceived differences in the role of Raptor for the biology of TEC during embryonic versus postnatal epithelial development, and the difference of Raptor's impact on cortical versus medullary TEC, a gene expression analysis was carried out, comparing Raptor-sufficient with Raptor-deficient TEC. The objective of this analysis was to gain insight into the availability and differential representation of signalling pathways linked to the phenotypic and functional differences observed between TEC that express Raptor and those that are deficient of Raptor.

The Affymetrix Mouse Gene 1.0 ST Array was performed on wild type and mutant TEC that were isolated from fetal thymi at E16 and postnatal thymi at 2 weeks of age. The postnatal time point was chosen, as 2 weeks old mutant thymi were already hypoplastic but did not yet display significant differences in the relative representation of TEC subpopulations within cTEC and mTEC. Therefore, the risk to obtain differences between wild type and mutant cTEC and mTEC, which would be linked to the specific TEC-subsets overrepresented in Raptor-deficient mice, was minimized. The TEC of 2 weeks old mice were separated into cTEC and mTEC. Since the epithelial compartment of thymi at E16 constitutes mostly cTEC, fetal TEC were not separated further.

The detailed analysis of gene networks and signalling pathways that are differentially represented between embryonic and post-natal TEC as well as between post-natal cortical and medullary TEC has been initiated and shown to be feasible. Preliminary data of the gene expression analysis revealed significant changes in the number of transcripts specific for central molecules of the canonical Wnt signalling pathway in adult cTEC, among them wingless-type MMTV integration site family, member 3A (Wnt3a) and the lymphoid enhancer-binding factor 1 (LEF1). A further in-depth analysis is beyond the scope of this thesis. Subsequent work in this direction will focus in particular on pathways related to cell size, proliferation and the expression of chemokines and cytokines that are essential for the interaction with developing thymocytes.

mTOR and the canonical Wnt pathway

Further analyses focussed on the canonical Wnt signalling pathway, as it was affected by the inhibition of mTORC1 in TEC and has been linked to epithelial cell fate, growth and differentiation (Miller, 2002). Moreover, stimulation of the canonical Wnt signalling pathway in TEC by secretion of Wnt glycoproteins increases the expression of Foxn1 (Balciunaite et al., 2002). Therefore, Wnt molecules provide regulatory signals critical for thymic function.

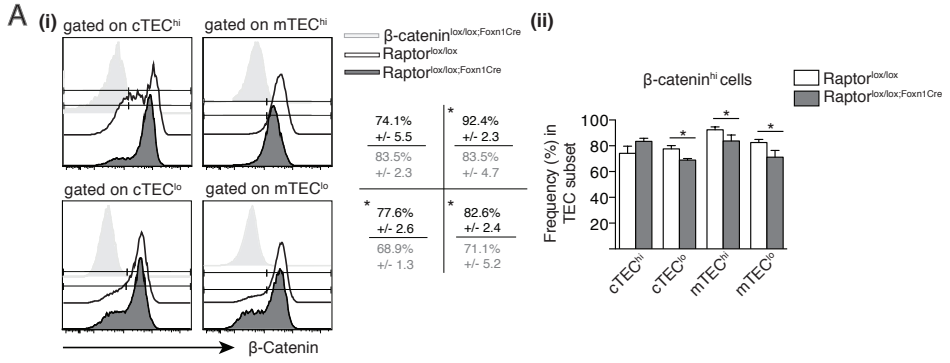

Figure 3.33: TEC subpopulations of Raptor$^{lox/lox;Foxn1Cre}$ mice display an altered expression of β-catenin compared to wild type mice; A (i) Histograms display β-catenin signal in different TEC subpopulations (cTEC^{hi}, cTEC^{lo}, mTEC^{hi}, mTEC^{lo}) of 7 weeks old Raptor$^{lox/lox}$ and Raptor$^{lox/lox;Foxn1Cre}$ mice. **A (ii)** Frequencies of β-catenin^{hi} cells in the respective TEC subset are depicted in bar graphs as mean values plus SD. Each experimental group consisted of at least 3 mice. p values were determined by Student's t test with $^*p < .05$; $^{**}p < .01$; $^{***}p < .005$)

Canonical Wnt signalling causes stabilization of β-catenin, which enables its translocation to the nucleus, where it interacts with the transcription factors that regulate expression of target genes. To measure Wnt signalling activity, β-catenin expression was detected in wild type and mutant TEC using flow cytometry. β-catenin expression intensities differed in TEC depending on the amount of MHCII cell surface expression and the TEC cell type (Fig. 3.33 A (i, ii)). In wild type and mutant mice the relative number of β-catenin^{pos} TEC was highest in the population of mTEC^{hi} when compared to the other TEC subsets. However, mutant mice displayed in general a significantly reduced frequency of β-catenin^{pos} cells within all TEC subsets with the exception of cTEC^{hi} when compared to wild type TEC populations (Fig. 3.33 A (i, ii)). This result demonstrates that mTORC1 activity is correlated with alterations in β-catenin expression specific for TEC subpopulations.

Chapter 4

Discussion

Regular thymic size requires both mTOR complexes

The goal of this study was to determine the role of the mTOR signalling pathway for the development, maintenance and function of thymic epithelia. As mTOR consists of two functionally different complexes (mTORC1 and mTORC2), three individual tissue-specific conditional knockout mice were generated, namely animals lacking either mTORC1 (Raptor$^{lox/lox;Foxn1Cre}$ mice), mTORC2 (Rictor$^{lox/lox;Foxn1Cre}$ mice), or both multi-protein complexes (Rictor$^{lox/lox}$Raptor$^{lox/lox;Foxn1Cre}$mice). The availability of these mice with a loss of Raptor, Rictor or the expression of both proteins in thymic epithelia allowed to interrogate the function of these molecules separately in the context of thymic function.

All three mouse models of partial or complete mTOR-inhibition displayed a significant change in thymic size, composition and functional competence at the age of 2 weeks. These results thus demonstrated the importance of intact mTOR signalling for thymic epithelial biology.

The concept that mTOR controls cellular (Fingar et al., 2002), and thus organ size (Csibi and Blenis, 2012; Cloëtta et al., 2013) is indeed consistent with the observation that the absence of Raptor and/or Rictor results in significant thymic hypoplasia. However, obvious differences in the severity of the thymic phenotype exist, when comparing the consequences of a TEC-targeted loss in mTORC1, mTORC2 or a general mTOR inhibition. Though the single loss of Raptor expression did not affect the thymic size in neonatal mice, the loss of Rictor and especially the combined loss of Raptor and Rictor reduced thymic cellularity. Later in life, Raptor-mutant mice also displayed a significant decrease in thymic cellularity. Thus, the absence of Raptor cannot be compensated after birth by the presence of Rictor whereas the latter is essential for both embryonic as well as post-natal TEC development. The concomitant and parallel availability of mTORC signalling by complex 1 and 2 is therefore required though with a different importance at distinct developmental stages. However, the stronger phenotype observed

in mice completely devoid of mTOR signalling implies that there is partial redundancy in the function of mTORC1 and mTORC2 during thymus organogenesis and post-natal organ maintenance.

mTORC1 and mTORC2 are interdependent in the context of TEC biology

mTORC1 and mTORC2 have initially been thought to be functionally independent though both mTOR complexes have now been shown to influence each others activity indirectly. Indeed, mTORC1 regulates via an internal feedback loop not only its own activity but also that of mTORC2. The steps involved in this negative feedback loop include the inhibition of PI3K downstream of the mTORC1 effector S6 kinase and the suppression of the growth factor insulin receptor substrate-1 (IRS1) function. Because growth factors act upstream of mTORC2 and stimulate its signalling activity, the suppression of IRS1 mediated signals dampens mTORC2 activity (Harrington et al., 2004; Um et al., 2004). Additionally, it was shown that mTORC1 activation promotes the phosphorylation of Rictor, and thus negatively regulates mTORC2 and Akt signalling (Julien et al., 2010). Conversely, it was found that Raptor-deficient bone marrow-derived dendritic cells display an enhanced mTORC2 activity, which in turn results in an increased Akt activity (Kellersch and Brocker, 2013).

However, an effect of mTORC2 on mTORC1 signalling activity has so far not been described. Although Akt regulates not only signalling events upstream of mTORC1 but also constitutes a substrate for mTORC2, it was shown that phosphorylation of Akt at Ser 473 - specifically mediated by mTORC2 - does not have an impact on the regulation of mTORC1. Therefore, mTORC2 is not considered to signal upstream of mTORC1 (Jacinto et al., 2006).

These examples show a mutually specific relation between mTORC1 and mTORC2 activity and provide some explanations for the differential effect of a loss of mTORC1 and mTORC2 signalling in the three mutant mouse models studied.

Effects of mTORC1-deficiency in TEC manifests postnatally

To investigate in depth the morphological, functional and molecular changes that ensue as a consequence of impaired mTOR signalling, my study focussed on the specific role of Raptor for the mouse thymic epithelia. The loss of Raptor was engineered to occur at around day 12 to 12.5 during embryogenesis (E12-12.5) since Raptor$^{lox/lox}$ and/or Rictor$^{lox/lox;Foxn1Cre}$ mice were crossed with the Foxn1-Cre transgenic mouse line, which starts Cre expression from gestational day 11.5 onwards (Zuklys et al., 2009).

A significant decrease in total thymic cellularity was only observed in

Raptor$^{lox/lox;Foxn1Cre}$ mice in comparison to controls once the mice were 1 week of age or older. The unchanged thymic cellularity early in development and immediately after birth was not due to a lack in recombination since Raptor transcripts and protein (as measured by qPCR and immunohistology) were reduced as early as E14 and absent by E16.5. Assuming that any remaining Raptor activity was significantly decreased or altogether lost, several explanations may account for the relatively late onset of a distinct phenotype in Raptor$^{lox/lox;Foxn1Cre}$ mice. Firstly, prenatal thymic development may proceed independently of a need for mTORC1 signalling. Secondly, prenatal mTORC2 activity could fully compensate for the loss of Raptor function. Finally, a prenatal loss of Raptor function may only become manifest one week after birth at the phenotypic level though molecular changes may already be apparent earlier.

The last explanation cannot easily be distinguished from a scenario in which early thymic development is independent of mTORC1 at all. Indeed, it has been established that thymocyte haematopoietic precursor seed in periodic waves to the thymic microenvironment and that only cells that have entered the primordium before E13 undergo proliferation and differentiation during the fetal period. In contrast, precursors that have entered the thymus later will have to await their turn in contributing to thymic T-cell development, which has been shown to occur in the weeks after birth (Le Douarin and Jotereau, 1975). Thus, the sequential seeding and expansion of T-cell precursors may partially account for the "delayed" (i.e. post-natal) onset of thymic hypoplasia in Raptor$^{lox/lox;Foxn1Cre}$ mice, though features other than low thymocyte numbers are the consequence of a loss of Raptor expression in TEC.

Loss of Raptor in TEC is dispensable for initial mTEC formation but is needed for their maintenance

A significant decrease in the absolute number of mTEC is apparent in Raptor$^{lox/lox;Foxn1Cre}$ mice as early as in the second week of life. This progressive decrease is accompanied by a replacement with mesenchymal fibroblasts. The mentioned timing in the loss of mTEC suggests that mTORC1 signalling is dispensable for the initial formation of the epithelial scaffold of the medulla, a process that depends amongst others on RelB- (Burkly et al., 1995) or lymphotoxin β receptor-mediated signals (Boehm et al., 2003).

The selective decrease in the absolute cell number of mTEC in Raptor-deficient mice was unexpected. This observation may link to the fact that mTEC devoid of Raptor display a decreased proliferation rate in comparison to wild type. This result is in keeping with a role of mTOR signalling in cell proliferation and its pharmacological blocking using Rapamycin, which results in an arrest in cell-cycle progression in the G1 phase (Dowling et al., 2010). Still it remains to be resolved, why cTEC are more resilient to the

loss of mTORC1. Gene expression profiling may provide molecular hints to this difference, which can further be investigated.

Raptor-ablation in TEC leads to a relative overrepresentation of AIRE^{pos} mTEC

The reduction of mTEC in Raptor$^{lox/lox;Foxn1Cre}$ mice affects the separate mTEC subpopulations differently. Mature mTEC can be distinguished into AIRE-expressing and AIRE-negative epithelia and it is the former that is progressively overrepresented in mTEC of Raptor$^{lox/lox;Foxn1Cre}$ mice.

Early embryonic differentiation of AIRE^{pos} mTEC involves receptor activator of NF-κB (RANK) interactions with its corresponding ligand (RANKL) provided by CD4^{pos}3^{neg} lymphoid tissue inducer cells (LTi) (Rossi et al., 2007), (White et al., 2008). The number of AIRE expressing mTEC in Raptor$^{lox/lox;Foxn1Cre}$ mice is unperturbed at both embryonic and newborn stages. This finding implies furthermore that mTORC1 signalling is not required for the developmental events in TEC differentiation that rely on RANK-RANKL interactions for the mechanisms that secure the presence of LTi in the embryonic thymus. However, the molecular and cellular requirements for the regular differentiation and maintenance of AIRE^{pos} mTEC in adult mice are still incompletely defined.

A possible explanation for the increased frequency of adult AIRE^{pos} mTEC in mutant mice may be provided by 3D visualization of the thymus, which demonstrated that AIRE^{pos} mTEC tend to congregate in the medullary area of the corticomedullary junction (CMJ) (Irla et al., 2013). In Raptor$^{lox/lox;Foxn1Cre}$ mice, the total number of mTEC is reduced. However, its distribution appeared much more dispatched than in wild type thymi. In this context, it would be interesting to evaluate whether the surface contact between medulla and cortex in mutant mice is comparable to that of wild type mice or whether the more fragmented spreading of mTEC that was observed in mutant mice results in a larger contact zone between cortex and medulla according to the principle of surface expansion and therefore in a higher frequency of AIRE-expressing mTEC.

Raptor-ablation in TEC favors the overrepresentation of MHCII^{hi} cells in TEC

In Raptor$^{lox/lox;Foxn1Cre}$ mice, the frequency of MHCII^{high} cells is increased in both TEC subsets. MHC class II expression in TEC depends strictly on the activation of the class II, major histocompatibility complex, transactivator (CIITA) (Chang et al., 1994), which can be modulated by environmental stimuli, such as interferon γ (Steimle et al., 1994). Recently, the inhibition of mTORC1 signalling via treatment with rapamycin was correlated with an increased surface expression of MHCII on professional antigen

presenting cells *in vitro* and *in vivo* (Schmid and Münz, 2007; Jagannath et al., 2009). The measurement of autophagic activity in both wild type or Raptor-deficient TEC revealed a positive correlation between MHCII expression and autophagy, which is in keeping with this previously noted association of MHCII-upregulation and autophagy. Therefore, a sequence of events is likely, whereby the loss of mTORC1 signalling results in MHCII^{hi} expression through promotion of autophagy.

Loss of Raptor expression in TEC impacts on thymopoiesis

In view of the many phenotypic changes, I also probed the function of TEC devoid of regular Raptor-expression.

T-cell maturation is a cell non-autonomous process, which requires the interaction with thymic epithelia. At first view, lack of mTORC1 signalling in TEC does not interfere with this interaction and is compatible with the generation of normal frequencies of CD4^{pos} and CD8^{pos} thymoyctes. A more detailed analysis, however, revealed alterations in the maturation of positively selected SP thymocytes from mutant mice, which resulted in an increased frequency of SP cells that are immature. The analysis of BrdU-incorporation after a 4 days chase showed identical frequencies of labelled SP cells in both strains of mice, which indicated that an altered kinetic in the transition from the DN to the SP stage was not the reason for the overrepresentation of immature SP thymocytes in mutant mice. An alternative explanation for the observed increase in immature SP thymocytes is based on the fact that Raptor$^{lox/lox;Foxn1Cre}$ mice display significantly fewer mTEC. As mTEC are functionally related to negative selection of self-reactive thymocytes, the paucity of these cells in Raptor$^{lox/lox;Foxn1Cre}$ mice could result in a decreased efficiency in the elimination — and therefore in an relative increase — of immature SP cells.

Since the relative increase in the immature SP cells was accompanied by a decrease in mature SP cells, the observed alterations could also arise from an accelerated egress of mature SP cells. Compatible with this hypothesis is the observation that the frequency of S1P1^{pos} cells mature SP thymocytes was significantly decreased in Raptor$^{lox/lox;Foxn1Cre}$ mice. This reduction correlated also with a higher vascular density and an increased number of pericytes in the medulla of Raptor-mutant mice. As pericytes promote thymocyte egress (Zachariah and Cyster, 2010) by producing S1P, the latter finding could additionally support the concept, that the exit of mature SP cells is accelerated in mice with a TEC-targeted inhibition of mTORC1. However, to identify the reason for the observed shifts in the frequencies of immature and mature thymocytes in Raptor$^{lox/lox;Foxn1Cre}$ mice the transit time of post-selection thymocytes in the medulla of wild type and mutant mice needs to be defined.

Raptor$^{lox/lox;Foxn1Cre}$ mice are lymphopenic and display changes in regulatory T-cells

Raptor$^{lox/lox;Foxn1Cre}$ mice suffered from peripheral lymphopenia due to reduced output of naïve T-cells and had significantly fewer intrathymically generated regulatory T-cells in relative and absolute terms. Moreover, there were indications that negative selection was less efficient in thymi of Raptor-deficient mice when compared to wild type mice.

Analysis of CD4^{pos} T-cell subpopulations in adult wild type and mutant mice revealed further that within the CD4^{pos} cells, memory T-cells mice were overrepresented in Raptor$^{lox/lox;Foxn1Cre}$ mice. The latter observation is ascribed to a well-known process, termed homeostatic proliferation, during which the expansion of few T-cell in a lymphopenic mouse is promoted due to an abundance of niches and cytokines. Typically, these homeostatically expanded T-cells show an activated, memory-like phenotype, which is marked by the expression of CD44 (Goldrath et al., 2000; Cho et al., 2000). Homeostatic proliferation can result in the expansion of auto-reactive T-cell clones. Despite these observations, Raptor$^{lox/lox;Foxn1Cre}$ mice did not display any signs characteristic for the development of autoimmune diseases or a decreased lifespan when compared to wild type mice.

This finding might be explained by the observation that lymphopenia is associated with a relative over-representation and an increased potency of T_{reg} (Barthlott et al. manuscript in preparation). Indeed, quantification of peripheral regulatory T-cells revealed at the age of 2 weeks and older both a significantly increased frequency of T_{reg} within the CD4^{pos} T-cells of mutant mice, and an increased suppressive potential of T_{reg} *in vitro* from Raptor$^{lox/lox;Foxn1Cre}$ mice. The latter finding correlated with an overrepresentation of a T_{reg} subsets in mutant mice which express CD103 and ICOS that has been described to suppress activation of T-cells best. Taken together, these data suggest that peripheral tolerance mediated by a T_{reg} subpopulation that is overrepresented in Raptor$^{lox/lox;Foxn1Cre}$ mice can account for the absence of autoimmunity, despite lymphopenia and an impaired generation of central tolerance in these mice.

Raptor$^{lox/lox;Foxn1Cre}$ mice display altered activity of canonical Wnt signalling in TEC

The frequency of β-catenin^{pos} TEC were significantly decreased in all TEC subsets of mutant mice with the exception of cTEC expressing high amounts of MHCII.

Wnt glycoproteins regulate Foxn1 expression (Balciunaite et al., 2002), and stabilization of β-catenin in TEC results in a block in thymus development and a loss of TEC identity (Zuklys et al., 2009). These implications of Wnt signalling in TEC biology suggest that the dysregulated levels of

β-catenin may contribute to the changes observed in the thymic microenvironment of Raptor$^{lox/lox;Foxn1Cre}$ mice. Thymi of mutant mice were hypoplastic and displayed in comparison to wild type thymi already at young age a remodelling of the organ with an increase in fibroblasts. These aspects — reminiscent of premature aging — may be also influenced by alterations of the level of β-catenin as the suppression of β-catenin dependent Wnt signalling in TEC was implicated in the initiation of thymic senescence (Varecza et al., 2011). The level of cytoplasmatic β-catenin is posttranslational strictly controlled by proteins that facilitate its degradation (Luckert et al., 2011), such as GSK3β. Therefore, a failure in GSK3β inactivation may account for decreased levels of β-catenin.

mTOR signalling can inhibit GSK3β activity through S6Kinase-mediated phosphorylation, which could provide an explanation for a lack of GSK3β inactivation in Raptor$^{lox/lox;Foxn1Cre}$ mice. However, it was shown that such a mechanism would only work if Akt-mediated inhibition of GSKβ is blocked as well. Since mTORC1 inhibition increases Akt activity (Zhang et al., 2006), the aforementioned mechanism is not a likely explanation for the decreased levels of β-catenin. Therefore, a different mTOR-dependent process needs to be responsible for this effect. Gene expression profile analysis revealed several candidates influencing the Wnt signalling pathway and may thus guide future understanding of the observed alterations.

Chapter 5

Conclusion

mTOR signalling is essential for TEC differentiation and maintenance. However, there is a differential requirement for the separate mTOR complexes with regards to TEC biology. Whereas mTORC1 signalling is dispensable for thymic organogenesis and further development during the embryonic stage, the absence of mTORC2 leads already prenatally to a reduced thymic cellularity. Despite their individual roles in TEC biology, both mTOR complexes display also a partial functional redundancy, as their combined loss results during both neonatal and postnatal stages in a phenotype that is stronger when compared to single mutant mice.

The absence of mTORC1-signalling at post-natal stages results in thymic hypoplasia and an increased fibrotic remodelling of the thymic microenviroment. Further changes are characterized by a significant reduction in medullary but not cortical TEC cellularity, a diminution of cell size, decreased TEC cell cycle activity, and a reduction in the transcription of TEC-specific chemokines that control the attraction of T-cell precursors to the thymus. Although the main steps during T-cell development are independent of the presence of mTORC1, its signalling in TEC is required for thymocyte selection and maturation.

In view of these essential thymic functions that are disturbed by the disruption of mTORC1 and mTORC2, any efforts integrating this pathway for medical therapeutic purposes will need to assure that disruption of T-cell maturation and thymic function are not an inadvertent complication.

Bibliography

Abraham, R. T. (1998). Mammalian target of rapamycin: immunosuppressive drugs uncover a novel pathway of cytokine receptor signaling. *Curr Opin Immunol*, 10(3):330–6.

Alessi, D. R., Pearce, L. R., and García-Martínez, J. M. (2009). New insights into mtor signaling: mtorc2 and beyond. *Sci Signal*, 2(67):pe27.

Anderson, G., Jenkinson, E. J., and Rodewald, H.-R. R. (2009). A roadmap for thymic epithelial cell development. *Eur J Immunol*, 39(7):1694–9.

Anderson, M. S., Venanzi, E. S., Klein, L., Chen, Z., Berzins, S. P., Turley, S. J., von Boehmer, H., Bronson, R., Dierich, A., Benoist, C., and Mathis, D. (2002). Projection of an immunological self shadow within the thymus by the aire protein. *Science*, 298(5597):1395–401.

Ara, T., Itoi, M., Kawabata, K., Egawa, T., Tokoyoda, K., Sugiyama, T., Fujii, N., Amagai, T., and Nagasawa, T. (2003). A role of cxc chemokine ligand 12/stromal cell-derived factor-1/pre-b cell growth stimulating factor and its receptor cxcr4 in fetal and adult t cell development in vivo. *J Immunol*, 170(9):4649–55.

Araki, K., Turner, A. P., Shaffer, V. O., Gangappa, S., Keller, S. A., Bachmann, M. F., Larsen, C. P., and Ahmed, R. (2009). mtor regulates memory cd8 t-cell differentiation. *Nature*, 460(7251):108–12.

Balciunaite, G., Keller, M. P., Balciunaite, E., Piali, L., Zuklys, S., Mathieu, Y. D., Gill, J., Boyd, R., Sussman, D. J., and Holländer, G. A. (2002). Wnt glycoproteins regulate the expression of foxn1, the gene defective in nude mice. *Nat Immunol*, 3(11):1102–8.

Barthlott, T., Kohler, H., and Eichmann, K. (1997). Asynchronous coreceptor downregulation after positive thymic selection: prolonged maintenance of the double positive state in cd8 lineage differentiation due to sustained biosynthesis of the cd4 coreceptor. *J Exp Med*, 185(2):357–62.

Bhasin, N., LaMantia, A.-S. S., and Lauder, J. M. (2004). Opposing regulation of cell proliferation by retinoic acid and the serotonin2b receptor in the mouse frontonasal mass. *Anat Embryol (Berl)*, 208(2):135–43.

Bleul, C. C. and Boehm, T. (2001). Laser capture microdissection-based expression profiling identifies pd1-ligand as a target of the nude locus gene product. *Eur J Immunol*, 31(8):2497–503.

Bleul, C. C., Corbeaux, T., Reuter, A., Fisch, P., Mönting, J. S., and Boehm, T. (2006). Formation of a functional thymus initiated by a postnatal epithelial progenitor cell. *Nature*, 441(7096):992–6.

Blommaart, E. F., Luiken, J. J., Blommaart, P. J., van Woerkom, G. M., and Meijer, A. J. (1995). Phosphorylation of ribosomal protein s6 is inhibitory for autophagy in isolated rat hepatocytes. *J Biol Chem*, 270(5):2320–6.

Bockman, D. E. and Kirby, M. L. (1984). Dependence of thymus development on derivatives of the neural crest. *Science*, 223(4635):498–500.

Boehm, T., Scheu, S., Pfeffer, K., and Bleul, C. C. (2003). Thymic medullary epithelial cell differentiation, thymocyte emigration, and the control of autoimmunity require lympho-epithelial cross talk via ltbetar. *J Exp Med*, 198(5):757–69.

Borgulya, P., Kishi, H., Uematsu, Y., and von Boehmer, H. (1992). Exclusion and inclusion of alpha and beta t cell receptor alleles. *Cell*, 69(3):529–37.

Brändle, D., Müller, C., Rülicke, T., Hengartner, H., and Pircher, H. (1992). Engagement of the t-cell receptor during positive selection in the thymus down-regulates rag-1 expression. *Proc Natl Acad Sci U S A*, 89(20):9529–33.

Brown, E. J., Albers, M. W., Shin, T. B., Ichikawa, K., Keith, C. T., Lane, W. S., and Schreiber, S. L. (1994). A mammalian protein targeted by g1-arresting rapamycin-receptor complex. *Nature*, 369(6483):756–8.

Burkly, L., Hession, C., Ogata, L., Reilly, C., Marconi, L. A., Olson, D., Tizard, R., Cate, R., and Lo, D. (1995). Expression of relb is required for the development of thymic medulla and dendritic cells. *Nature*, 373(6514):531–6.

Carrière, A., Cargnello, M., Julien, L.-A. A., Gao, H., Bonneil, E., Thibault, P., and Roux, P. P. (2008). Oncogenic mapk signaling stimulates mtorc1 activity by promoting rsk-mediated raptor phosphorylation. *Curr Biol*, 18(17):1269–77.

Carriere, A., Romeo, Y., Acosta-Jaquez, H. A., Moreau, J., Bonneil, E., Thibault, P., Fingar, D. C., and Roux, P. P. (2011). Erk1/2 phosphorylate raptor to promote ras-dependent activation of mtor complex 1 (mtorc1). *J Biol Chem*, 286(1):567–77.

Carson, D. A., Kaye, J., and Seegmiller, J. E. (1977). Lymphospecific toxicity in adenosine deaminase deficiency and purine nucleoside phosphorylase deficiency: possible role of nucleoside kinase(s). *Proc Natl Acad Sci U S A*, 74(12):5677–81.

Chang, C. H., Fontes, J. D., Peterlin, M., and Flavell, R. A. (1994). Class ii transactivator (ciita) is sufficient for the inducible expression of major histocompatibility complex class ii genes. *J Exp Med*, 180(4):1367–74.

Chisaka, O. and Capecchi, M. R. (1991). Regionally restricted developmental defects resulting from targeted disruption of the mouse homeobox gene hox-1.5. *Nature*, 350(6318):473–9.

Cho, B. K., Rao, V. P., Ge, Q., Eisen, H. N., and Chen, J. (2000). Homeostasis-stimulated proliferation drives naive t cells to differentiate directly into memory t cells. *J Exp Med*, 192(4):549–56.

Cloëtta, D., Thomanetz, V., Baranek, C., Lustenberger, R. M., Lin, S., Oliveri, F., Atanasoski, S., and Rüegg, M. A. (2013). Inactivation of mtorc1 in the developing brain causes microcephaly and affects gliogenesis. *J Neurosci*, 33(18):7799–810.

Cordier, A. C. and Haumont, S. M. (1980). Development of thymus, parathyroids, and ultimo-branchial bodies in nmri and nude mice. *Am J Anat*, 157(3):227–63.

Csibi, A. and Blenis, J. (2012). Hippo-yap and mtor pathways collaborate to regulate organ size. *Nat Cell Biol*, 14(12):1244–5.

Cunningham, J. T., Rodgers, J. T., Arlow, D. H., Vazquez, F., Mootha, V. K., and Puigserver, P. (2007). mtor controls mitochondrial oxidative function through a yy1-pgc-1alpha transcriptional complex. *Nature*, 450(7170):736–40.

Cybulski, N., Polak, P., Auwerx, J., Rüegg, M. A., and Hall, M. N. (2009). mtor complex 2 in adipose tissue negatively controls whole-body growth. *Proc Natl Acad Sci U S A*, 106(24):9902–7.

Danielian, P. S., Muccino, D., Rowitch, D. H., Michael, S. K., and McMahon, A. P. (1998). Modification of gene activity in mouse embryos in utero by a tamoxifen-inducible form of cre recombinase. *Curr Biol*, 8(24):1323–6.

Davodeau, F., Difilippantonio, M., Roldan, E., Malissen, M., Casanova, J. L., Couedel, C., Morcet, J. F., Merkenschlager, M., Nussenzweig, A., Bonneville, M., and Malissen, B. (2001). The tight interallelic positional coincidence that distinguishes t-cell receptor jalpha usage does not result from homologous chromosomal pairing during valphajalpha rearrangement. *EMBO J*, 20(17):4717–29.

Dehner, M., Hadjihannas, M., Weiske, J., Huber, O., and Behrens, J. (2008). Wnt signaling inhibits forkhead box o3a-induced transcription and apoptosis through up-regulation of serum- and glucocorticoid-inducible kinase 1. *J Biol Chem*, 283(28):19201–10.

Delgoffe, G. M., Kole, T. P., Zheng, Y., Zarek, P. E., Matthews, K. L., Xiao, B., Worley, P. F., Kozma, S. C., and Powell, J. D. (2009). The mtor kinase differentially regulates effector and regulatory t cell lineage commitment. *Immunity*, 30(6):832–44.

Delgoffe, G. M., Pollizzi, K. N., Waickman, A. T., Heikamp, E., Meyers, D. J., Horton, M. R., Xiao, B., Worley, P. F., and Powell, J. D. (2011). The kinase mtor regulates the differentiation of helper t cells through the selective activation of signaling by mtorc1 and mtorc2. *Nat Immunol*, 12(4):295–303.

Delgoffe, G. M. and Powell, J. D. (2009). mtor: taking cues from the immune microenvironment. *Immunology*, 127(4):459–65.

Derbinski, J., Gäbler, J., Brors, B., Tierling, S., Jonnakuty, S., Hergenhahn, M., Peltonen, L., Walter, J., and Kyewski, B. (2005). Promiscuous gene expression in thymic epithelial cells is regulated at multiple levels. *J Exp Med*, 202(1):33–45.

Derbinski, J., Schulte, A., Kyewski, B., and Klein, L. (2001). Promiscuous gene expression in medullary thymic epithelial cells mirrors the peripheral self. *Nat Immunol*, 2(11):1032–9.

DeVoss, J., Hou, Y., Johannes, K., Lu, W., Liou, G. I., Rinn, J., Chang, H., Caspi, R. R., Caspi, R., Fong, L., and Anderson, M. S. (2006). Spontaneous autoimmunity prevented by thymic expression of a single self-antigen. *J Exp Med*, 203(12):2727–35.

Dowling, R. J. O., Topisirovic, I., Alain, T., Bidinosti, M., Fonseca, B. D., Petroulakis, E., Wang, X., Larsson, O., Selvaraj, A., Liu, Y., Kozma, S. C., Thomas, G., and Sonenberg, N. (2010). mtorc1-mediated cell proliferation, but not cell growth, controlled by the 4e-bps. *Science*, 328(5982):1172–6.

Doyle, C. and Strominger, J. L. (1987). Interaction between cd4 and class ii mhc molecules mediates cell adhesion. *Nature*, 330(6145):256–9.

Dunlop, E. A., Hunt, D. K., Acosta-Jaquez, H. A., Fingar, D. C., and Tee, A. R. (2011). Ulk1 inhibits mtorc1 signaling, promotes multisite raptor phosphorylation and hinders substrate binding. *Autophagy*, 7(7):737–47.

Echelard, Y., Vassileva, G., and McMahon, A. P. (1994). Cis-acting regulatory sequences governing wnt-1 expression in the developing mouse cns. *Development*, 120(8):2213–24.

Fingar, D. C., Richardson, C. J., Tee, A. R., Cheatham, L., Tsou, C., and Blenis, J. (2004). mtor controls cell cycle progression through its cell growth effectors s6k1 and 4e-bp1/eukaryotic translation initiation factor 4e. *Mol Cell Biol*, 24(1):200–16.

Fingar, D. C., Salama, S., Tsou, C., Harlow, E., and Blenis, J. (2002). Mammalian cell size is controlled by mtor and its downstream targets s6k1 and 4ebp1/eif4e. *Genes Dev*, 16(12):1472–87.

Flanagan, S. P. (1966). 'nude', a new hairless gene with pleiotropic effects in the mouse. *Genet Res*, 8(3):295–309.

Foster, K. G., Acosta-Jaquez, H. A., Romeo, Y., Ekim, B., Soliman, G. A., Carriere, A., Roux, P. P., Ballif, B. A., and Fingar, D. C. (2010). Regulation of mtor complex 1 (mtorc1) by raptor ser863 and multisite phosphorylation. *J Biol Chem*, 285(1):80–94.

Frauwirth, K. A. and Thompson, C. B. (2004). Regulation of t lymphocyte metabolism. *J Immunol*, 172(8):4661–5.

Frias, M. A., Thoreen, C. C., Jaffe, J. D., Schroder, W., Sculley, T., Carr, S. A., and Sabatini, D. M. (2006). msin1 is necessary for akt/pkb phosphorylation, and its isoforms define three distinct mtorc2s. *Curr Biol*, 16(18):1865–70.

Fry, T. J. and Mackall, C. L. (2005). The many faces of il-7: from lymphopoiesis to peripheral t cell maintenance. *J Immunol*, 174(11):6571–6.

Fumarola, C., La Monica, S., Alfieri, R. R., Borra, E., and Guidotti, G. G. (2005). Cell size reduction induced by inhibition of the mtor/s6k-signaling pathway protects jurkat cells from apoptosis. *Cell Death Differ*, 12(10):1344–57.

Ganley, I. G., Lam, D. H. u. . H., Wang, J., Ding, X., Chen, S., and Jiang, X. (2009). Ulk1.atg13.fip200 complex mediates mtor signaling and is essential for autophagy. *J Biol Chem*, 284(18):12297–305.

Godfrey, D. I., Izon, D. J., Wilson, T. J., Tucek, C. L., and Boyd, R. L. (1988). Thymic stromal elements defined by m.abs: ontogeny, and modulation in vivo by immunosuppression. *Adv Exp Med Biol*, 237:269–75.

Goldrath, A. W., Bogatzki, L. Y., and Bevan, M. J. (2000). Naive t cells transiently acquire a memory-like phenotype during homeostasis-driven proliferation. *J Exp Med*, 192(4):557–64.

Gordon, J., Bennett, A. R., Blackburn, C. C., and Manley, N. R. (2001). Gcm2 and foxn1 mark early parathyroid- and thymus-specific domains in the developing third pharyngeal pouch. *Mech Dev*, 103(1-2):141–3.

Gray, D., Abramson, J., Benoist, C., and Mathis, D. (2007). Proliferative arrest and rapid turnover of thymic epithelial cells expressing aire. *J Exp Med*, 204(11):2521–8.

Gray, D. H. D., Seach, N., Ueno, T., Milton, M. K., Liston, A., Lew, A. M., Goodnow, C. C., and Boyd, R. L. (2006). Developmental kinetics, turnover, and stimulatory capacity of thymic epithelial cells. *Blood*, 108(12):3777–85.

Guertin, D. A., Stevens, D. M., Thoreen, C. C., Burds, A. A., Kalaany, N. Y., Moffat, J., Brown, M., Fitzgerald, K. J., and Sabatini, D. M. (2006). Ablation in mice of the mtorc components raptor, rictor, or mlst8 reveals that mtorc2 is required for signaling to akt-foxo and pkcalpha, but not s6k1. *Dev Cell*, 11(6):859–71.

Gupta, M., Hendrickson, A. E. W., Yun, S. S., Han, J. J., Schneider, P. A., Koh, B. D., Stenson, M. J., Wellik, L. E., Shing, J. C., Peterson, K. L., Flatten, K. S., Hess, A. D., Smith, B. D., Karp, J. E., Barr, S., Witzig, T. E., and Kaufmann, S. H. (2012). Dual mtorc1/mtorc2 inhibition diminishes akt activation and induces puma-dependent apoptosis in lymphoid malignancies. *Blood*, 119(2):476–87.

Gwinn, D. M., Shackelford, D. B., Egan, D. F., Mihaylova, M. M., Mery, A., Vasquez, D. S., Turk, B. E., and Shaw, R. J. (2008). Ampk phosphorylation of raptor mediates a metabolic checkpoint. *Mol Cell*, 30(2):214–26.

Hamazaki, Y., Fujita, H., Kobayashi, T., Choi, Y., Scott, H. S., Matsumoto, M., and Minato, N. (2007). Medullary thymic epithelial cells expressing aire represent a unique lineage derived from cells expressing claudin. *Nat Immunol*, 8(3):304–11.

Hara, K., Maruki, Y., Long, X., Yoshino, K.-i., Oshiro, N., Hidayat, S., Tokunaga, C., Avruch, J., and Yonezawa, K. (2002). Raptor, a binding partner of target of rapamycin (tor), mediates tor action. *Cell*, 110(2):177–89.

Hara, K., Yonezawa, K., Weng, Q. P., Kozlowski, M. T., Belham, C., and Avruch, J. (1998). Amino acid sufficiency and mtor regulate p70 s6 kinase and eif-4e bp1 through a common effector mechanism. *J Biol Chem*, 273(23):14484–94.

Hardie, D. G., Carling, D., and Carlson, M. (1998). The amp-activated/snf1 protein kinase subfamily: metabolic sensors of the eukaryotic cell? *Annu Rev Biochem*, 67:821–55.

Harrington, L. S., Findlay, G. M., Gray, A., Tolkacheva, T., Wigfield, S., Rebholz, H., Barnett, J., Leslie, N. R., Cheng, S., Shepherd, P. R., Gout, I., Downes, C. P., and Lamb, R. F. (2004). The tsc1-2 tumor suppressor controls insulin-pi3k signaling via regulation of irs proteins. *J Cell Biol*, 166(2):213–23.

Haxhinasto, S., Mathis, D., and Benoist, C. (2008). The akt-mtor axis regulates de novo differentiation of cd4+foxp3+ cells. *J Exp Med*, 205(3):565–74.

Hay, N. and Sonenberg, N. (2004). Upstream and downstream of mtor. *Genes Dev*, 18(16):1926–45.

Heitman, J., Movva, N. R., and Hall, M. N. (1991). Targets for cell cycle arrest by the immunosuppressant rapamycin in yeast. *Science*, 253(5022):905–9.

Hetzer-Egger, C., Schorpp, M., Haas-Assenbaum, A., Balling, R., Peters, H., and Boehm, T. (2002). Thymopoiesis requires pax9 function in thymic epithelial cells. *Eur J Immunol*, 32(4):1175–81.

Hikosaka, Y., Nitta, T., Ohigashi, I., Yano, K., Ishimaru, N., Hayashi, Y., Matsumoto, M., Matsuo, K., Penninger, J. M., Takayanagi, H., Yokota, Y., Yamada, H., Yoshikai, Y., Inoue, J.-i. . I., Akiyama, T., and Takahama, Y. (2008). The cytokine {RANKL} produced by positively selected thymocytes fosters medullary thymic epithelial cells that express autoimmune regulator. *Immunity*, 29(3):438 – 450.

Hirokawa, K., Utsuyama, M., Moriizumi, E., and Handa, S. (1986). Analysis of the thymic microenvironment by monoclonal antibodies with special reference to thymic nurse cells. *Thymus*, 8(6):349–60.

Hirose, E., Nakashima, N., Sekiguchi, T., and Nishimoto, T. (1998). Raga is a functional homologue of s. cerevisiae gtr1p involved in the ran/gsp1-gtpase pathway. *J Cell Sci*, 111 (Pt 1):11–21.

Holländer, G. A., Wang, B., Nichogiannopoulou, A., Platenburg, P. P., van Ewijk, W., Burakoff, S. J., Gutierrez-Ramos, J. C., and Terhorst, C. (1995). Developmental control point in induction of thymic cortex regulated by a subpopulation of prothymocytes. *Nature*, 373(6512):350–3.

Hosokawa, N., Hara, T., Kaizuka, T., Kishi, C., Takamura, A., Miura, Y., Iemura, S.-i., Natsume, T., Takehana, K., Yamada, N., Guan, J.-L. L., Oshiro, N., and Mizushima, N. (2009). Nutrient-dependent mtorc1 association with the ulk1-atg13-fip200 complex required for autophagy. *Mol Biol Cell*, 20(7):1981–91.

Inoki, K., Li, Y., Xu, T., and Guan, K.-L. L. (2003a). Rheb gtpase is a direct target of tsc2 gap activity and regulates mtor signaling. *Genes Dev*, 17(15):1829–34.

Inoki, K., Li, Y., Zhu, T., Wu, J., and Guan, K.-L. . L. (2002). Tsc2 is phosphorylated and inhibited by akt and suppresses mtor signalling. *Nature Cell Biology*, 4(9):648–657.

Inoki, K., Ouyang, H., Zhu, T., Lindvall, C., Wang, Y., Zhang, X., Yang, Q., Bennett, C., Harada, Y., Stankunas, K., Wang, C.-Y. Y., He, X., MacDougald, O. A., You, M., Williams, B. O., and Guan, K.-L. L. (2006). Tsc2 integrates wnt and energy signals via a coordinated phosphorylation by ampk and gsk3 to regulate cell growth. *Cell*, 126(5):955–68.

Inoki, K., Zhu, T., and Guan, K.-L. L. (2003b). Tsc2 mediates cellular energy response to control cell growth and survival. *Cell*, 115(5):577–90.

Irla, M., Guenot, J., Sealy, G., Reith, W., Imhof, B. A., and Sergé, A. (2013). Three-dimensional visualization of the mouse thymus organization in health and immunodeficiency. *J Immunol*, 190(2):586–96.

Jacinto, E., Facchinetti, V., Liu, D., Soto, N., Wei, S., Jung, S. Y., Huang, Q., Qin, J., and Su, B. (2006). Sin1/mip1 maintains rictor-mtor complex integrity and regulates akt phosphorylation and substrate specificity. *Cell*, 127(1):125–37.

Jacinto, E., Loewith, R., Schmidt, A., Lin, S., Rüegg, M. A., Hall, A., and Hall, M. N. (2004). Mammalian tor complex 2 controls the actin cytoskeleton and is rapamycin insensitive. *Nat Cell Biol*, 6(11):1122–8.

Jaeschke, A., Hartkamp, J., Saitoh, M., Roworth, W., Nobukuni, T., Hodges, A., Sampson, J., Thomas, G., and Lamb, R. (2002). Tuberous sclerosis complex tumor suppressor-mediated s6 kinase inhibition by phosphatidylinositide-3-oh kinase is mtor independent. *J Cell Biol*, 159(2):217–24.

Jagannath, C., Lindsey, D. R., Dhandayuthapani, S., Xu, Y., Hunter, R. L., and Eissa, N. T. (2009). Autophagy enhances the efficacy of bcg vaccine by increasing peptide presentation in mouse dendritic cells. *Nat Med*, 15(3):267–76.

Jenkinson, W. E., Jenkinson, E. J., and Anderson, G. (2003). Differential requirement for mesenchyme in the proliferation and maturation of thymic epithelial progenitors. *J Exp Med*, 198(2):325–32.

Jenkinson, W. E., Rossi, S. W., Parnell, S. M., Jenkinson, E. J., and Anderson, G. (2007). Pdgfralpha-expressing mesenchyme regulates thymus growth and the availability of intrathymic niches. *Blood*, 109(3):954–60.

Jiang, X., Rowitch, D. H., Soriano, P., McMahon, A. P., and Sucov, H. M. (2000). Fate of the mammalian cardiac neural crest. *Development*, 127(8):1607–16.

Julien, L.-A. A., Carriere, A., Moreau, J., and Roux, P. P. (2010). mtorc1-activated s6k1 phosphorylates rictor on threonine 1135 and regulates mtorc2 signaling. *Mol Cell Biol*, 30(4):908–21.

Jung, C. H., Jun, C. B., Ro, S.-H. H., Kim, Y.-M. M., Otto, N. M., Cao, J., Kundu, M., and Kim, D.-H. H. (2009). Ulk-atg13-fip200 complexes mediate mtor signaling to the autophagy machinery. *Mol Biol Cell*, 20(7):1992–2003.

Kadish, J. L. and Basch, R. S. (1976). Hematopoietic thymocyte precursors. i. assay and kinetics of the appearance of progeny. *J Exp Med*, 143(5):1082–99.

Kaizuka, T., Hara, T., Oshiro, N., Kikkawa, U., Yonezawa, K., Takehana, K., Iemura, S.-I., Natsume, T., and Mizushima, N. (2010). Tti1 and tel2 are critical factors in mammalian target of rapamycin complex assembly. *J Biol Chem*, 285(26):20109–16.

Kay, J. E., Kromwel, L., Doe, S. E., and Denyer, M. (1991). Inhibition of t and b lymphocyte proliferation by rapamycin. *Immunology*, 72(4):544–9.

Kellersch, B. and Brocker, T. (2013). Langerhans cell homeostasis in mice is dependent on mtorc1 but not mtorc2 function. *Blood*, 121(2):298–307.

Kim, D.-H. H., Sarbassov, D. D., Ali, S. M., King, J. E., Latek, R. R., Erdjument-Bromage, H., Tempst, P., and Sabatini, D. M. (2002). mtor interacts with raptor to form a nutrient-sensitive complex that signals to the cell growth machinery. *Cell*, 110(2):163–75.

Kim, D.-H. H., Sarbassov, D. D., Ali, S. M., Latek, R. R., Guntur, K. V. P., Erdjument-Bromage, H., Tempst, P., and Sabatini, D. M. (2003). Gbetal, a positive regulator of the rapamycin-sensitive pathway required for the nutrient-sensitive interaction between raptor and mtor. *Mol Cell*, 11(4):895–904.

Kim, E., Goraksha-Hicks, P., Li, L., Neufeld, T. P., and Guan, K.-L. L. (2008). Regulation of torc1 by rag gtpases in nutrient response. *Nat Cell Biol*, 10(8):935–45.

Kim, J. E. and Chen, J. (2004). regulation of peroxisome proliferator-activated receptor-gamma activity by mammalian target of rapamycin and amino acids in adipogenesis. *Diabetes*, 53(11):2748–56.

Kishimoto, H. and Sprent, J. (1997). Negative selection in the thymus includes semimature t cells. *J Exp Med*, 185(2):263–71.

Klein, L. and Jovanovic, K. (2011). Regulatory t cell lineage commitment in the thymus. *Semin Immunol*, 23(6):401–9.

Klug, D. B., Carter, C., Crouch, E., Roop, D., Conti, C. J., and Richie, E. R. (1998). Interdependence of cortical thymic epithelial cell differentiation and t-lineage commitment. *Proc Natl Acad Sci U S A*, 95(20):11822–7.

Klug, D. B., Carter, C., Gimenez-Conti, I. B., and Richie, E. R. (2002). Cutting edge: thymocyte-independent and thymocyte-dependent phases of epithelial patterning in the fetal thymus. *J Immunol*, 169(6):2842–5.

Kuo, C. J., Chung, J., Fiorentino, D. F., Flanagan, W. M., Blenis, J., and Crabtree, G. R. (1992). Rapamycin selectively inhibits interleukin-2 activation of p70 s6 kinase. *Nature*, 358(6381):70–73.

Kyewski, B., Hunsmann, G., Friedrich, R., Ketelsen, U. P., and Wekerle, H. (1981). Thymic nurse cells: intraepithelial thymocyte sojourn and its possible relevance for the pathogenesis of akr lymphomas. *Haematol Blood Transfus*, 26:372–6.

Kyewski, B. and Klein, L. (2006). A central role for central tolerance. *Annu Rev Immunol*, 24:571–606.

Langlais, P., Yi, Z., and Mandarino, L. J. (2011). The identification of raptor as a substrate for p44/42 mapk. *Endocrinology*, 152(4):1264–73.

Laplante, M. and Sabatini, D. M. (2009). mtor signaling at a glance. *J Cell Sci*, 122(Pt 20):3589–94.

Le Douarin, N. M. and Jotereau, F. V. (1975). Tracing of cells of the avian thymus through embryonic life in interspecific chimeras. *J Exp Med*, 142(1):17–40.

Le Douarin, N. M., Jotereau, F. V., Houssaint, E., and Belo, M. (1976). Ontogeny of the avian thymus and bursa of fabricius studied in interspecific chimeras. *Ann Immunol (Paris)*, 127(6):849–56.

Le Lièvre, C. S. and Le Douarin, N. M. (1975). Mesenchymal derivatives of the neural crest: analysis of chimaeric quail and chick embryos. *J Embryol Exp Morphol*, 34(1):125–54.

Lee, C.-H. H., Inoki, K., Karbowniczek, M., Petroulakis, E., Sonenberg, N., Henske, E. P., and Guan, K.-L. L. (2007). Constitutive mtor activation in tsc mutants sensitizes cells to energy starvation and genomic damage via p53. *EMBO J*, 26(23):4812–23.

Lee, K., Gudapati, P., Dragovic, S., Spencer, C., Joyce, S., Killeen, N., Magnuson, M. A., and Boothby, M. (2010). Mammalian target of rapamycin protein complex 2 regulates differentiation of th1 and th2 cell subsets via distinct signaling pathways. *Immunity*, 32(6):743–53.

Lepault, F. and Weissman, I. L. (1981). An in vivo assay for thymus-homing bone marrow cells. *Nature*, 293(5828):151–4.

Leuchars, E., Davies, A. J., and Wallis, V. (1973). Studies on t-cell precursors. *Int Arch Allergy Appl Immunol*, 45(1):237–9.

Liu, C., Ueno, T., Kuse, S., Saito, F., Nitta, T., Piali, L., Nakano, H., Kakiuchi, T., Lipp, M., Hollander, G. A., and Takahama, Y. (2005). The role of ccl21 in recruitment of t-precursor cells to fetal thymi. *Blood*, 105(1):31–9.

Long, X., Lin, Y., Ortiz-Vega, S., Yonezawa, K., and Avruch, J. (2005). Rheb binds and regulates the mtor kinase. *Curr Biol*, 15(8):702–13.

Lu, M., Wang, J., Ives, H. E., and Pearce, D. (2011). msin1 protein mediates sgk1 protein interaction with mtorc2 protein complex and is required for selective activation of the epithelial sodium channel. *J Biol Chem*, 286(35):30647–54.

Luckert, K., Götschel, F., Sorger, P. K., Hecht, A., Joos, T. O., and Pötz, O. (2011). Snapshots of protein dynamics and post-translational modifications in one experiment–beta-catenin and its functions. *Mol Cell Proteomics*, 10(5):M110.007377.

Lumeng, C. N., Bodzin, J. L., and Saltiel, A. R. (2007). Obesity induces a phenotypic switch in adipose tissue macrophage polarization. *J Clin Invest*, 117(1):175–84.

Ma, X. M. and Blenis, J. (2009). Molecular mechanisms of mtor-mediated translational control. *Nat Rev Mol Cell Biol*, 10(5):307–18.

Manley, N. R. (2000). Thymus organogenesis and molecular mechanisms of thymic epithelial cell differentiation. *Semin Immunol*, 12(5):421–8.

Manley, N. R. and Capecchi, M. R. (1995). The role of hoxa-3 in mouse thymus and thyroid development. *Development*, 121(7):1989–2003.

Maródi, L. and Notarangelo, L. D. (2007). Immunological and genetic bases of new primary immunodeficiencies. *Nat Rev Immunol*, 7(11):851–61.

Martel, R. R., Klicius, J., and Galet, S. (1977). Inhibition of the immune response by rapamycin, a new antifungal antibiotic. *Can J Physiol Pharmacol*, 55(1):48–51.

Matloubian, M., Lo, C. G., Cinamon, G., Lesneski, M. J., Xu, Y., Brinkmann, V., Allende, M. L., Proia, R. L., and Cyster, J. G. (2004). Lymphocyte egress from thymus and peripheral lymphoid organs is dependent on s1p receptor 1. *Nature*, 427(6972):355–60.

Matsuoka, T., Ahlberg, P. E., Kessaris, N., Iannarelli, P., Dennehy, U., Richardson, W. D., McMahon, A. P., and Koentges, G. (2005). Neural crest origins of the neck and shoulder. *Nature*, 436(7049):347–55.

McDonald, P. C., Oloumi, A., Mills, J., Dobreva, I., Maidan, M., Gray, V., Wederell, E. D., Bally, M. B., Foster, L. J., and Dedhar, S. (2008). Rictor and integrin-linked kinase interact and regulate akt phosphorylation and cancer cell survival. *Cancer Res*, 68(6):1618–24.

Medzhitov, R. and Janeway, C. A. (2002). Decoding the patterns of self and nonself by the innate immune system. *Science*, 296(5566):298–300.

Medzhitov, R., Preston-Hurlburt, P., and Janeway, C. A. (1997). A human homologue of the drosophila toll protein signals activation of adaptive immunity. *Nature*, 388(6640):394–7.

Merkenschlager, M. and von Boehmer, H. (2010). Pi3 kinase signalling blocks foxp3 expression by sequestering foxo factors. *J Exp Med*, 207(7):1347–50.

Miller, J. F. (1964). The thymus and the development of immunologic responsiveness. *Science*, 144(3626):1544–51.

Miller, J. R. (2002). The wnts. *Genome Biol*, 3(1):REVIEWS3001.

Moore, M. A. and Owen, J. J. (1967). Experimental studies on the development of the thymus. *J Exp Med*, 126(4):715–26.

Mori, K., Itoi, M., Tsukamoto, N., Kubo, H., and Amagai, T. (2007). The perivascular space as a path of hematopoietic progenitor cells and mature t cells between the blood circulation and the thymic parenchyma. *Int Immunol*, 19(6):745–53.

Nakagawa, Y., Ohigashi, I., Nitta, T., Sakata, M., Tanaka, K., Murata, S., Kanagawa, O., and Takahama, Y. (2012). Thymic nurse cells provide microenvironment for secondary t cell receptor α rearrangement in cortical thymocytes. *Proc Natl Acad Sci U S A*, 109(50):20572–7.

Naspetti, M., Aurrand-Lions, M., DeKoning, J., Malissen, M., Galland, F., Lo, D., and Naquet, P. (1997). Thymocytes and relb-dependent medullary epithelial cells provide growth-promoting and organization signals, respectively, to thymic medullary stromal cells. *Eur J Immunol*, 27(6):1392–7.

Nazio, F., Strappazzon, F., Antonioli, M., Bielli, P., Cianfanelli, V., Bordi, M., Gretzmeier, C., Dengjel, J., Piacentini, M., Fimia, G. M., and Cecconi, F. (2013). mtor inhibits autophagy by controlling ulk1 ubiquitylation, self-association and function throughambra1 and traf6. *Nat Cell Biol*, 15(4):406–16.

Nehls, M., Pfeifer, D., Schorpp, M., Hedrich, H., and Boehm, T. (1994). New member of the winged-helix protein family disrupted in mouse and rat nude mutations. *Nature*, 372(6501):103–7.

Nitta, T., Ohigashi, I., Nakagawa, Y., and Takahama, Y. (2011). Cytokine crosstalk for thymic medulla formation. *Curr Opin Immunol*, 23(2):190–7.

Nojima, H., Tokunaga, C., Eguchi, S., Oshiro, N., Hidayat, S., Yoshino, K.-i., Hara, K., Tanaka, N., Avruch, J., and Yonezawa, K. (2003). The mammalian target of rapamycin (mtor) partner, raptor, binds the mtor substrates p70 s6 kinase and 4e-bp1 through their tor signaling (tos) motif. *J Biol Chem*, 278(18):15461–4.

Norment, A. M., Salter, R. D., Parham, P., Engelhard, V. H., and Littman, D. R. (1988). Cell-cell adhesion mediated by cd8 and mhc class i molecules. *Nature*, 336(6194):79–81.

Ouchi, N., Parker, J. L., Lugus, J. J., and Walsh, K. (2011). Adipokines in inflammation and metabolic disease. *Nat Rev Immunol*, 11(2):85–97.

Owen, J. J. and Ritter, M. A. (1969). Tissue interaction in the development of thymus lymphocytes. *J Exp Med*, 129(2):431–42.

Palmer, E. and Naeher, D. (2009). Affinity threshold for thymic selection through a t-cell receptor-co-receptor zipper. *Nat Rev Immunol*, 9(3):207–13.

Pantelouris, E. M. (1968). Absence of thymus in a mouse mutant. *Nature*, 217(5126):370–1.

Pearce, L. R., Huang, X., Boudeau, J., Pawowski, R., Wullschleger, S., Deak, M., Ibrahim, A. F. M., Gourlay, R., Magnuson, M. A., and Alessi, D. R. (2007). Identification of protor as a novel rictor-binding component of mtor complex-2. *Biochem J*, 405(3):513–22.

Pearce, L. R., Sommer, E. M., Sakamoto, K., Wullschleger, S., and Alessi, D. R. (2011). Protor-1 is required for efficient mtorc2-mediated activation of sgk1 in the kidney. *Biochem J*, 436(1):169–79.

Perry, S. S., Wang, H., Pierce, L. J., Yang, A. M., Tsai, S., and Spangrude, G. J. (2004). L-selectin defines a bone marrow analog to the thymic early t-lineage progenitor. *Blood*, 103(8):2990–6.

Peters, H., Neubüser, A., Kratochwil, K., and Balling, R. (1998). Pax9-deficient mice lack pharyngeal pouch derivatives and teeth and exhibit craniofacial and limb abnormalities. *Genes Dev*, 12(17):2735–47.

Peterson, T. R., Laplante, M., Thoreen, C. C., Sancak, Y., Kang, S. A., Kuehl, W. M., Gray, N. S., and Sabatini, D. M. (2009). Deptor is an mtor inhibitor frequently overexpressed in multiple myeloma cells and required for their survival. *Cell*, 137(5):873–86.

Petrie, H. T., Livak, F., Schatz, D. G., Strasser, A., Crispe, I. N., and Shortman, K. (1993). Multiple rearrangements in t cell receptor alpha chain genes maximize the production of useful thymocytes. *J Exp Med*, 178(2):615–22.

Picca, C. C., Oh, S., Panarey, L., Aitken, M., Basehoar, A., and Caton, A. J. (2009). Thymocyte deletion can bias treg formation toward low-abundance self-peptide. *Eur J Immunol*, 39(12):3301–6.

Porstmann, T., Santos, C. R., Lewis, C., Griffiths, B., and Schulze, A. (2009). A new player in the orchestra of cell growth: Srebp activity is regulated by mtorc1 and contributes to the regulation of cell and organ size. *Biochem Soc Trans*, 37(Pt 1):278–83.

Ramírez-Valle, F., Badura, M. L., Braunstein, S., Narasimhan, M., and Schneider, R. J. (2010). Mitotic raptor promotes mtorc1 activity, g(2)/m cell cycle progression, and internal ribosome entry site-mediated mrna translation. *Mol Cell Biol*, 30(13):3151–64.

Rao, R. R., Li, Q., Odunsi, K., and Shrikant, P. A. (2010). The mtor kinase determines effector versus memory cd8+ t cell fate by regulating the expression of transcription factors t-bet and eomesodermin. *Immunity*, 32(1):67–78.

Raught, B., Peiretti, F., Gingras, A.-C. C., Livingstone, M., Shahbazian, D., Mayeur, G. L., Polakiewicz, R. D., Sonenberg, N., and Hershey, J. W. B. (2004). Phosphorylation of eucaryotic translation initiation factor 4b ser422 is modulated by s6 kinases. *EMBO J*, 23(8):1761–9.

Revest, J. M., Suniara, R. K., Kerr, K., Owen, J. J., and Dickson, C. (2001). Development of the thymus requires signaling through the fibroblast growth factor receptor r2-iiib. *J Immunol*, 167(4):1954–61.

Ricklin, D., Hajishengallis, G., Yang, K., and Lambris, J. D. (2010). Complement: a key system for immune surveillance and homeostasis. *Nat Immunol*, 11(9):785–97.

Ritter, M. A. and Boyd, R. L. (1993). Development in the thymus: it takes two to tango. *Immunol Today*, 14(9):462–9.

Robitaille, A. M., Christen, S., Shimobayashi, M., Cornu, M., Fava, L. L., Moes, S., Prescianotto-Baschong, C., Sauer, U., Jenoe, P., and Hall, M. N. (2013). Science.

Rodewald, H.-R. R. (2008). Thymus organogenesis. *Annu Rev Immunol*, 26:355–88.

Rossi, S. W., Jenkinson, W. E., Anderson, G., and Jenkinson, E. J. (2006). Clonal analysis reveals a common progenitor for thymic cortical and medullary epithelium. *Nature*, 441(7096):988–91.

Rossi, S. W., Kim, M.-Y. Y., Leibbrandt, A., Parnell, S. M., Jenkinson, W. E., Glanville, S. H., McConnell, F. M., Scott, H. S., Penninger, J. M., Jenkinson, E. J., Lane, P. J. L., and Anderson, G. (2007). Rank signals from cd4(+)3(-) inducer cells regulate development of aire-expressing epithelial cells in the thymic medulla. *J Exp Med*, 204(6):1267–72.

Roux, P. P., Ballif, B. A., Anjum, R., Gygi, S. P., and Blenis, J. (2004). Tumor-promoting phorbol esters and activated ras inactivate the tuberous sclerosis tumor suppressor complex via p90 ribosomal s6 kinase. *Proc Natl Acad Sci U S A*, 101(37):13489–94.

Sabatini, D. M., Erdjument-Bromage, H., Lui, M., Tempst, P., and Snyder, S. H. (1994). Raft1: a mammalian protein that binds to fkbp12 in a rapamycin-dependent fashion and is homologous to yeast tors. *Cell*, 78(1):35–43.

Sabers, C. J., Martin, M. M., Brunn, G. J., Williams, J. M., Dumont, F. J., Wiederrecht, G., and Abraham, R. T. (1995). Isolation of a protein target of the fkbp12-rapamycin complex in mammalian cells. *J Biol Chem*, 270(2):815–22.

Sancak, Y., Bar-Peled, L., Zoncu, R., Markhard, A. L., Nada, S., and Sabatini, D. M. (2010). Ragulator-rag complex targets mtorc1 to the lysosomal surface and is necessary for its activation by amino acids. *Cell*, 141(2):290–303.

Sancak, Y., Peterson, T. R., Shaul, Y. D., Lindquist, R. A., Thoreen, C. C., Bar-Peled, L., and Sabatini, D. M. (2008). The rag gtpases bind raptor and mediate amino acid signaling to mtorc1. *Science*, 320(5882):1496–501.

Sancak, Y., Thoreen, C. C., Peterson, T. R., Lindquist, R. A., Kang, S. A., Spooner, E., Carr, S. A., and Sabatini, D. M. (2007). Pras40 is an insulin-regulated inhibitor of the mtorc1 protein kinase. *Mol Cell*, 25(6):903–15.

Sarbassov, D. D., Ali, S. M., Kim, D.-H. H., Guertin, D. A., Latek, R. R., Erdjument-Bromage, H., Tempst, P., and Sabatini, D. M. (2004). Rictor, a novel binding partner of mtor, defines a rapamycin-insensitive and

raptor-independent pathway that regulates the cytoskeleton. *Curr Biol*, 14(14):1296–302.

Sarbassov, D. D., Ali, S. M., Sengupta, S., Sheen, J.-H. H., Hsu, P. P., Bagley, A. F., Markhard, A. L., and Sabatini, D. M. (2006). Prolonged rapamycin treatment inhibits mtorc2 assembly and akt/pkb. *Mol Cell*, 22(2):159–68.

Sathaliyawala, T., O'Gorman, W. E., Greter, M., Bogunovic, M., Konjufca, V., Hou, Z. E., Nolan, G. P., Miller, M. J., Merad, M., and Reizis, B. (2010). Mammalian target of rapamycin controls dendritic cell development downstream of flt3 ligand signaling. *Immunity*, 33(4):597–606.

Sauer, S., Bruno, L., Hertweck, A., Finlay, D., Leleu, M., Spivakov, M., Knight, Z. A., Cobb, B. S., Cantrell, D., O'Connor, E., Shokat, K. M., Fisher, A. G., and Merkenschlager, M. (2008). T cell receptor signaling controls foxp3 expression via pi3k, akt, and mtor. *Proc Natl Acad Sci U S A*, 105(22):7797–802.

Schmid, D. and Münz, C. (2007). Immune surveillance via self digestion. *Autophagy*, 3(2):133–5.

Schürmann, A., Brauers, A., Massmann, S., Becker, W., and Joost, H. G. (1995). Cloning of a novel family of mammalian gtp-binding proteins (raga, ragbs, ragb1) with remote similarity to the ras-related gtpases. *J Biol Chem*, 270(48):28982–8.

Sekiguchi, T., Hirose, E., Nakashima, N., Ii, M., and Nishimoto, T. (2001). Novel g proteins, rag c and rag d, interact with gtp-binding proteins, rag a and rag b. *J Biol Chem*, 276(10):7246–57.

Settembre, C., Zoncu, R., Medina, D. L., Vetrini, F., Erdin, S., Erdin, S., Huynh, T., Ferron, M., Karsenty, G., Vellard, M. C., Facchinetti, V., Sabatini, D. M., and Ballabio, A. (2012). A lysosome-to-nucleus signalling mechanism senses and regulates the lysosome via mtor and tfeb. *EMBO J*, 31(5):1095–108.

Shakib, S., Desanti, G. E., Jenkinson, W. E., Parnell, S. M., Jenkinson, E. J., and Anderson, G. (2009). Checkpoints in the development of thymic cortical epithelial cells. *J Immunol*, 182(1):130–7.

Shaw, A. S., Amrein, K. E., Hammond, C., Stern, D. F., Sefton, B. M., and Rose, J. K. (1989). The lck tyrosine protein kinase interacts with the cytoplasmic tail of the cd4 glycoprotein through its unique amino-terminal domain. *Cell*, 59(4):627–36.

Shinohara, T. and Honjo, T. (1996). Epidermal growth factor can replace thymic mesenchyme in induction of embryonic thymus morphogenesis in vitro. *Eur J Immunol*, 26(4):747–52.

Sinclair, L. V., Finlay, D., Feijoo, C., Cornish, G. H., Gray, A., Ager, A., Okkenhaug, K., Hagenbeek, T. J., Spits, H., and Cantrell, D. A. (2008). Phosphatidylinositol-3-oh kinase and nutrient-sensing mtor pathways control t lymphocyte trafficking. *Nat Immunol*, 9(5):513–21.

Singer, A., Adoro, S., and Park, J.-H. H. (2008). Lineage fate and intense debate: myths, models and mechanisms of cd4- versus cd8-lineage choice. *Nat Rev Immunol*, 8(10):788–801.

Smith, C. (1965). Studies on the thymus of the mammal. xiv. histology and histochemistry of embryonic and early postnatal thymuses of c57bl-6 and akr strain mice. *Am J Anat*, 116(3):611–29.

Starr, T. K., Jameson, S. C., and Hogquist, K. A. (2003). Positive and negative selection of t cells. *Annu Rev Immunol*, 21:139–76.

Steimle, V., Siegrist, C. A., Mottet, A., Lisowska-Grospierre, B., and Mach, B. (1994). Regulation of mhc class ii expression by interferon-gamma mediated by the transactivator gene ciita. *Science*, 265(5168):106–9.

Surh, C. D., Ernst, B., and Sprent, J. (1992). Growth of epithelial cells in the thymic medulla is under the control of mature t cells. *J Exp Med*, 176(2):611–6.

Takeda, K., Kaisho, T., and Akira, S. (2003). Toll-like receptors. *Annu Rev Immunol*, 21:335–76.

Thedieck, K., Polak, P., Kim, M. L., Molle, K. D., Cohen, A., Jenö, P., Arrieumerlou, C., and Hall, M. N. (2007). Pras40 and prr5-like protein are new mtor interactors that regulate apoptosis. *PLoS One*, 2(11):e1217.

Tsan, M.-F. F. and Gao, B. (2004). Endogenous ligands of toll-like receptors. *J Leukoc Biol*, 76(3):514–9.

Ueno, T., Saito, F., Gray, D. H. D., Kuse, S., Hieshima, K., Nakano, H., Kakiuchi, T., Lipp, M., Boyd, R. L., and Takahama, Y. (2004). Ccr7 signals are essential for cortex-medulla migration of developing thymocytes. *J Exp Med*, 200(4):493–505.

Um, S. H., Frigerio, F., Watanabe, M., Picard, F., Joaquin, M., Sticker, M., Fumagalli, S., Allegrini, P. R., Kozma, S. C., Auwerx, J., and Thomas, G. (2004). Absence of s6k1 protects against age- and diet-induced obesity while enhancing insulin sensitivity. *Nature*, 431(7005):200–5.

Vander Haar, E., Lee, S.-I. I., Bandhakavi, S., Griffin, T. J., and Kim, D.-H. H. (2007). Insulin signalling to mtor mediated by the akt/pkb substrate pras40. *Nat Cell Biol*, 9(3):316–23.

Varecza, Z., Kvell, K., Talabér, G., Miskei, G., Csongei, V., Bartis, D., Anderson, G., Jenkinson, E. J., and Pongracz, J. E. (2011). Multiple suppression pathways of canonical wnt signalling control thymic epithelial senescence. *Mech Ageing Dev*, 132(5):249–56.

Veillette, A., Bookman, M. A., Horak, E. M., Samelson, L. E., and Bolen, J. B. (1989a). Signal transduction through the cd4 receptor involves the activation of the internal membrane tyrosine-protein kinase p56lck. *Nature*, 338(6212):257–9.

Veillette, A., Zúñiga Pflücker, J. C., Bolen, J. B., and Kruisbeek, A. M. (1989b). Engagement of cd4 and cd8 expressed on immature thymocytes induces activation of intracellular tyrosine phosphorylation pathways. *J Exp Med*, 170(5):1671–80.

Wallin, J., Eibel, H., Neubüser, A., Wilting, J., Koseki, H., and Balling, R. (1996). Pax1 is expressed during development of the thymus epithelium and is required for normal t-cell maturation. *Development*, 122(1):23–30.

Wang, B., Simpson, S. J., Holländer, G. A., and Terhorst, C. (1997). Development and function of t lymphocytes and natural killer cells after bone marrow transplantation of severely immunodeficient mice. *Immunol Rev*, 157:53–60.

Wang, L., Harris, T. E., Roth, R. A., and Lawrence, J. C. (2007). Pras40 regulates mtorc1 kinase activity by functioning as a direct inhibitor of substrate binding. *J Biol Chem*, 282(27):20036–44.

Wang, L., Lawrence, J. C., Sturgill, T. W., and Harris, T. E. (2009). Mammalian target of rapamycin complex 1 (mtorc1) activity is associated with phosphorylation of raptor by mtor. *J Biol Chem*, 284(22):14693–7.

Weichhart, T., Costantino, G., Poglitsch, M., Rosner, M., Zeyda, M., Stuhlmeier, K. M., Kolbe, T., Stulnig, T. M., Hörl, W. H., Hengstschläger, M., Müller, M., and Säemann, M. D. (2008). The tsc-mtor signaling pathway regulates the innate inflammatory response. *Immunity*, 29(4):565–77.

Weinreich, M. A. and Hogquist, K. A. (2008). Thymic emigration: when and how t cells leave home. *J Immunol*, 181(4):2265–70.

Wekerle, H. and Ketelsen, U. P. (1980). Thymic nurse cells–ia-bearing epithelium involved in t-lymphocyte differentiation? *Nature*, 283(5745):402–4.

White, A. J., Nakamura, K., Jenkinson, W. E., Saini, M., Sinclair, C., Seddon, B., Narendran, P., Pfeffer, K., Nitta, T., Takahama, Y., Caamano, J. H., Lane, P. J. L., Jenkinson, E. J., and Anderson, G. (2010). Lymphotoxin signals from positively selected thymocytes regulate the terminal differentiation of medullary thymic epithelial cells. *J Immunol*, 185(8):4769–76.

White, A. J., Withers, D. R., Parnell, S. M., Scott, H. S., Finke, D., Lane, P. J. L., Jenkinson, E. J., and Anderson, G. (2008). Sequential phases in the development of aire-expressing medullary thymic epithelial cells involve distinct cellular input. *Eur J Immunol*, 38(4):942–7.

Wilkinson, R. W., Anderson, G., Owen, J. J., and Jenkinson, E. J. (1995). Positive selection of thymocytes involves sustained interactions with the thymic microenvironment. *J Immunol*, 155(11):5234–40.

Wurbel, M. A., Malissen, M., Guy-Grand, D., Meffre, E., Nussenzweig, M. C., Richelme, M., Carrier, A., and Malissen, B. (2001). Mice lacking the ccr9 cc-chemokine receptor show a mild impairment of early t- and b-cell development and a reduction in t-cell receptor gammadelta(+) gut intraepithelial lymphocytes. *Blood*, 98(9):2626–32.

Xu, P.-X. X., Zheng, W., Laclef, C., Maire, P., Maas, R. L., Peters, H., and Xu, X. (2002). Eya1 is required for the morphogenesis of mammalian thymus, parathyroid and thyroid. *Development*, 129(13):3033–44.

Yamashita, I., Nagata, T., Tada, T., and Nakayama, T. (1993). Cd69 cell surface expression identifies developing thymocytes which audition for t cell antigen receptor-mediated positive selection. *Int Immunol*, 5(9):1139–50.

Yamazaki, H., Sakata, E., Yamane, T., Yanagisawa, A., Abe, K., Yamamura, K.-I., Hayashi, S.-I., and Kunisada, T. (2005). Presence and distribution of neural crest-derived cells in the murine developing thymus and their potential for differentiation. *Int Immunol*, 17(5):549–58.

Yan, L., Mieulet, V., and Lamb, R. F. (2008). mtorc2 is the hydrophobic motif kinase for sgk1. *Biochem J*, 416(3):e19–21.

Zachariah, M. A. and Cyster, J. G. (2010). Neural crest-derived pericytes promote egress of mature thymocytes at the corticomedullary junction. *Science*, 328(5982):1129–35.

Zhang, H., Stallock, J. P., Ng, J. C., Reinhard, C., and Neufeld, T. P. (2000). Regulation of cellular growth by the drosophila target of rapamycin dtor. *Genes Dev*, 14(21):2712–24.

Zhang, H. H., Lipovsky, A. I., Dibble, C. C., Sahin, M., and Manning, B. D. (2006). S6k1 regulates gsk3 under conditions of mtor-dependent feedback inhibition of akt. *Mol Cell*, 24(2):185–97.

Zhang, S., Readinger, J. A., DuBois, W., Janka-Junttila, M., Robinson, R., Pruitt, M., Bliskovsky, V., Wu, J. Z., Sakakibara, K., Patel, J., Parent, C. A., Tessarollo, L., Schwartzberg, P. L., and Mock, B. A. (2011). Constitutive reductions in mtor alter cell size, immune cell development, and antibody production. *Blood*, 117(4):1228–38.

Zinzalla, V., Stracka, D., Oppliger, W., and Hall, M. N. (2011). Activation of mtorc2 by association with the ribosome. *Cell*, 144(5):757–68.

Zoncu, R., Efeyan, A., and Sabatini, D. M. (2011). mtor: from growth signal integration to cancer, diabetes and ageing. *Nat Rev Mol Cell Biol*, 12(1):21–35.

Zuklys, S., Gill, J., Keller, M. P., Hauri-Hohl, M., Zhanybekova, S., Balciunaite, G., Na, K.-J. J., Jeker, L. T., Hafen, K., Tsukamoto, N., Amagai, T., Taketo, M. M., Krenger, W., and Holländer, G. A. (2009). Stabilized beta-catenin in thymic epithelial cells blocks thymus development and function. *J Immunol*, 182(5):2997–3007.